

**Improved Pulse Pressure Variability Algorithm: Design and Development of
Data Collection Software and Development of a Standard Algorithm for Pulse Pressure
Variability for Research Purposes**

Submitted by

Kevyn Nyland

Bachelor of Engineering Electrical and Computing (Honours), 1992 Monash University

A thesis submitted in total fulfilment

Of the requirements for the degree of

Master of Engineering

Department of Engineering

College of Science, Health and Engineering

La Trobe University

Victoria, Australia

March 2020

Statement of Authorship

Except where reference is made in the text of the thesis, this thesis contains no material published elsewhere or extracted in whole or in part from a thesis accepted for the award of any other degree or diploma. No other person's work has been used without due acknowledgment in the main text of the thesis. This thesis has not been submitted for the award of any degree or diploma in any other tertiary institution.

Kevyn Nyland

6 March 2020

This work was supported by an Australian Government Research Training Program Scholarship

Abstract

The Pulse Pressure Variability (PPV) index, determined by an algorithm based on the change in blood pressure response due to the action of mechanical ventilation, can measure and predict fluid responsiveness of patients in surgery or Intensive Care. When intravenous fluids are administered, fluid responsiveness relates to a desirable increase in cardiac output, which is beneficial to patient recovery, but too much fluid can be detrimental, causing oedema, sepsis, and patient mortality. My intention was to improve on the currently used PPV algorithm (Aboy, 2004), which exhibits difficulty coping with abrupt hemodynamic changes encountered in clinical scenarios.

This required data acquisition from patient monitoring systems, with software to simulate the existing PPV algorithm. To maintain a platform consistent with existing systems in the hosting clinical environment, a communication program was developed in LabVIEW, enabling collection of required data from patient monitoring systems. Condensing the software and hardware to a LabVIEW platform (for example, establishing the working communication interface) was advantageous as a consolidated tool for ongoing clinical research.

Aboy's PPV algorithm was replicated and extended into development of a frequency-domain method to improve on the currently used time-domain PPV algorithms.

Both the developed Aboy and the novel test algorithms worked successfully with simulated data. After comparison with clinical data from the output of an actual patient monitor, the result of the replicated algorithm showed accuracy of 19.1% across all classifications (fluid responders, non-responders or within a 'grey zone'). The accuracy of the novel 'test' algorithm was a disappointing 36.3%, but the overall proportion of fluid responders to non-responders was 5.7% for both algorithms.

But if the proposed frequency-domain model can be enhanced, the new, simpler algorithm, promising as a first step to predict PPV, will be worthy of further development.

Acknowledgements

Here I would like to thank the following people for all the help they have given during this work. Most notably are Supervisors; Adjunct Senior Lecturer Paul Junor, Adjunct Professor Richard Kirsner and Professor Philip Peyton, all of whom have been there throughout the journey towards completing this Thesis. I want to thank them for their patience and support while I have endeavoured to produce something that could be useful to ongoing research in this area.

Special thanks to my beautiful wife Urvashi who has been with me for most of the journey and spent countless nights alone while I worked. Thank you to my children Kai and Elijah for being patient while Dad was not around.

I have dedicated this work to Peter Atkin, who was a quick friend but was too quick to leave us.

Figures

Figure 1. Simultaneous recording of systemic arterial and airway pressure with Pulse Pressure variations [4]	16
Figure 2. Block diagram of a circulatory system [6].....	17
Figure 3. Basic cardiac anatomy anterior view [7].....	18
Figure 4. Stroke Volume Vs End-diastolic filling pressure induced by mechanical ventilation[11]	20
Figure 5. Ventricular preload relating to stroke volume including failing ventricle [10].....	20
Figure 6. Effects of positive pressure ventilation on the heart[13]	21
Figure 7. Arterial line placement[14]	22
Figure 8. Arterial blood pressure waveform Systolic and Diastolic phases (adapted from [15])	23
Figure 9. ABP waveforms with variation due to damping of the system [16]	23
Figure 10. PP_{max} and PP_{min} due to the effect of a mechanical ventilator	26
Figure 11. Relationship between PPV before Volume Expansion and Percentages CO induced. Grey zone 9-13% shows the limits of uncertainty[23]	28
Figure 12. Gold Standard PPV_{man} (%) calculated using data collected from Philips Monitor	31
Figure 13. The complexity of the blood pressure waveform[35]	31
Figure 14. Simulated ABP waveform that shows a pressure amplitude change with each simulated respiratory cycle resulting in PP_{max} and PP_{min} [1]	35
Figure 15. Simple amplitude modulated signal made of two sinusoidal signals.	36
Figure 16. Amplitude modulation represented in the frequency-domain[48].....	36
Figure 17. Differences in Modulation of 50 to 100%.....	37
Figure 18. Simulated ‘Modulated’ waveform, Systolic/Diastolic 120/80 mmHg with PPV 15%.....	38
Figure 19. Patient Data ABP Waveform, Systolic/Diastolic peaks changing with Respiration	38
Figure 20. Simulated “Simple” Simulated Waveform, 15% change in amplitude, Systolic/Diastolic 120/80 mmHg	38
Figure 21. Power Spectrum Display (PSD) of ABP signal with signal peaks	39
Figure 22. Main-VI and Sub-VIs used in the project	40
Figure 23. Simulated ‘Simple’ Simulated Waveform, 30% change in amplitude, Systolic/Diastolic 120/80 mmHg	41
Figure 42. Power spectrum of “Simple” with relative peaks for $SPRR$ and $SPHR$	41
Figure 25. Beat minima and maxima, in the time series	44
Figure 26. Envelope upper $ue(n)$ and lower $le(n)$ taken from patient data shown in Figure 24.	44
Figure 27. Estimated $ue(n)$ and lower $le(n)$ resampled and smoothed with Gaussian function	45

Figure 28. Pulse pressure amplitude estimate pan , showing effects of respiration on the pulse pressure	46
Figure 29. Simulation data with $\alpha = 0.2$ (PPV= 20%)	48
Figure 30. PSD Second harmonic, proportionally raised from a factor of 1x respiratory sideband	49
Figure 31. PSD Second-harmonic, proportionally raised 2x respiratory sideband	50
Figure 32. Crossover cable connection for Laptop to Monitor communications	52
Figure 33. RJ45 LAN connection location Philips MP70	53
Figure 34. Protocol diagram for communication between Server (MP70) and Client (Laptop) [49]. ..	56
Figure 35. Steps for establishing a communications, polling data and releasing client Intellivue Monitor	57
Figure 36. Arterial blood pressure waveform scaled correctly	60
Figure 37. LabVIEW screen layout for communication with Philips MX800 with simulated data	60
Figure 43. Correlation plot $\%PPV_{test}$ vs reference $\%PPV_{rec}$	64
Figure 44. Bland Altman plot $\%PPV_{test}$ vs reference $\%PPV_{rec}$	65
Figure 45. Correlation plot $\%PPV_{Aboy}$ vs reference $\%PPV_{rec}$	65
Figure 46. Bland-Altman plot $\%PPV_{Aboy}$ vs reference $\%PPV_{rec}$	66
Figure 47. Patient data, normal pulse pressure with $PPV \approx 30\%$	73
Figure 48. PP Envelope for Test method 30% envelope change	74
Figure 49. PP Envelope that satisfies Aboy algorithm $PPV = 30\%$	74
Figure 50. Initiate and Close UDP	76
Figure 51. Increase UDP buffer size	77
Figure 52. Stop error 56 for UDP, No Timeout	77
Figure 53. UDP Reading packets of data and converting to string arrays	77
Figure 54. Request to start communication	78
Figure 55. Single Poll Data (numeric)	78
Figure 56. Vi for conversion from 32-bit hex to float type numeric display	80
Figure 57. Conversion of relative time Hex to Integer data in milliseconds	81
Figure 58 Selection of polled waveforms and numerics	82
Figure 59. Writing to *.CSV file	83
Figure 60. Sample Excel data recorded from the monitor	83
Figure 61. Aboy Algorithm <i>Sub-VI</i> coding snippet	84
Figure 62. Front panel created for Aboy Algorithm thesis	84
Figure 63 <i>Sub-VI</i> for CO2 wave capture	88
Figure 64. Resultant CO2 waveform	89

Figure 65. GE Code Example Code sample	90
Figure 66. Hex commands for GE Carescape monitor for the initiation of Wave and Numerical data	91
Figure 67. Electrical interference on the bit	92

Tables

Table 1. Recorded patient data waveforms from this study	24
Table 2. Showing mean PPV% \pm SD for Responders and Non-Responders where fluid responsiveness is > 15% Cardiac Output after volume expansion[23].....	27
Table 3. Summarising different algorithm/methods	33
Table 4. Manufacturer-specific technologies and methods	34
Table 5. Estimation $\%\Delta PP$ using a window of 3 samples or approximately 10 seconds	47
Table 6. Simulation data vs Aboy Algorithm.....	48
Table 7. Percentage error with changing respiratory signal phase θc 2 nd harmonic x1.....	49
Table 8. Percentage error with changing respiratory signal phase θc 2 nd harmonic x2.....	50
Table 9. Different Objects available with examples of their attributes [49].	55
Table 10. Polling frequency and sample period and size [49].	58
Table 11. Solving for y to determine a scaling factor for Invasive Blood Pressure measurement	59
Table 12. Different PSDs for different wave-types	69
Table 13. Signal quality affected the ability of PPV Algorithm	70
Table 14. Polling frequency and sample period and size.....	81

Notations and Abbreviations

PPV	Pulse Pressure Variation
CO	Cardiac Output
SV	Stroke Volume
LVSV	Left Ventricular Stroke Volume
PP	Pulse Pressure
ABP	Arterial Blood Pressure
HR	Heart Rate
RR	Respiratory Rate
PSD	Power Spectral Density
SPeR	Spectral Peak Ratio

Table of Contents

Statement of Authorship	i
Abstract.....	ii
Acknowledgements.....	iii
Figures.....	iv
Tables	vii
Notations and Abbreviations	viii
Table of Contents.....	ix
1.0 Introduction	13
1.1 Project Scope	14
2.0 Physiology	15
2.1 The Heart and Cardiac Cycle	17
2.2 Stroke Volume (Cardiac Output).....	19
2.3 Frank-Starling Mechanism	19
2.4 Effects of Positive Pressure Mechanical Ventilation.....	21
2.5 Blood Pressure Monitoring	22
2.6 Blood Pressure Waveforms.....	22
3.0 Background Literature	25
3.1 Pulse Pressure Variation PPV	25
3.2 Fluid Responsiveness and PPV	26
3.2.1 PPV and Unreliable Grey Zones	27
3.2.2 PPV Performance and Efficacy	28
3.3 PPV Calculation	30
3.3.1 Manual PPV Calculation	30
3.3.2 Automatic PPV Algorithms.....	31
3.4 Other PPV Experimental Algorithm Research.....	32
3.4.1 Time-Domain-Based Algorithms	32

3.4.1 Frequency-Domain-Based Algorithms	33
3.4.2 PPV/SSV Commercial Products	34
4.0 PPV Algorithms.....	35
4.1 Mathematical Steps	35
4.1.1 PPV Equation.....	35
4.1.2 Amplitude modulation	36
4.1.3 Simulation waveforms – Modulated and Simple	37
4.1.4 Time-domain vs Frequency-domain.	39
4.1.5 Integration of the Algorithms in LabView	40
4.2 Novel ‘test’ algorithm	41
4.2.1 Justification for novel ‘test’ algorithm	42
4.3 Aboy Method Steps for Pulse Pressure Estimate	43
4.3.1 Step 1: Beat Minima detection	43
4.3.2 Step 2: Beat Maxima detection.....	43
4.3.3 Step 3: Beat Mean Calculation.....	44
4.3.4 Step 4: Pulse Amplitude Pressure	44
4.3.5 Step 5: Envelope Estimation	44
4.3.6 Step 6: Pulse Amplitude Pressure Estimate	45
4.3.7 Step 7: Pulse Pressure Variation Estimation	46
4.4 Effectiveness of “Aboy” Algorithm with Simulation Data.....	48
5.0 Data Collection Software for Philips Intellivue Monitor	51
5.1 Requirements for Intellivue LabVIEW communication program	52
5.1.1 Design requirements.....	52
5.1.2 Extra software tools required	52
5.1.3 Connectivity to Laptop.....	52
5.1.4 Configuring Network Address and Network Settings	53
5.2 Data Export Interface	53
5.2.1 Supported Protocols	54

5.2.2 Protocol Model	55
5.2.3 Protocol Diagram	56
5.2.4 Selection of Wave and Numerical Data.	58
5.3 Program Output	59
5.3.1 Parsing polled messages	59
5.3.2 Screen layout	60
6.0 Method	61
6.1 Method Summary	61
6.1.1 Measurements	61
6.1.2 Statistical analysis	61
6.1.3 Primary endpoint	61
6.2 Clinical Study	62
6.2.1 Patient selection	62
6.2.2 Data collection	62
6.3 Data Collection and Analysis	63
6.3.1 Dataset Length	63
6.3.2 Correlation Plot	63
6.3.3 Bland-Altman Plot	63
7.0 Results	64
7.1 Clinical Results % <i>PPV</i> _{rec} vs % <i>PPV</i> _{test}	64
7.2 Clinical Results % <i>PPV</i> _{Aboy} vs % <i>PPV</i> _{rec}	65
8.0 Discussion.....	67
8.1 Software Development	67
8.1.1 Data Collection Software Sub-VI	67
8.1.2 Aboy Algorithm Sub-VI	68
8.1.3 Novel ‘Test’ Algorithm	70
8.2 Clinical Results Observations	72
8.3 Other observations and improvements	73

9.0 Conclusion.....	75
Appendix 1. Philips monitoring LabVIEW Documentation	76
Appendix 2 – Aboy Algorithm coding	84
Appendix 3 – Communication with Other Monitors	85
Appendix 4. Cyclic Redundancy Checks used in Philips Intellivue Monitor	92
References	96

1.0 Introduction

Pulse Pressure Variation (PPV) is a calculated dynamic index derived from fluctuations in the blood pressure waveform during mechanical ventilation and gives clinical information related to blood volume for a particular range of values. Maintaining an acceptable blood volume level is particularly important as it effects the hearts Cardiac Output (CO) at all times and is associated with patient recovery or morbidity.

The clinical setting for this project was the Austin Hospital, Melbourne, where Principal Investigator Prof Philip Peyton had observed that for some periods during cardiac rate or rhythm irregularities, also known as cardiac arrhythmias, the prevailing PPV algorithm was displaying unreliable values or not delivering a reading. This PPV algorithm based on original work by Aboy et al. [1] in 2004, had been adopted by Philips Medical Systems for use in its patient monitors, and it had been validated by Cannesson et al. [2] as accurate enough for use within operating theatres. However, Aboy et al. [3] later noted that the algorithm was not able to work in periods of abrupt haemodynamic change, such as during cardiac irregularities.

As with all information displayed on patient monitoring equipment, it is reasonable that these values rely on a biological signal being present. This is because there can be irregularities in signal strength due to loss of organ function, as can be the case for PPV since it is derived from blood pressure, and blood pressure being dependent on the working heart. In the case of PPV, this index is also derived from the increase and decrease of blood pressure induced by positive pressure ventilation from a mechanical ventilator. Therefore, it may be considered that if a pulse pressure exists during heart irregularities then in principle it should be possible to measure the pulse pressure variability. A novel approach to calculating the PPV is required, a more robust method that would work during periods of cardiac arrhythmia.

Where this thesis sits within the larger clinical context is to provide tools to validate newer PPV methods, by first creating a means to communicate with and download patient data from Philips patient monitors during surgery, create a working algorithm based on Aboy et al., and finally attempt a novel PPV algorithm, and assessing its reliability by comparison with work by Aboy et al.

1.1 Project Scope

The following steps outline the scope of works for this project:

1. Develop communication software to access patient data in real-time, using LabVIEW (National Instruments) programming language and Philips Communication Protocol (Philips Medical Systems).
2. Determine the method for collection of the patient data, how it will be stored and analysed, including integrating with LabVIEW software already created.
3. Duplicate the original algorithm of Aboy et al. [1], again using the LabVIEW program as a means of comparison with any future attempts at PPV algorithm improvement. To test the efficacy of the algorithm using simulated and patient data
4. Comparison of a novel 'test' algorithm by clinical study to validate its efficacy with statistical comparisons such as Bland-Altman plots and correlation methods.

2.0 Physiology

During a normal breath, there is a lowering of blood pressure as the lungs inflate, and a rise of blood pressure during deflation; this 'swing' in blood pressure does not usually exceed 5-10 mmHg [4]. When exaggerated, and exceeding 10mmHg during inspiration, this is known as *pulsus paradoxus* and is described as the cardiac pulse disappearing during inspiration and returning during expiration. The term "paradox" was used because the heartbeat was audible at the chest through a stethoscope although there was a quietening of radial pulse pressure (at the wrist) [6].

When first observed in 1872, this became known as Kussmaul's Sign and was used as a guide for possible issues with the patient's cardiac status. One example is pericardial tamponade, where fluid fills the pericardium, the sac around the heart, thus hindering the heart filling during cardiac relaxation, and resulting in the patient having a low blood pressure; pulsus paradox is observed during this interval [5].

However, during some types of surgery, anaesthesia or critical care, a patient is paralysed and not breathing on their own therefore requiring mechanical ventilation. Mechanical inspiration/expiration airway pressures affect the heart and create a different type of blood pressure response. During positive pressure ventilation, the effect is reversed from a normal breath, this time, there is a rise in blood pressure during inflation and a decrease in blood pressure during exhalation. An arterial *Pulse Pressure* (PP) recorded as part of a patient's vital sign observations is shown in Figure 1 below, illustrating the effect of the positive pressure ventilation recorded with a capnograph *Airway Pressure* (AP) on the blood pressure waveform. This phenomenon discovered by Massumi et al., in 1974 [5] was dubbed reversed pulsus paradox. However, more recently, it has been called *Systolic Pressure Variation* (SPV), or, as used in this thesis, *Pulse Pressure Variation* (PPV)[4].

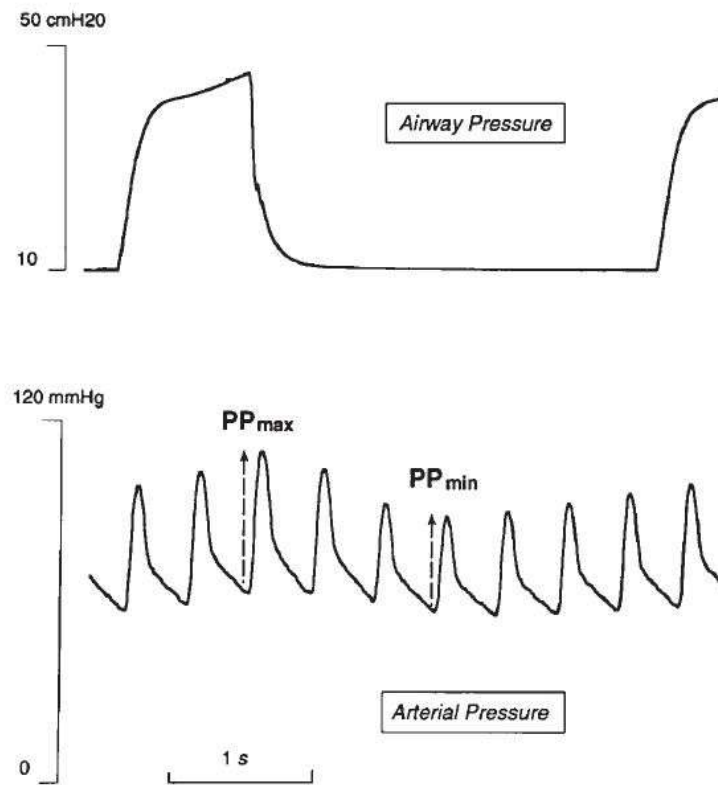


Figure 1. Simultaneous recording of systemic arterial and airway pressure with Pulse Pressure variations [4]

2.1 The Heart and Cardiac Cycle

The heart is an essential part of the haemodynamic system (see Figure 2) and with each stroke of the heart creates pressure Pulse Pressure (PP) and blood flow. The heart is a two-sided pump contained in a single cardiac muscle. The left side pumps freshly oxygenated blood from the lungs to the body, and the right side receives deoxygenated blood back from the body to return to the lungs and thus completing a cardiac cycle.

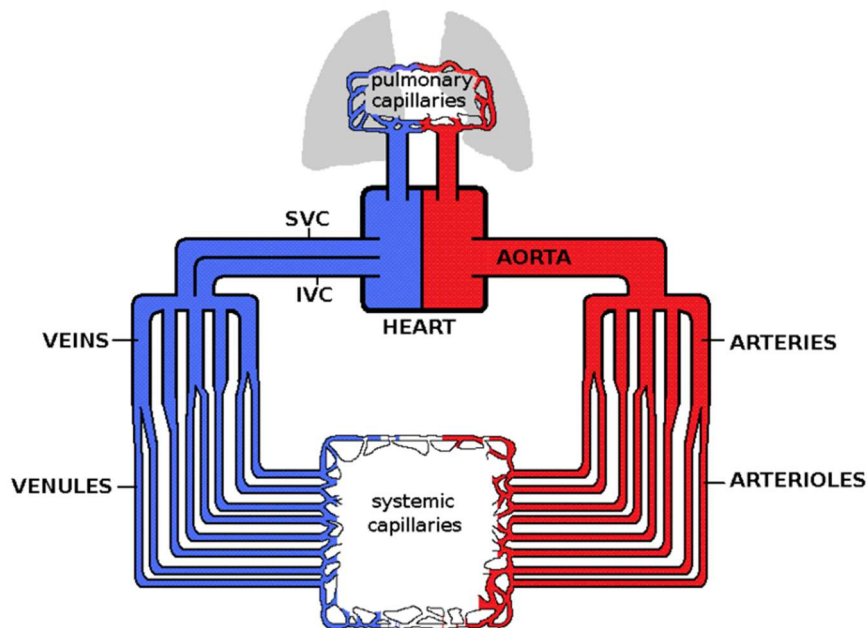


Figure 2. Block diagram of a circulatory system [6]

Like any mechanical pump, the heart has a means of forcing a particular volume out at a required pressure; this is achieved by contraction of the cardiac muscle from top to bottom sections, with one-way valves to stop flow returning. These chambers hold the blood volumes for filling and subsequent ejection. The four chambers are upper *Right Atrium* (RA) and *Left Atrium* (LA) and lower *Right Ventricle* (RV) and *Left Ventricle* (LV). All blood vessels that return blood to the heart from the lungs (pulmonary) or body *Superior Vena Cava* (SVC) and *Inferior Vena Cava* (IVC) are veins, and blood vessels with blood flow exiting from the heart, are called arteries. Heart valves called mitral (RV/RA) and tricuspid (LV/LA) respectively sit between each of the atria/ventricles, and between the heart and the arteries there is another set of heart valves: pulmonary (to the lungs) and left aorta (to the body). The heart is a contractile pump, with contraction (systole) and relaxation (diastole) phases.

See Figure 3 for basic anatomy, where blue vessels symbolise deoxygenated blood flow and red vessels are for oxygenated blood flow paths.

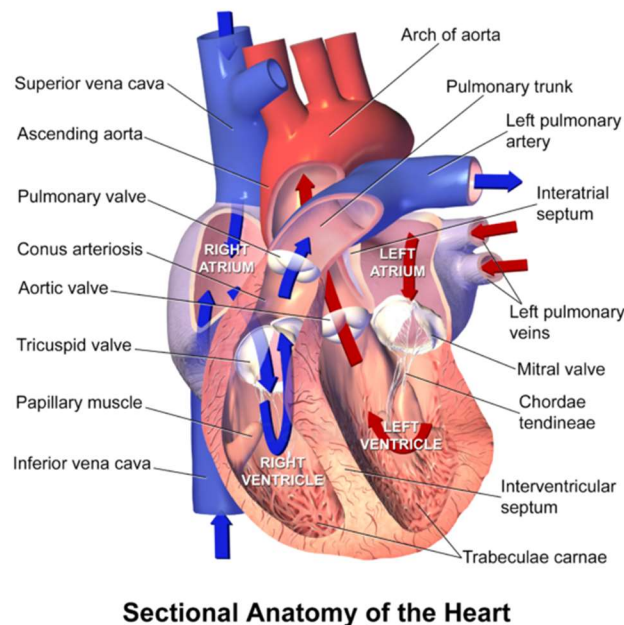


Figure 3. Basic cardiac anatomy anterior view [7]

The cycle starts with a period of low-pressure (or relaxation) called *Diastole*, when filling occurs, and the subsequent high-pressure period of contraction or *Systole*. When the pressure in the ventricles falls below filling pressure in the systemic veins and pulmonary veins, blood fills the ventricles via the atria. About 75% of the blood moves from the atria into the ventricles during the relaxation, or filling phase, but during the contraction of the atria, a further 25% adds to increase the ventricular expansion, before contraction of the ventricles forces blood out of the heart. Valves inhibit blood from returning to preceding chambers; almost all blood that enters the heart is pumped out, although a vital small proportion is required to perfuse the organ itself via the coronary arteries [8].

The body regulates the necessary blood volume such that when exercising, the heart must pump more blood to the body than when resting. This volume difference is regulated in part by the ability of the heart ventricles to expand to meet these requirements, e.g. larger volumes will be ejected because of the ventricle's ability to expand (to a limit) to hold the larger volumes. Therefore because the blood moving towards the body leaves through the aorta and starting from LV, when this aortic pressure meets the resistance from the body and creates the pulse pressure PP, any variations in pulse pressure are known as *Pulse Pressure Variation* or ΔPPV , which originates from left ventricular filling. The cardiac output ejected by the heart per beat (stroke) is known as *stroke volume*.

2.2 Stroke Volume (Cardiac Output)

With each beat/stroke of the heart, the flow of re-oxygenated blood from the lungs via the pulmonary vein and the left atrium is ejected from the left ventricle into the arterial system. This volume of blood is known as the *Stroke Volume*, (SV) or *Left-Ventricular Stroke Volume*, (LVSV). When this is recorded over a period of time (minute), it is known as *Cardiac Output* CO (Litres/minute).

As previously discussed, the body acts as a resistance to the blood flow. Arterial pulse pressure (PP) (the difference between the systolic and the preceding diastolic pressure) is created. This PP is directly proportional to SV and inversely related to the compliance of the arterial system [9]. Therefore, for a given arterial compliance, the amplitude of PP is directly related to the SV. Because of this relationship, the variation in left ventricular stroke volume due to respiratory variation can be the primary determinant of the respiratory variation in pulse pressure.

Systolic pressure is less closely related to stroke volume and arterial compliance because it is also dependent on diastolic pressure and changes in extramural or external pleural (airway) pressure exerted by the lungs on the aorta. What is common, however, is that pressure is related to volume status, and there must be enough blood in the body to supply oxygen to tissues and organs. In clinical practice, a common clinical question is whether the use of administered fluids will improve blood flow or haemodynamic output of the heart to the body [10].

2.3 Frank-Starling Mechanism

The mechanism by which the heart can adapt to changing blood volume is known as the Frank-Starling Mechanism. The heart, or more precisely, the ventricle, can expand or stretch during relaxation phase (diastole) within a specific range, and this relates to the amount of fluid returned to the heart from the veins. SV will increase if the ventricular preload volume entering the heart increases; this higher volume will create a greater contractile force and increase Cardiac Output (CO). Therefore, with the administration of more fluid, or volume expansion, the patient's cardiac output should increase.

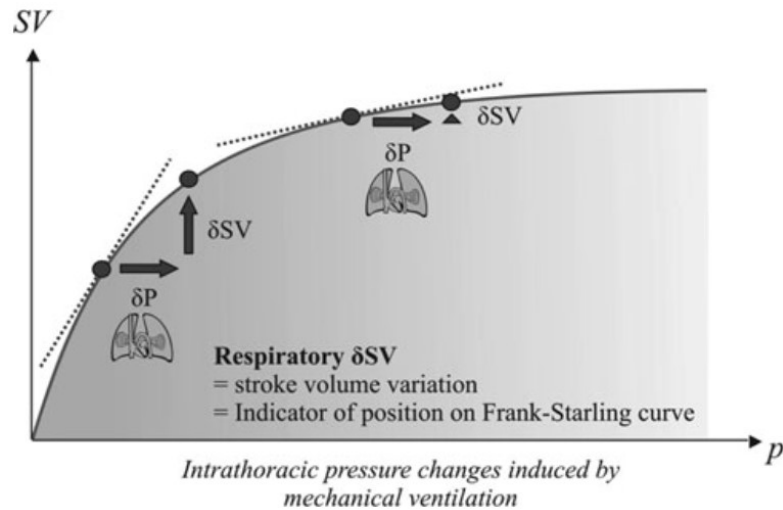


Figure 4. Stroke Volume Vs End-diastolic filling pressure induced by mechanical ventilation[11]

Figure 4 above shows the relationship between increasing the filling pressure in the ventricle and the increase in stroke volume. There is a range (steep curve) in which giving fluid and increasing filling pressure will have a more significant effect on the stroke volume, whereas by administering fluid when the pressure is higher (plateau area), the benefit to stroke volume will be relatively small.

This concept can be more complicated though because ventricular preload, ventricular volume and ventricular filling-pressure are in part related to ventricular compliance. For example, in a sick patient with a less-compliant or a hypertrophic left ventricle, there will be a smaller left ventricular end-diastolic volume and elevation of left ventricular filling pressure due to a diastolic dysfunction[11]. Figure 5 can be used to show the lower stroke volumes occurring when a ventricle is failing.

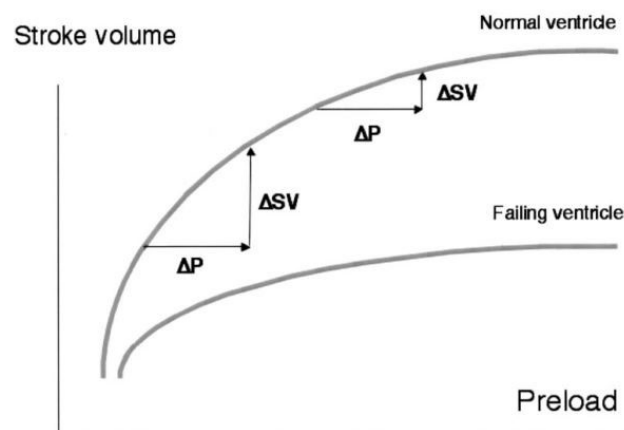


Figure 5. Ventricular preload relating to stroke volume including failing ventricle [10]

2.4 Effects of Positive Pressure Mechanical Ventilation

Controlled positive pressure ventilation is a necessary component of anaesthesia for major surgery and critical care. The effects of the positive mechanical pressure exerted into the lungs can be regarded as both good and detrimental. With mechanical ventilation, airway pressures, and therefore pleural pressures, affect the blood flow of major vessels surrounding the heart [12], the vena cava, pulmonary artery and aorta. It also affects the systolic and diastolic pressures and hence the pulse pressure. Stroke Volumes change depending on the position on the Frank-Starling curve, and volume stasis. Figure 6 shows other effects that could be detrimental to pulmonary and cardiac haemodynamics.

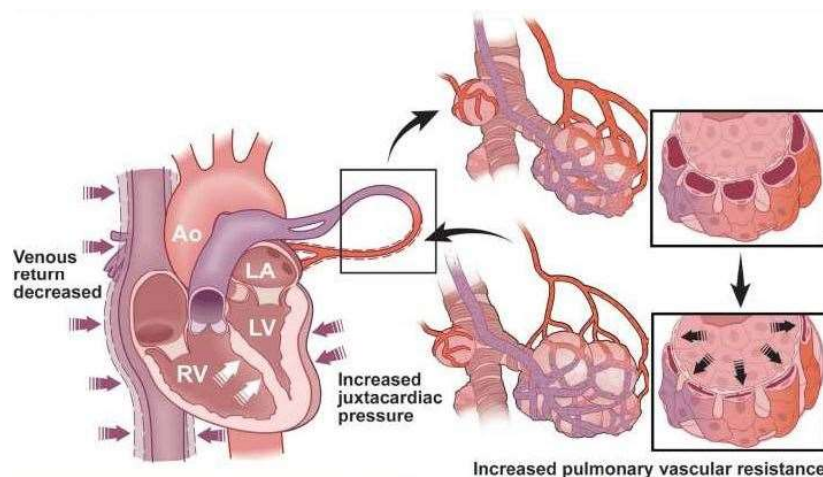


Figure 6. Effects of positive pressure ventilation on the heart[13]

An unfavourable effect of positive mechanical airway pressure could be a diminishing venous return due to external pressure on the inferior vena cava that also affects its calibre, increased right ventricular dilation with septal shift (shown in white arrows in Figure 6), with the result of elevation on the right ventricular afterload and decreased left ventricular filling and cardiac output.

However, as stated earlier, the benefits of mechanical ventilation far outweigh these factors in a majority of cases, and since the function of a steady and predictable machine such as a mechanical ventilator is a 'constant', it provides clinicians with static inputs to a variable human system. Pulse Pressure Variation (PPV) is one such derivative of the effects of the mechanical system that is a useful indicator to predict the fluid responsiveness of the patient.

2.5 Blood Pressure Monitoring

Arterial blood pressure monitoring is routinely performed by the insertion of a catheter (or 'arterial line') into a peripheral artery Figure 7. The catheter has a pressure transducer attached in-line with a tap for zeroing the pressure sensor. A secondary benefit of an arterial line is the ability for blood gas monitoring, and other laboratory tests to be performed.

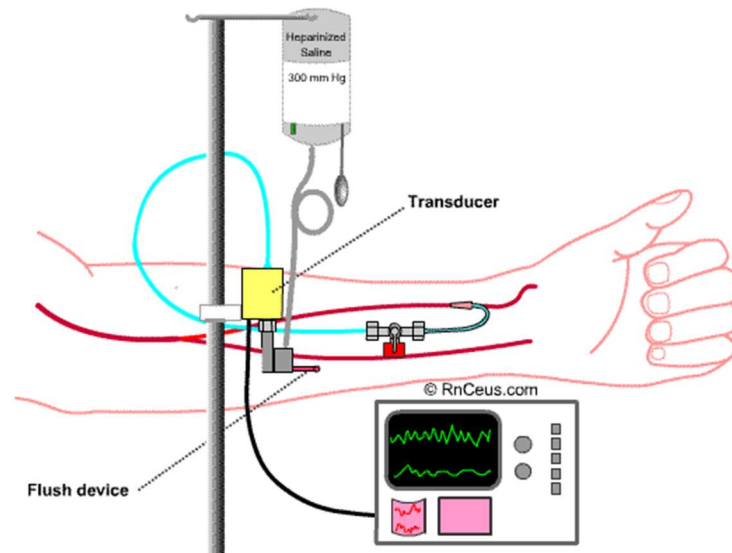


Figure 7. Arterial line placement[14]

2.6 Blood Pressure Waveforms

Understandably, it is important that the signal provides a good waveform. When recorded on the patient monitor, the waveform appears as shown in Figure 8. The dicrotic notch marks the closure of the aortic valve after injection of blood into the arterial system, and delineates between the ejection phase of high pressure during systole and the drop in arterial pressure as the blood moves passively along its pressure gradient peripherally down the arterial tree during diastole.

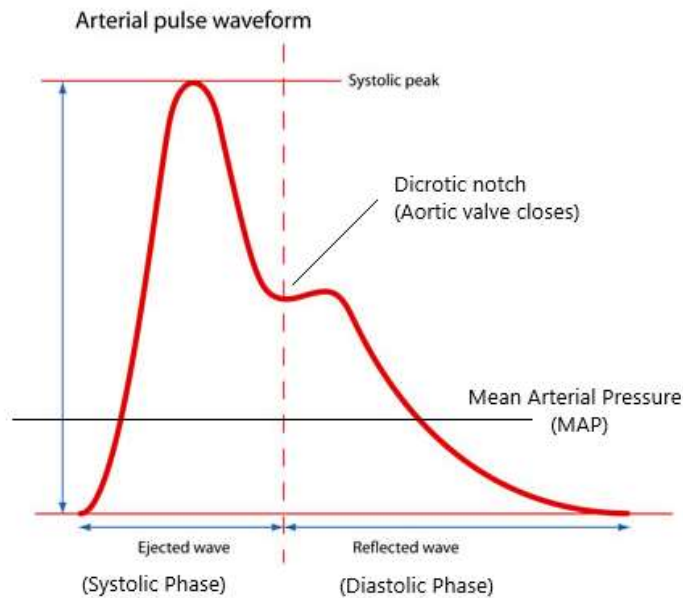


Figure 8. Arterial blood pressure waveform Systolic and Diastolic phases (adapted from [15])

PPV signals rely on good arterial blood pressure signals. Placement and maintenance of the sensor are important as the signal waveform can be overdamped or underdamped; ideally, the Dicrotic notch should be visible. Enough damping is needed so that underdamping does not occur, where excessive resonance (ringing) is displayed: this causes an overestimation of the systolic pressures and an underestimation of the diastolic pressures and is characterised by high initial spike, see Figure 9. below. Overdamping results in false low-systolic pressure, but usually accurate mean pressure, and may be due to clot or fibrin build-up in the catheter tip. In both cases, the *Mean Arterial Pressure* MAP is relatively accurate (see Table 1: recorded patient data example waveforms).

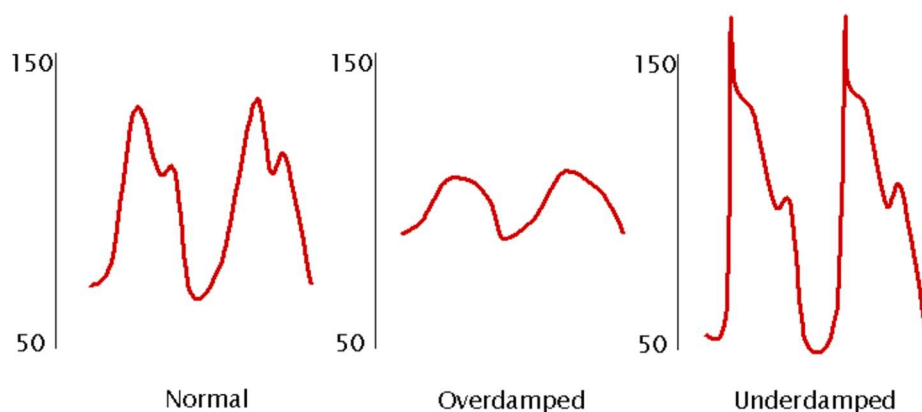


Figure 9. ABP waveforms with variation due to damping of the system [16]

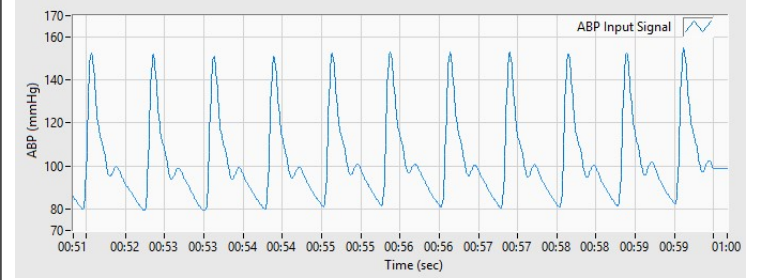
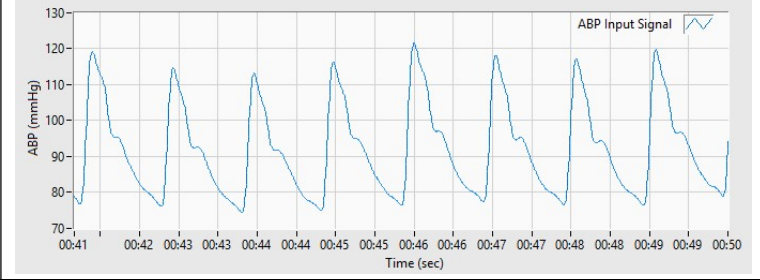
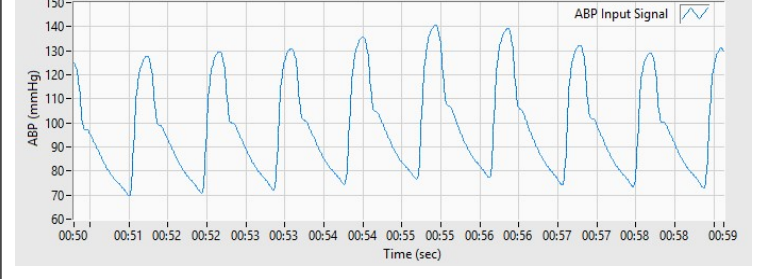
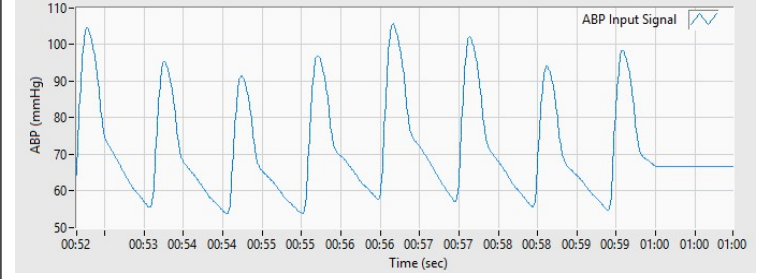
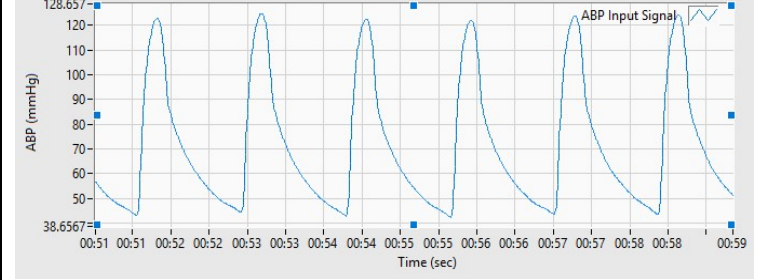
High-frequency components, dicrotic notch sharp (possible underdamped)	 <p>ABP (mmHg)</p> <p>Time (sec)</p> <p>ABP Input Signal</p>
High-frequency components, dicrotic notch evident	 <p>ABP (mmHg)</p> <p>Time (sec)</p> <p>ABP Input Signal</p>
Less high-frequency components, dicrotic notch less-evident	 <p>ABP (mmHg)</p> <p>Time (sec)</p> <p>ABP Input Signal</p>
Less high-frequency components, dicrotic notch not displayed	 <p>ABP (mmHg)</p> <p>Time (sec)</p> <p>ABP Input Signal</p>
Less high-frequency components, dicrotic notch not displayed. (overdamped)	 <p>ABP (mmHg)</p> <p>Time (sec)</p> <p>ABP Input Signal</p>

Table 1. Recorded patient data waveforms from this study

3.0 Background Literature

This chapter aims to increase an understanding of the PPV index and show how clinicians can use this to predict fluid responsiveness: for the benefit of a particular group of mechanically ventilated patients. Given that the Aboy algorithm is the primary comparison method for this thesis, the background here will focus mostly on this method of PPV calculation, however a review of the literature will show predicting fluid responsiveness is performed by other means.

To begin, PPV and fluid responsiveness will be defined and the original method for calculation shown. PPV's efficacy through the years as a predictor of blood volume responsiveness will be explored, and this will provide an understanding as to the limitations of PPV. Given that there are other commercial technologies and methods available to similarly predict fluid responsiveness, these will be shown for comparison. Finally, as the scope of this thesis is to explore potential improvement of the existing PPV algorithm, other novel algorithms will be examined with particular focus on those that attempt to work during abrupt haemodynamic change.

3.1 Pulse Pressure Variation PPV

PPV is a 'dynamic' index of blood volume status, used clinically to assess the volume status of ventilated patients. It is considered superior to traditional 'static' indices such as central venous pressure CVP or left ventricular end-diastolic or 'wedge' pressure LVEDP measured using a balloon-tipped pulmonary artery catheter [11, 17]: it has been shown to predict fluid responsiveness [18, 19].

Pulse pressure variation $\Delta PPV(\%)$ is an index first considered by Micard et al. [4], derived from the difference between the maximum pulse pressure PP_{max} and PP_{min} (see Figure 10) calculated by equation (1) [4].

$$\Delta PPV(\%) = \frac{PP_{max} - PP_{min}}{\frac{PP_{max} + PP_{min}}{2}} * 100 \quad (1)$$

Pulse Pressure is calculated on a beat-to-beat basis as the difference between systolic and diastolic pressure. Maximal Pulse Pressure (PP_{max}) and minimal (PP_{min}) values are determined over a single respiratory cycle, where $\Delta PPV(\%)$ is expressed as a percentage [4], and originally the standard method to identify the start of each breath was to record airway pressure at the same time as per Figure 1 and find PP maxima and minima for that period.

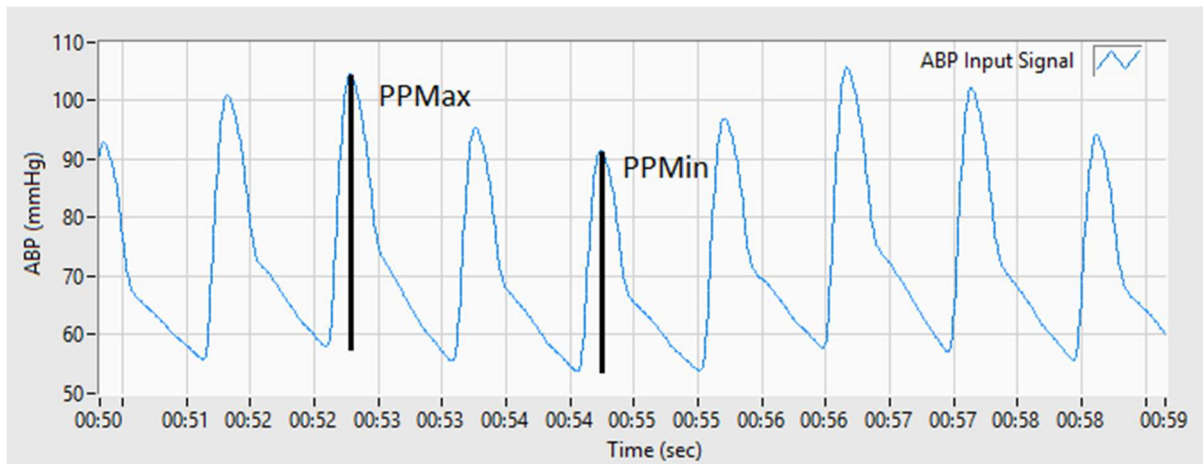


Figure 10. PP_{max} and PP_{min} due to the effect of a mechanical ventilator

As part of this original study, Micard et al. found a correlation between the patients Cardiac Index (CI) (or Cardiac Output vs Body Size), and a decrease in ΔPPV after a fluid bolus was administered to patients whilst mechanically ventilated: Micard concluded that ΔPPV may be useful for monitoring the haemodynamic effects of fluid loading.

3.2 Fluid Responsiveness and PPV

Fluid responsiveness, a measured response to intravenous fluid loading, reflects the hemodynamic status of the patient and their hemodynamic response to administered fluids. PPV is commonly used for this purpose, as both a monitor and a predictor of fluid responsiveness.

A PPV within a specific range [10, 19-22] helps to predict to what degree a patient's stroke volume (or cardiac output) can increase with an increase in fluid loading. Moreover, the heart is capable of filling or having a preload (filling pressure) which relates to the degree of tension in the heart tissue. However, continually increasing the blood pressure by the addition of fluid will not continually increase the cardiac output as described by the Frank-Starling mechanism (see Figure 4).

Michard et al [21] was the first to use the term *responder* in relation to PPV where 50% of all treated patients responded to an intravenous bolus with cardiac output benefit. Similarly in their study of 413 patients undergoing surgery, Cannesson et al [23]. found that only roughly 50% of treated patients will respond to plasma volume expansion in terms of a measured increase in cardiac output of 15% or greater. Fluid administration in the absence of demonstrated fluid responsiveness may result in excessive fluid loading and become dangerous, leading to heart failure and interstitial tissue oedema [24]. But as intravenous fluid administration is the first intervention to correct hemodynamic instability in critically ill patients, predicting fluid responsiveness in advance is advantageous in intensive care medicine to ensure the patient's survival and recovery. Given also that PPV calculations

are performed in real-time, any changes in PPV can be observed at some time after the administration of fluid and provide a practical feedback loop for clinicians managing ventilated patients.

To keep the patient in a normal physiological range is essential, and maintaining or being able to increase cardiac output is important, however since there is no measurement for cardiac filling or any way of quickly determining this, the PPV index is able to provide a method to measure fluid responsiveness [10]. Furthermore, getting fluid management right is also significant because it has a known influence on the patient both at the time of surgery and later during recovery and the postoperative period [25].

3.2.1 PPV and Unreliable Grey Zones

The effectiveness of PPV to adequately determine *responders* or *non-responders* came into question with the Cannesson et al. 2011 [23] study when it was discovered that there was an intermediate range of PPV values (or “grey zone”) for which the index is unable to predict fluid responsiveness. Patients were grouped as either responders or non-responders based on whether administered fluids provided enough volume expansion such that their Cardiac Output would increase by >15%. Table 2 below shows cases where patients respond to increase in volume relating to %PPV. Patients that responded had PPV measurements between 10-22% prior to fluid administration, and non-responding patients PPV between 4-12%. The overlap between the two groups created the “grey zone”.

	Responders to Volume Expansion (51% patients)	Non-Responders to Volume Expansion (49% patients)
PPV (%)	16 ± 6%	8±4%

Table 2. Showing mean PPV% ± SD for Responders and Non-Responders where fluid responsiveness is > 15% Cardiac Output after volume expansion[23]

The grey zone (shown in Figure 11 below) has been shown to represent approximately 25% of patients who require further management tools, because the response to fluid is not statistically predictable. These findings have been obtained in patients ventilated with tidal volumes of at least 7-8 mL/kg body weight. Smaller tidal volumes will be less influential in generating reliable predictions of fluid responsiveness. Optimal cut-offs for the grey zone are also dependent on the type of controls, whether tight vs liberal fluid. Nevertheless, in general, the higher the %PPV value, the greater the predictability that fluid administration will increase cardiac output. The limits of the grey zone for PPV as a predictor of fluid responsiveness reported were 9 – 13%.

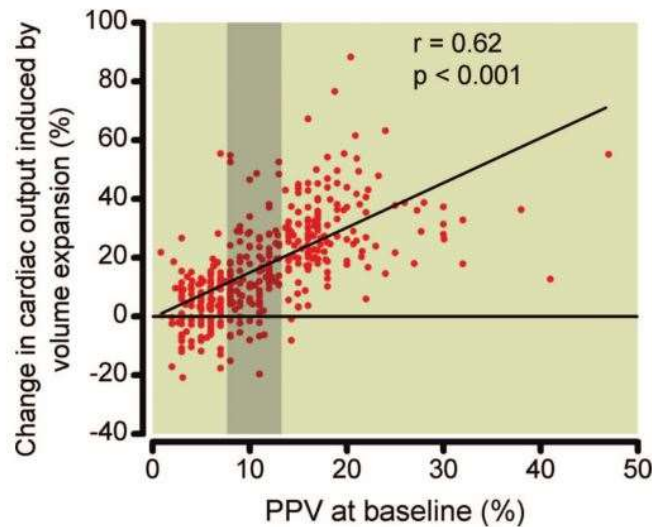


Figure 11. Relationship between PPV before Volume Expansion and Percentages CO induced. Grey zone 9-13% shows the limits of uncertainty[23]

3.2.2 PPV Performance and Efficacy

After the initial promise that PPV would be a useful tool to measure and predict fluid responsiveness, the discovery of the “grey zone” considerably reduced the patient population that could benefit from this index. However, multiple other factors had become understood since its inception related to PPVs inability to function correctly: these related to anything that may interfere with any of the physiological inputs. The first relates to pleural pressure (the pressure induced by the heart from the filling of the lungs); the second the heart’s ability to create and maintain blood pressure.

3.2.2.1 Effects of Pleural Pressure

Tidal volume (the amount of gas delivered into the patient per breath, approx. 8 ml/Kg body weight [26]) is required to create pleural pressures effective for pressure transfer of the lungs onto the heart. PPV measurements can be effected even for patients that are fluid responsive [27], for example with reduced tidal volumes of 6 ml/Kg. Other factors that affect the PPV measurement include Acute Respiratory Distress Syndrome (or ARDS) [28], low lung compliance [29], spontaneous breathing [4] and other factors such as an open chest during an operation [30]. At present it is also rare for ventilation to be mandatory, and many other ventilation modes are available in which the patient may be awake (in this case PPV is not a viable option).

3.2.2.2 Effects of Cardiac Arrhythmias

The ability for the heart to pump effectively will influence the suitability of PPV. Mechanical issues with the heart, including right ventricular dysfunction, will contribute to poor PPV performance [31]: cardiac arrhythmias include extrasystoles (extra beats) that can be difficult to detect in patients with tachycardia [32], atrial fibrillation or cardiac ectopy rule out continuous and automatic monitoring

systems [10]. In general, candidates for PPV should have few cardiac arrhythmias, otherwise detection of beats will be difficult for the particular algorithm to work.

3.2.2.3 Other factors

Increasing intra-abdominal pressure can affect PPV measurement, the added pressure can raise the threshold values discriminating between responders and non-responders [33]. Also, if the ratio of heart rate/respiratory rate is too low (<3.6), then PPV is difficult to determine, as the number of beats during the respiratory cycle would be insufficient to allow stroke volume variation to occur, and decrease the predictive value of fluid responsiveness [34].

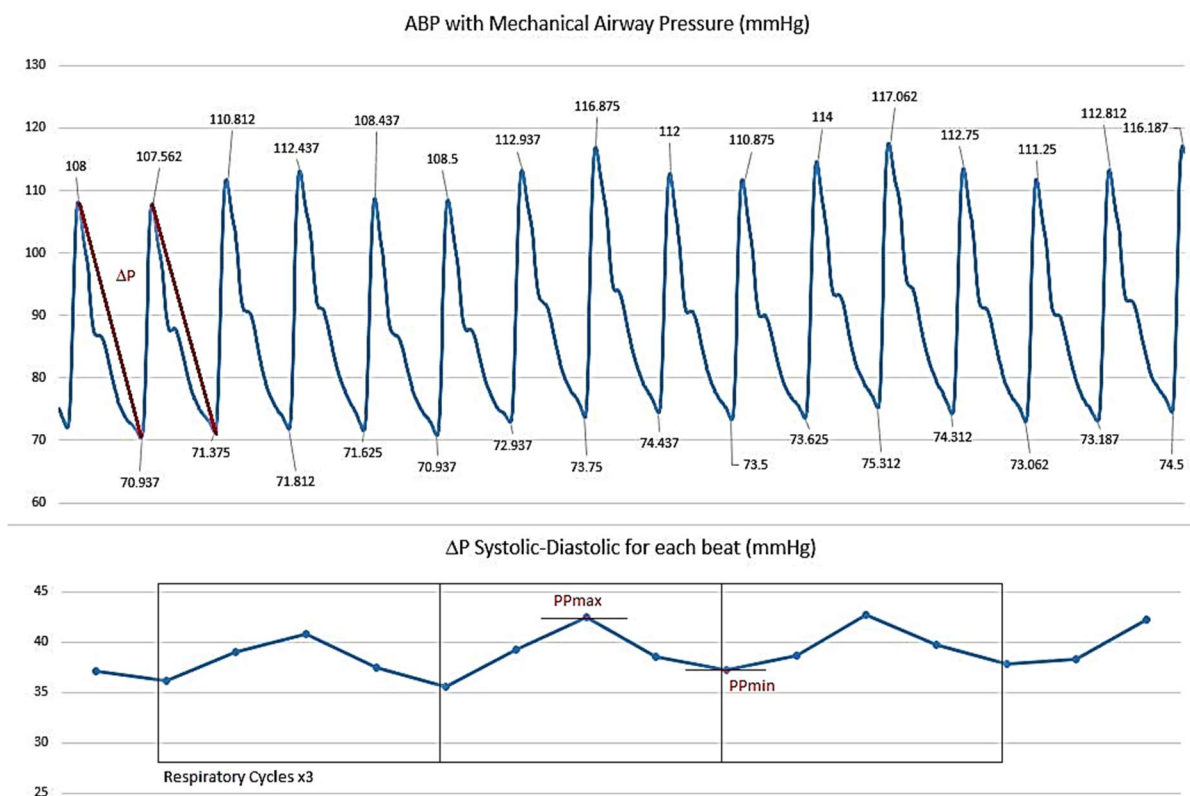
Therefore, for each additional factor, PPV determination and its ability to successfully measure and predict fluid responsiveness reduces. In an ICU setting, some studies have suggested that unrestricted PPV use was as low as 17%, but this may vary depending on the type of patient: 39% for patients with sepsis and 53% with patients with trauma [31].

3.3 PPV Calculation

Initially, PPV calculations required analogue data to be collected from the patient and calculations performed offline, and although there was some commercial proprietary software, these were not available to researchers.

3.3.1 Manual PPV Calculation

Figure 12 below shows the iterative means of manually determining PPV from real patient data from the patient monitor during each respiratory cycle. This is still the accepted gold standard as it is determined precisely with each iteration and is known as ΔPPV_{man} . It is noted that the ΔPPV_{man} is a difference between PP maxima and minima *over a single respiratory cycle*. $PPV_{man}(\%)$ can swing considerably between each breath and as shown in Figure 12 this swing from 12% to 18% and back to 11% would also give quite an erratic trace. However, as will be shown later, median filters are used to smooth out the PPV value over several respiratory cycles.



$$PPV(\%) = \frac{PPmax - PPmin}{\frac{PPmax + PPmin}{2}} * 100 \quad (1)$$

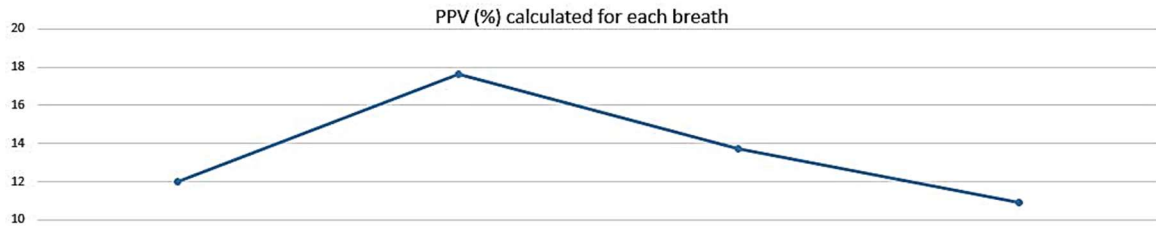


Figure 12. Gold Standard PPV_{man} (%) calculated using data collected from Philips Monitor

3.3.2 Automatic PPV Algorithms

The original non-proprietary algorithm [35] created by Aboy et al. (in 2004) that could calculate the PPV reliably took only the arterial pressure wave as an input. The algorithm was made up from various linear and non-linear (rank-order) filters, decision logic, and peak detection methods. Many recursive steps are required to ensure the wave was ready for PPV calculation because although only the PP Maximum and PP Minimum for each respiratory cycle were required as inputs to the equation (1), there are multiple peaks of the blood pressure waveform (Figure 13). The diastolic (or low pressure) and a systolic (or high pressure) are only two of the 'peaks', and with the addition of the respiratory pressure, the sample wave can be more complex.

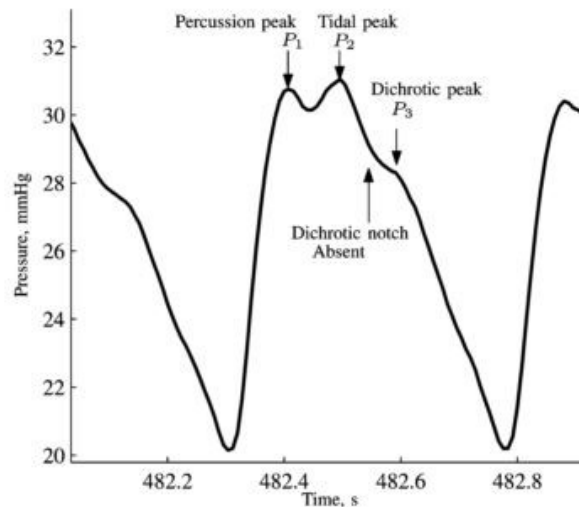


Figure 13. The complexity of the blood pressure waveform[35]

This algorithm had a positive predictive value of 98.43% on a dataset of 42,539 beats, had compared favourably to a gold standard for PPV measurement [2], and after publication was used by in Philips Intellivue MP70 monitors (Philips Medical Systems).

3.4 Other PPV Experimental Algorithm Research

This section describes research to improve the PPV algorithm. Some work (in the time-domain) concerns better detection of beats, envelopes, and isolation of respiratory and cardiac amplitudes of the blood pressure signal; in the frequency-domain, spectral components of blood pressure signals have been used. Both time domain and frequency domain methods are employed in the case of fast haemodynamic changes such as blood loss and other work applied in particular to abrupt heart arrhythmias, performed by predictive statistical modelling or by removal of detrimental beats.

Although non-proprietary algorithms developed to improve PPV calculations can be separated into time-domain-based algorithms and frequency-domain-based algorithms, it should be noted that frequency domain methods are often used in programming even in time-domain-based work to determine the location of heart and respiratory rates, so that filters will have a cut-off required to suppress unwanted signals. Discussion follows regarding algorithm attempts, and a summary of the progression of research is shown in Table 3.

3.4.1 Time-Domain-Based Algorithms

Since development, the Aboy method has worked reliably but is sensitive to abrupt irregularities in heart rate [2, 36], failing to deliver a measurement for a significant period. To address these shortcomings, in 2005 Aboy et al. [35] released improvements to the peak detection algorithm as part of an enhanced PPV algorithm 2009 [3], showing its ability to cope with fast blood loss: performance proved better than the PiCCO (Pulsion Medical System), a commercially available monitor typically used for comparison during experimental research.

After the first non-commercial version by Aboy et al., others made attempts to improve performance, or find a surrogate method for PPV. The method of Austin et al. [37] did not require beat detection but used a non-linear filter after removing the signal mean to find the upper and lower envelopes of the Pulse Pressure waveform. This approximated the envelope by determining when the blood pressure waveform switched from systolic to diastolic periods.

McNames et al. [38] used Extended Kalman Filters to statistically model the complete respiratory and cardiac states including PPV. Estimation and tracking of the PPV index were based on knowledge of the previous state, predicting the next state, measuring what had occurred, and updating current state. In this way the artefacts or signal loss can be predicted (and skipped), inserted or isolated for recording. Similarly Kim et al. [39] uses Monte Carlo (a state-space model) estimation, that automatically tracks and predicts PPV based on statistical estimates of the system, maximising the probability of replacing a missing sequence (beats) given previous sequence data. An estimate of the

missing beat can be reinserted, minimizing failure of the PPV algorithm. Cannesson et al. [40] successfully dealt with extrasystoles (extra beats) in a porcine model, by detecting and rejecting abnormal beats, followed by interpolation and restoration of missing beats.

3.4.1 Frequency-Domain-Based Algorithms

The work of Thieles et al. [41] is an example of a frequency-domain-based algorithm. However, it is not focused on PPV but correlation between PPV and a spectral peak ratio at HR and RR frequencies was demonstrated. Finally, Soltesz [42] used a Lomb-Scargle spectral density estimator with least squares spectral analysis. This method can work on non-uniformly sampled data and creates a spectral power density estimate at isolated frequencies in the sample. The upper and lower envelopes are at non-uniform frequencies and therefore the Lomb-Scargle method estimates systolic and diastolic peaks.

Algorithm Specific Factors	Primary comparison	Notes/Performance	Reference (Year)
Time -domain-based algorithms			
Automatic detection algorithm Kernel Smoothing Rank-order filters Median Filters	manual annotation	Original method, Validated Cannesson et al. 2008 [2]	Aboy et al. 2004 [1] Aboy et al. 2005 [35]
Non-linear technique envelope	manual annotation, PiCCO	Better than PiCCO during periods of blood loss	Austin et al. 2006 [37]
Statistical Modelling Extended Kalman Filter	manual annotation, PiCCO	Better than PiCCO during periods of blood loss	McNames et al.2008 [38]
Model based prediction	manual annotation, PiCCO	Discards PPV measurements if outside predicted model Better than PiCCO during periods of blood loss	Aboy et al. 2009 [3]
Statistical Modelling Asymmetrical estimation	Previous algorithms	Better PPV estimation of upper and lower Blood pressure waveform	McNames et al. 2011 [38]
Detection and rejection of abnormal beats	Previous algorithms Flotrack	Interpolation and restoration of missing beats	Cannesson et al. 2012 [40]
Sequential Monte Carlo method Statistical State-Space Model	manual annotation	Maximizes the probability of a missing sequence given previous data	Kim et al. 2013 Kim et al. 2016
Frequency-based-domain algorithms			
Frequency-domain analysis Spectral Peak Ratio	Time-domain analysis (many previous methods)	Comparable to time-based methods, PPV calculation not site specific	Theile et al. 2012 [41]
Lomb-Scargle Spectral Density Estimator Least Squares method	Previous data-set and previous methods	Non-uniform sampling computes spectral power density (PSD) estimates at isolated frequencies, rather than over frequency intervals	Soltesz K. 2018

Table 3. Summarising different algorithm/methods

3.4.2 PPV/SSV Commercial Products

Pulse Pressure Variation calculated using the signal from a blood pressure transducer is just one of the methods used to assist clinicians' haemodynamic monitoring of patients. Commercial products exist that can approximate PPV using non-invasive techniques or other parameters such as *Stroke Volume Variation* SVV and *Pulse Contour Cardiac Output* PiCCO methods to provide haemodynamic monitoring in ICU or during surgery. Table 4 below summarises commercially available products.

There are other “novel algorithms” that are worth mentioning: these devices or methods have proprietary software and therefore the algorithm is not known, but they can still approximate PPV. Non-invasive methods, evaluated in [43, 44] include regulating blood flow in a finger by a volume clamp method, where a pump regulates air into a small finger cuff in order to keep blood flow constant by removing the pulsatile effect of the blood pressure. The blood pressure pulse is approximated by the amount of air pressure regulation required and a PPV or SSV estimate is calculated from the waveform. Another method evaluated here in [45-47] uses the actual display of a patient monitor to access the arterial blood pressure waveform, by taking a photo snapshot and using a mobile phone application to convert the image into digital values so the PPV can be estimated.

Method/Algorithm	Notes	Manufacturer	Model
Systolic and Diastolic Respiratory induced peaks/Aboy et al.	Invasive ABP measurement for PPV calculation	Philips	Intellivue PPV
Volume clamp method/proprietary	Non-invasive finger cuff for SSV calculation	Edwards	Nexfin
Volume clamp method Volume clamp method/proprietary	Non-invasive finger cuff for PPV calculation	Drager	CNAP
Thermodilution Pulse contour method/proprietary	Invasive Cardiac Output and PPV, often used as a comparative monitor for research	Pulsion Medical Systems	PiCCO
Systolic respiratory induced peaks/proprietary	Invasive ABP measurement for SSV calculations	Edwards Lifesciences	Flotrack
Unsure of method/proprietary	Non-invasive - mobile application that takes snapshot of patient monitor for PPV calculation	Galenic App	Capstesia

Table 4. Manufacturer-specific technologies and methods

4.0 PPV Algorithms

This section describes the basis for the novel ‘test’ algorithm and describes Aboy et al. 2004 [1] algorithm replicated for this thesis. Included in this chapter will be exposition of the mathematical processes, signal processing, programming steps, generation of simulated data, and comparison methods used with patient data.

4.1 Mathematical Steps

At each stage of the algorithm, an understanding of the signal processing is required; this will assist in the assessment of results and give a better understanding of how an estimate of PPV (%) is achieved.

4.1.1 PPV Equation

As previously described the PPV is calculated over a single respiratory cycle (Figure 14)

$$PPV(\%) = \frac{PP_{max} - PP_{min}}{\frac{PP_{max} + PP_{min}}{2}} * 100 \quad (1)$$

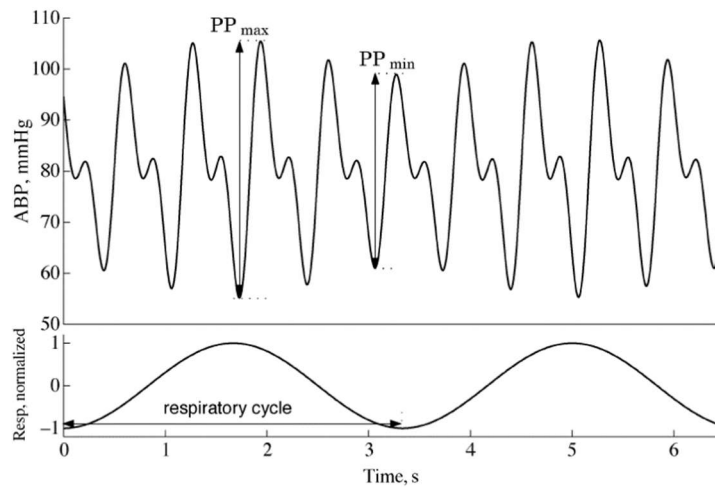


Figure 14. Simulated ABP waveform that shows a pressure amplitude change with each simulated respiratory cycle resulting in PPmax and PPmin[1]

4.1.2 Amplitude modulation

The Pulse Pressure PP component of an ABP waveform (Figure 14) closely resembles that of amplitude modulation techniques as used in broadcast radio. This technique uses a high frequency (AC) “carrier” waveform with a lower frequency “signal” (AM) to modulate the waveform.

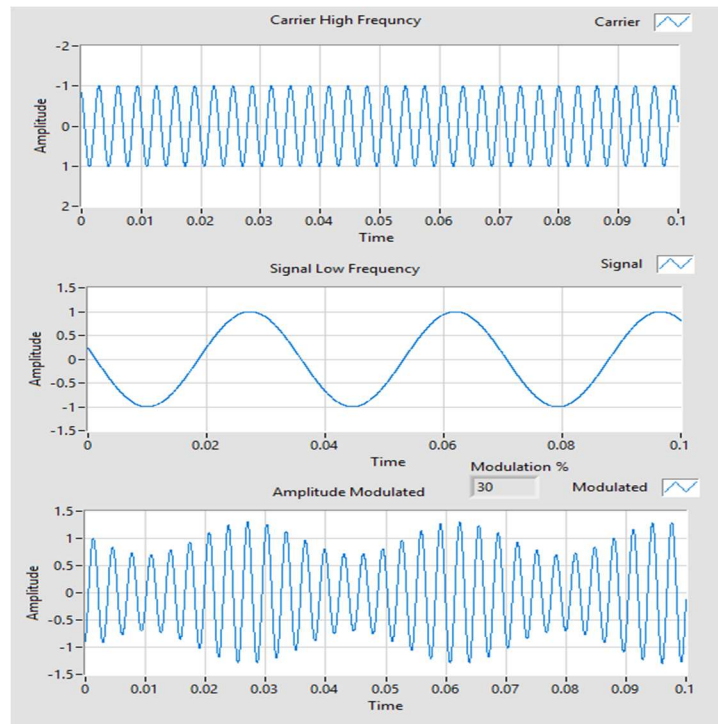


Figure 15. Simple amplitude modulated signal made of two sinusoidal signals.

Figure 15 above shows amplitude modulation in the time-domain, this is represented as a waveform, but in the frequency-domain spectrum Figure 16, the AM signal is represented by sidebands, the addition and subtraction of the AM modulation frequency with the carrier frequency.

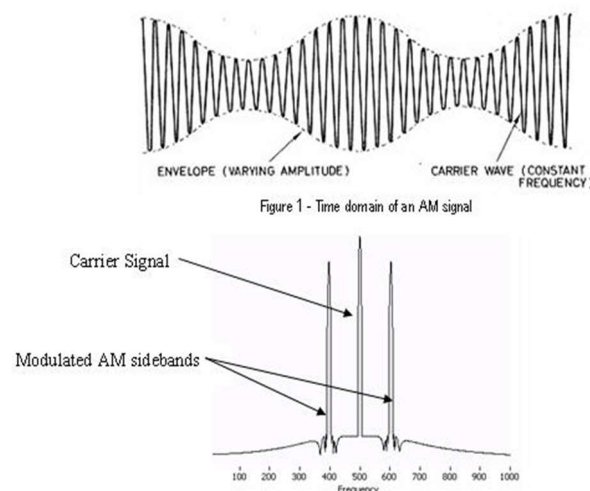


Figure 16. Amplitude modulation represented in the frequency-domain[48]

The amount of modulation (m) that can occur on a waveform is known as the Modulation Index and expressed by a percentage where 100% modulated ($m=1$) infers that the carrier waveform is fully utilised, at 50% ($m=0.5$) where half of the waveform is used. See figure 17.

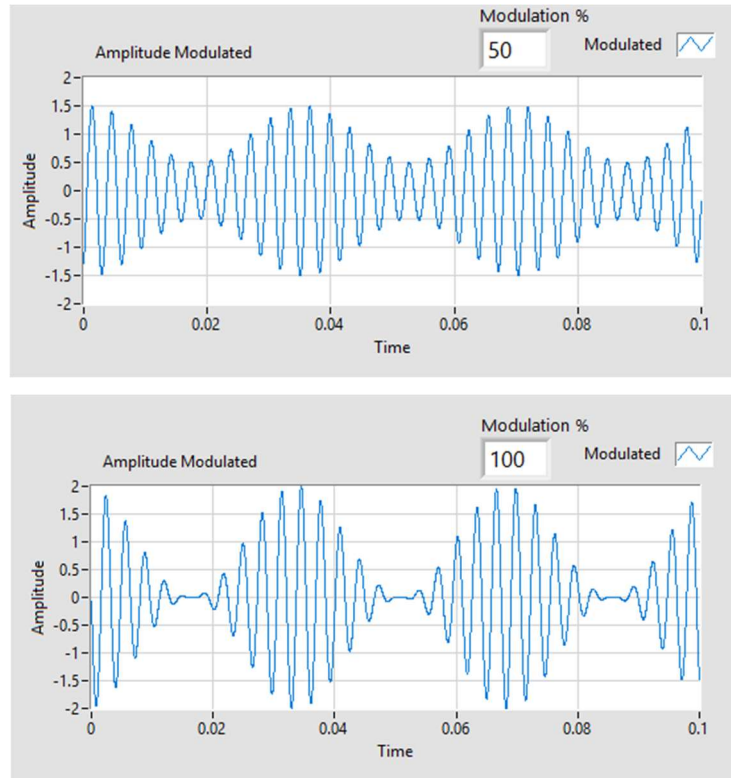


Figure 17. Differences in Modulation of 50 to 100%

Aboy et al. realised that ΔPP or the change in ABP amplitude was similar to amplitude modulation and that ΔPP could, therefore, be an estimation of the modulation index.

4.1.3 Simulation waveforms – Modulated and Simple

PPV Simulated data can be modelled using equation (2):

$$p(t) = u_p + [1 + ar_n(t)] \cdot [\alpha \cos 2\pi f_c t + \beta \cos(4\pi f_c t + \theta_c)] \quad (2)$$

$$r_n(t) = \cos(2\pi f_r t + \theta) \quad (3)$$

where $p(t)$ is the ABP waveform, u_p is the mean ABP pressure, a is the amplitude modulation, $r_n(t)$, equation (3), is the normalised respiratory frequency, and $c(t) = \alpha \cos 2\pi f_c t + \beta \cos(4\pi f_c t + \theta_c)$ are the first two harmonics of the ABP signal. A synthesized waveform created using LabVIEW is shown in Figure 18 below and will be used as a test.

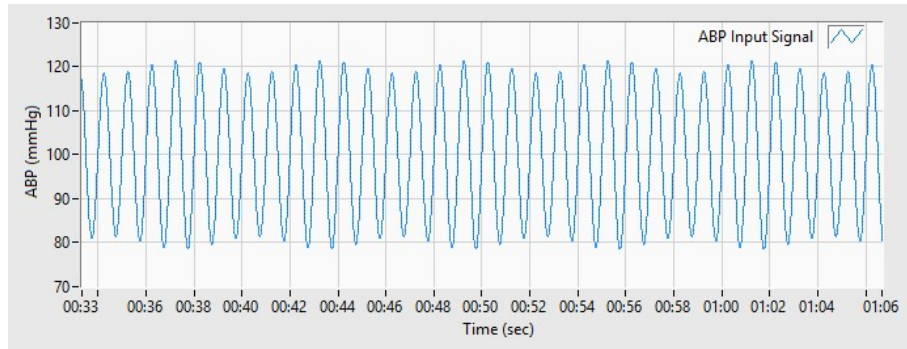


Figure 18. Simulated 'Modulated' waveform, Systolic/Diastolic 120/80 mmHg with PPV 15%

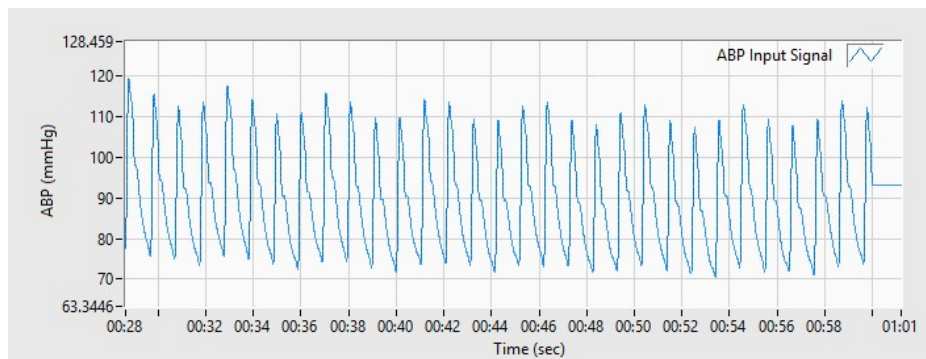


Figure 19. Patient Data ABP Waveform, Systolic/Diastolic peaks changing with Respiration

As a comparison, Figure 19 is patient data (also see Table 1); what is noticeable is that not only does it appear to have more modulation on top of the waveform than the bottom, but the whole waveform amplitude rises and falls at the same time, and therefore although "modulated", the systolic/diastolic amplitudes also moved in the same direction with the respiratory pressure wave. Thus, a simulated 'simple' waveform was also created by the addition of two sinusoidal waveforms as shown in Figure 20. In classical terms, there is zero $\% \Delta PP$, because pulse pressure amplitude does not change $PP_{max} - PP_{min} = 0$; however, the relative amplitudes do change. This type of unmodulated waveform, however, was chosen by the Lead Investigator because it is more physiological, and became the basis for a frequency-domain-based PPV 'test' algorithm, see Section 4.2.

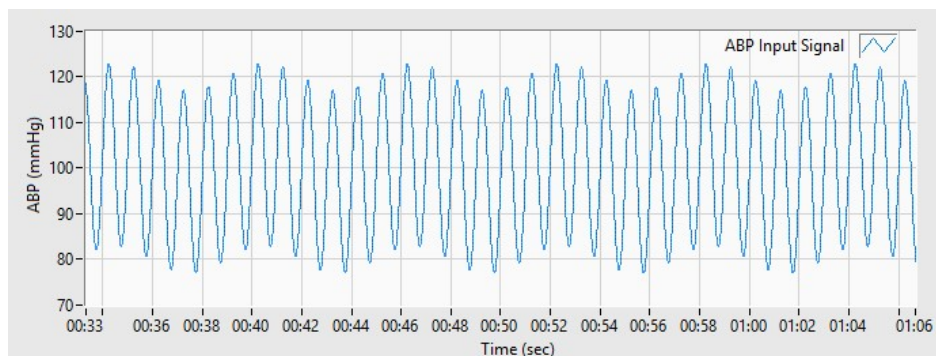


Figure 20. Simulated "Simple" Simulated Waveform, 15% change in amplitude, Systolic/Diastolic 120/80 mmHg

4.1.4 Time-domain vs Frequency-domain.

When a signal is displayed with the x-axis displaying time in seconds, a signal is viewed in the time-domain and this shows moment-by-moment information. However, it is good to view the individual frequencies that make up the signal, and this is achieved by *Fast Fourier Transform* FFT which displays the signal in the frequency-domain. This takes the form of a *Power Spectral Density* PSD and displays the relative power of particular frequencies within a signal, for a specific time period. Figure 21 below shows this for a real patient ABP signal, for this signal, the respiratory frequencies (0.24 Hz) and heart rate frequencies ECG (0.97 Hz), are evident, as are their harmonics. Also, as described in Section 4.1.2, the modulation caused by the respiration on the ECG signal is evident as sidebands. The relative size of the amplitudes is of interest when thinking about PPV. A PSD does not show any phase information or positioning of the individual frequencies in real-time. Therefore, a PSD cannot be reconstituted back into the original time-domain waveform.

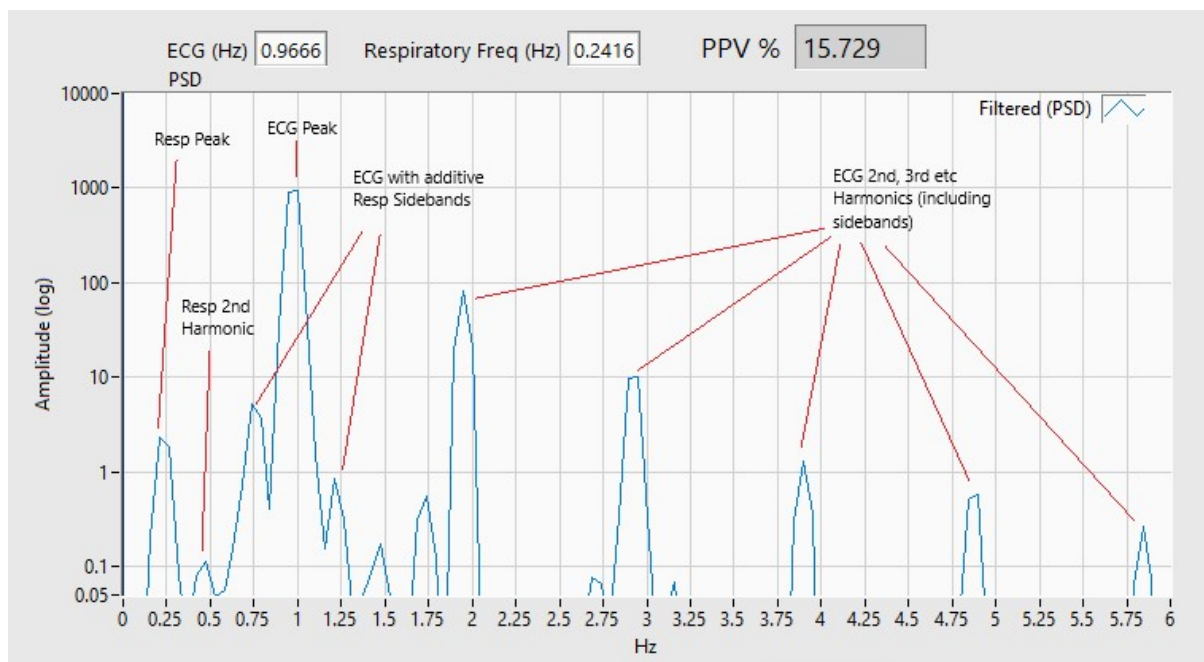


Figure 21. Power Spectrum Display (PSD) of ABP signal with signal peaks

4.1.5 Integration of the Algorithms in LabVIEW

All programming is achieved using National Instruments LabVIEW 2011 *Virtual Instruments* ('VIs'). Figure 22 below shows (in blue) the Main-VI and Sub-VI previously developed by the Principal Investigator, and the two green Sub-VIs created by the author of this thesis. The Main-VI takes stored patient data and sends it to two Sub-VIs; the resultant PPV values are returned to the Main-VI, which compares the results of these Sub-VIs statistically. A working Aboy algorithm is reproduced based on the steps outlined below in Section 4.3; programming examples are displayed in Appendix 4. Another PPV Development Sub-VI creates simulation data and is the location of any developed 'test' algorithms. Integration of the algorithms required some work to ensure timing and dataset sizes were accurate. A second Sub-VI developed for the project is a standalone VI used for communication and data collection, see Chapter 5 for more information.

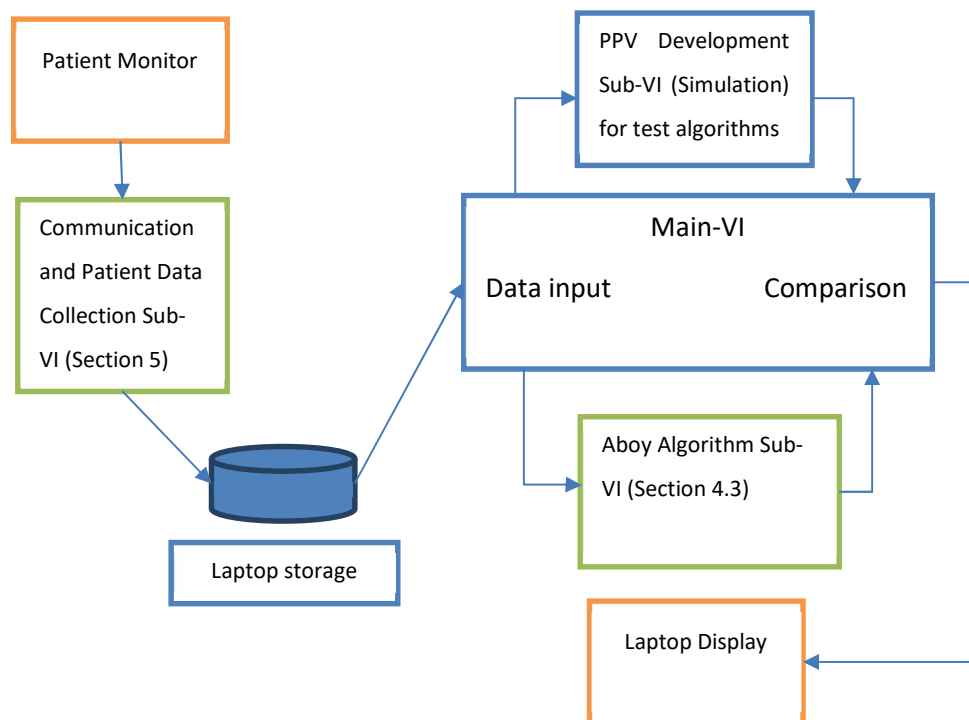


Figure 22. Main-VI and Sub-VIs used in the project

4.2 Novel 'test' algorithm

The path taken to find a novel 'test' algorithm began with inspecting simulated data in the spectral domain. This came about due to awareness of the potential of frequency-domain alternatives, as investigated by Thiele et al. [41]. Whilst viewing patient blood pressure signals (see Figure 19), the similarities with the simulated waveform previously noted as Figure 23 are evident, and for a given amount of %PPV the power spectral density displayed an interesting spectral peaks ratio of *Spectral Power* (SP) at HR and RR frequencies (displayed as SP_{HR} or SP_{RR}). Alternatively, compared to the path taken by Aboy, the 1st harmonic of the spectral power is located with the help of capnography data for *Respiratory Rate* (RR), and the *Echo Cardiogram* (ECG) for Heart Rate (HR).

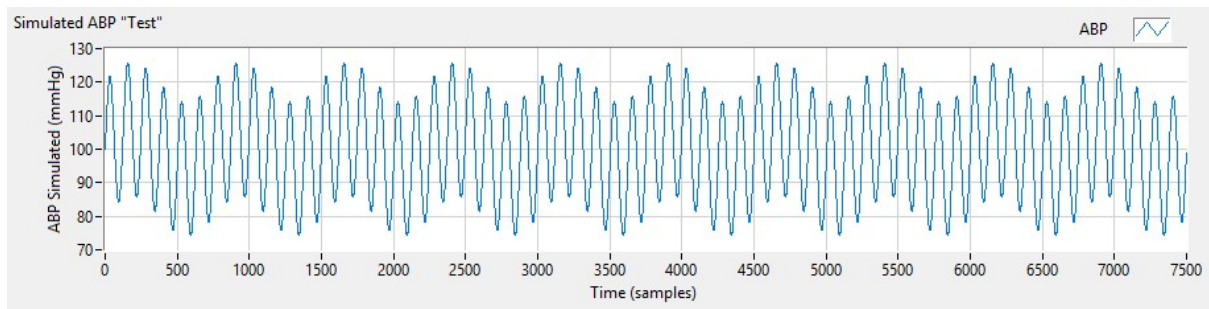


Figure 23. Simulated 'Simple' Simulated Waveform, 30% change in amplitude, Systolic/Diastolic 120/80 mmHg

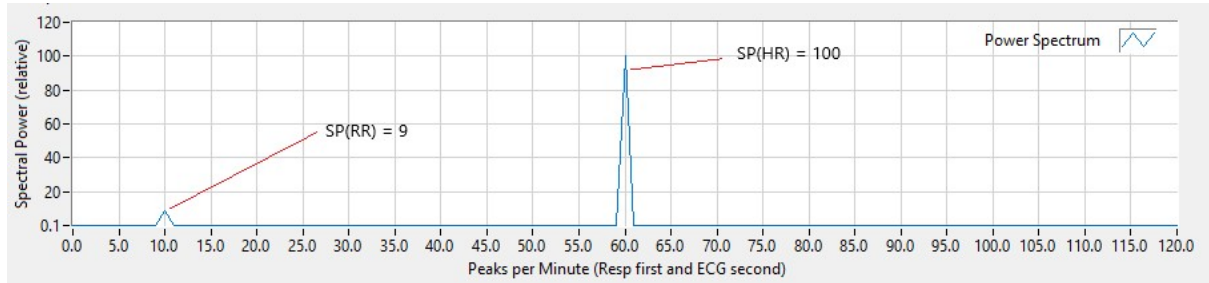


Figure 24. Power spectrum of "Simple" with relative peaks for SP_{RR} and SP_{HR}

Figure 24 above shows the relative spectral power at RR and HR, and the following equation (4) is used to determine $\%PPV_{test}$.

$$\%PPV_{test} = 100 \times \sqrt{\frac{SP_{RR}}{SP_{HR}}} \quad (4)$$

Using the values from Figure 24, $SP_{RR}=9$ and $SP_{HR} = 100$

$$\%PPV_{test} = 100 \times \sqrt{\frac{9}{100}}$$

And therefore:

$$\%PPV_{test} = 30\%$$

When other values of simulated simple %PPV waveform are used and amplitudes extracted, the equation based on the relative as SP_{HR} or SP_{RR} resolve correctly with equation (4).

4.2.1 Justification for novel 'test' algorithm

Using the insight provided by direct observation enabled the straightforward application of frequency domain-based methods in LabVIEW. With fewer filters for pre-processing and no recursive steps, LabVIEW Vis can use raw patient data, and with the appropriate VI, can provide instant magnitude information. Phase information is lost but in any event is not required for the calculation. Thiele et al. [41] found that the correlation of their ratio of SP_{HR} or SP_{RR} gave a result indicating that the site of the recording of blood pressure mattered less: there was greater variability with the traditional PPV when recorded at different sites. This would indicate that frequency-domain-based algorithm may have a benefit above time-based-algorithms.

4.3 Aboy Method Steps for Pulse Pressure Estimate

The ABP signal varies with the steady respiratory airway pressure from the ventilator and isolating the upper and lower envelopes of this waveform is the key to estimating the pulse amplitude pressure variation using the Aboy method, or modulation created by the respiration and therefore % Δ PPV.

4.3.1 Step 1: Beat Minima detection

The starting point is to find the sequence of beat minima, the time location corresponding to each beat a_k equation (5).

$$a = (a_1, a_2, \dots, a_{k-1}, a_k, a_{k+1}, \dots)^T \quad (5)$$

Heart rate is estimated via a bandpass filter and power spectral density (PSD); once determined, this frequency is used later. The signal is filtered, and peak detection and decision logic using rank-percentile based non-linear filters plus relative slope and amplitude information coarsely estimates the beat locations a_k . A nearest neighbour algorithm uses this estimation and interbeat interval with the estimated heart rate for classification of the beat minima. Although this is performed on the filtered wave, another nearest neighbour is used to find the minima on the raw signal.

4.3.2 Step 2: Beat Maxima detection

Now that beat minima are determined, the beat maxima b_k equation (6,7) are detected using a_k components.

$$b_k \triangleq \arg \max_{a_k \leq n \leq k+1} x(n) \quad (6)$$

$$b = (b_1, b_2, \dots, b_{k-1}, b_k, b_{k+1}, \dots)^T \quad (7)$$

where $x(n)$ is the ABP sampled signal at a sampling rate of f_s . The Philips patient monitor used in this project outputs data at a sampling rate of 125 samples per second, which is high enough to capture adequate amplitude and waveform information. Aboy uses steps 1 and 2 but recommends that any good beat detection algorithm can be used for this purpose. LabVIEW *Peak Detector.Vi* is used for this purpose, results are shown in Figure 25.

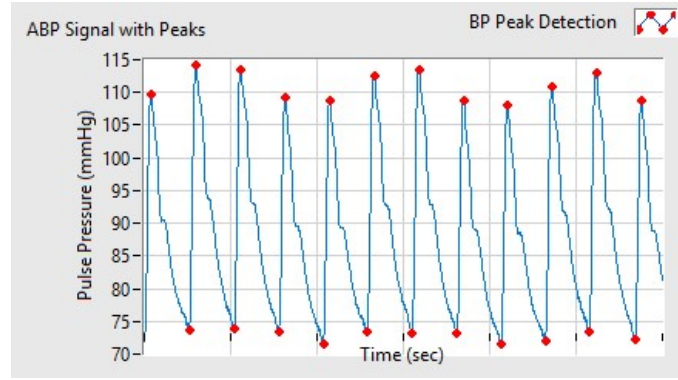


Figure 25. Beat minima and maxima, in the time series

4.3.3 Step 3: Beat Mean Calculation

The beat mean pressure \bar{x}_k is used as an estimate of the additive effect of the respiration on ABP. The use of a high-pass filter removed the effect of the respiration works for simulated data.

4.3.4 Step 4: Pulse Amplitude Pressure

The pulse amplitude pressure is simply obtained by finding the difference between the peaks found during the minima a_k and maxima b_k ,

4.3.5 Step 5: Envelope Estimation

The upper and lower envelopes of the ABP waveform are required; upper $u_e(n)$ and lower $l_e(n)$ from the lower $x(a)$ and upper $x(b)$ time series. Figure 26 shows the envelope points.

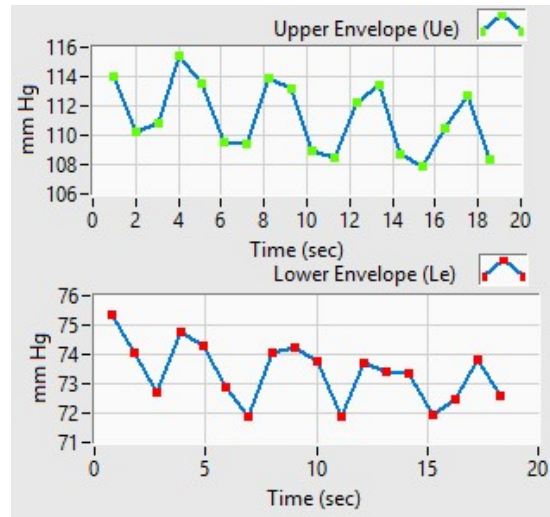


Figure 26. Envelope upper $u_e(n)$ and lower $l_e(n)$ taken from patient data shown in Figure 24.

To estimate the envelope, $x(a)$ and $x(b)$ are smoothed and resampled again at the sampling frequency f_s with a kernel smoother equation (8,9):

$$d(k) = \frac{\sum_{n=1}^N \delta(n) b(\frac{|kT_s - t(n)|}{\sigma_b})}{\sum_{n=1}^N b(\frac{|kT_s - t(n)|}{\sigma_b})} \quad (8)$$

$$b(u) = \begin{cases} \exp\left(\frac{-u^2}{2}\right) & \text{if } -5 \leq u \leq 5 \\ 0 & \text{otherwise} \end{cases} \quad (9)$$

where $kT_s = 1/f_s$ is the sampling interval, σ_b is the kernel width and $b(\cdot)$ is the clipped Gaussian kernel function. In reality, this is a Gaussian function that moves through the upper and lower envelope beats with a kernel width of approximately 0.2 seconds to create a resampled waveform Figure 27.

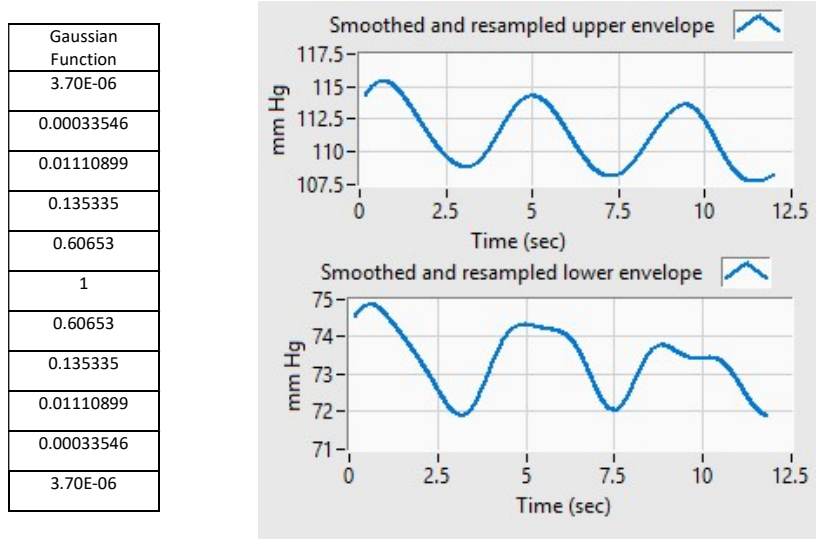


Figure 27. Estimated $u_e(n)$ and lower $l_e(n)$ resampled and smoothed with Gaussian function

4.3.6 Step 6: Pulse Amplitude Pressure Estimate

In this step, the pulse pressure is estimated by subtraction of upper $u_e(n)$ and lower $l_e(n)$ and creates a sample-by-sample difference $\hat{p}_\alpha(n)$ equation (10):

$$\hat{p}_\alpha(n) \triangleq u_e(n) - l_e(n) \quad (20)$$

The two waveforms are essentially subtracted from each other to create a Pulse Pressure amplitude estimate, being primarily the change in blood pressure due to respiration (Figure 28). What can be noted already is that there is a swing of approximately 4 mmHg for each breath at a mean pulse pressure of about 38 mmHg, this should give a $\% \Delta PPV \cong 11\%$.

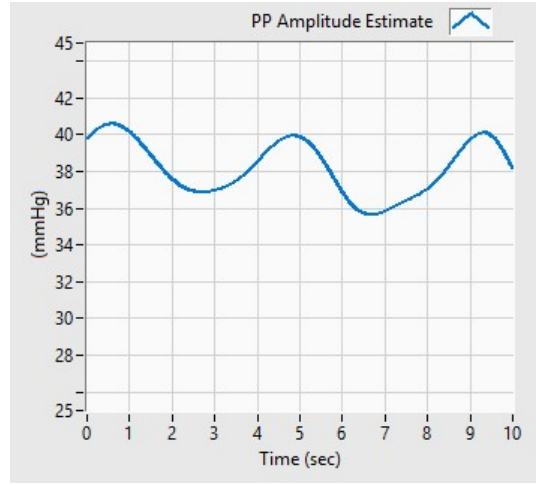


Figure 28. Pulse pressure amplitude estimate $\hat{p}_\alpha(n)$, showing effects of respiration on the pulse pressure

4.3.7 Step 7: Pulse Pressure Variation Estimation

The final step is to determine $\% \Delta PPV$ from the time series $\hat{p}_\alpha(n)$. This involves taking the time series and now finding the peaks that correlate with the maxima and minima pressure variations. To do this, firstly a low-pass filter at $1.75 \times f_r$ Hz is used to remove the respiratory trend frequency f_r , determined using power spectral density. Minima a_p and maxima b_p detection is performed on the pulse pressure waveform, and an estimated maximum $\widehat{PP_{max}}$ and minimum $\widehat{PP_{min}}$ pulse pressures can be identified over each respiratory cycle:

$$\widehat{PP_{max}} = \hat{p}_\alpha(b_p)$$

$$\widehat{PP_{min}} = \hat{p}_\alpha(a_p)$$

Using these estimates, a ΔPP for each period of samples is calculated in equation (11), μ being the average pulse pressure over the respiratory period and to ensure a more robust output equation (12), median filter $\mathcal{Fmed}(\cdot, \omega_l)$, is applied where ω_l is the window over the period of the samples (a window between 3 and 10 respiratory cycles is suggested):

$$\Delta \widehat{PP} = \mathcal{Fmed}\left(\frac{\widehat{PP_{max}} - \widehat{PP_{min}}}{\mu}, \omega_l\right) \quad (11)$$

$$\mu = \frac{1}{a_{p_{k+1}} - a_{p_k} + 1} \sum_{k=a_{p_k}}^{a_{p_{k+1}}} \hat{p}_\alpha(n) \quad (12)$$

Table 5 below performs the final calculations from the pulse pressure estimate using data shown in Figure 28 above. As previously expected, the $\% \Delta \widehat{PP}$ or the estimate of the pulse pressure variation using the Aboy averages was as anticipated.

time (sec)	\widehat{PP}_{max} (mmHg)	\widehat{PP}_{min} (mmHg)	$\widehat{PP}_{max} - \widehat{PP}_{min}$	Average μ (mmHg)	$\frac{\widehat{PP}_{max} - \widehat{PP}_{min}}{\mu}$	$\% \Delta \widehat{PP}$ $\omega_i = 3$
0.774058	39.1888					
2.91106		35.6037	3.5851	37.39625	9.586790119	
5.04901	38.5698					
6.8837		34.4134	4.1564	36.4916	11.39001852	11.39001852
9.50756	38.7202					
11.1619		34.1115	4.6087	36.41585	12.65575292	

Table 5. Estimation $\% \Delta \widehat{PP}$ using a window of 3 samples or approximately 10 seconds

4.4 Effectiveness of “Aboy” Algorithm with Simulation Data

As a test of the efficacy of the now programmed Aboy algorithm, simulation data was used as described in 4.1.3 and equation (2,3), previously described.

$$p(t) = u_p + [1 + ar_n(t)] \cdot [\alpha \cos 2\pi f_c t + \beta \cos(4\pi f_c t + \theta_c)]$$

$$r_n(t) = \cos(2\pi f_r t + \theta)$$

This equation contains first and second harmonics of the simulated ABP signal, α is the modulation index, and $r_n(t)$ is the amount of normalized respiratory pressure added to the ABP signal.

With only one sideband on a PSD and $\alpha = 0.2$ (i.e. PPV= 20%), in the following PSD (Figure 29) a single sideband is visible, and the Aboy Algorithm gives PPV \approx 19.3%. When tested with multiple PPV values, an error of approximately 3.5% was displayed (Table 6).

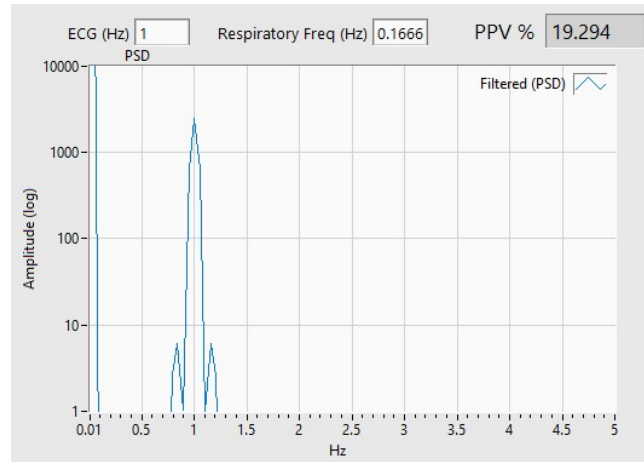


Figure 29. Simulation data with $\alpha = 0.2$ (PPV= 20%)

PPV simulated (%)	Aboy Algorithm (%)	Error %
5.0	4.8	4
10	9.6	4
15	14.5	3.3
20	19.3	3.5
25	24.1	3.6
30	29.0	3.3

Table 6. Simulation data vs Aboy Algorithm

An error of 3.6 % could be considered acceptable for values of PPV as described in Section 3.1, fluid responders are shown to be predictable within the range of PPV($16 \pm 6\%$), and typically the higher the PPV, the greater the chance the patient will respond to fluid administration. However, the closer the recorded PPV% is to the grey zone (9%-13%) the higher the chance of misclassifying a patient.

To illustrate artefact or noise the addition of a second respiratory harmonic with the same power as the respiratory harmonic (Figure 30), and leaving constant at PPV = 20%, but changing the phase θ_c , this is displayed below.

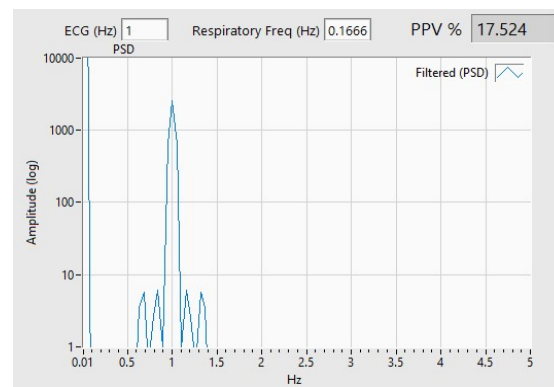


Figure 30. PSD Second harmonic, proportionally raised from a factor of 1x respiratory sideband

2 nd Harmonic x1		
θ_c deg PPV simulated 20 (%)	Aboy Algorithm (%)	Error %
0	17.5	12.5
45	19	5
90	20.5	2.5
135	19	5
180	17.5	12.5

Table 7. Percentage error with changing respiratory signal phase θ_c 2nd harmonic x1

Figure 30, along with Table 7, shows the effect of adding a second harmonic to the signal, whilst the proportion of energy in the second harmonic is the same as for the respiratory signal, the error is as much as 12.5%.

In Figure 31, corresponding to Table 8, again keeping PPV constant at 20%, but now adding twice as much power (to emulate more noise or other frequencies) to the second harmonic the algorithm is not able to determine the PPV with any degree of accuracy and 74% error is shown.

This will become important if there are proportionally higher frequencies in the PSD than the sideband ‘respiratory’ frequency, or additional 2nd , 3rd or 4th harmonic ABP frequencies with high power content, these will have a great influence on the Aboy Algorithm’s ability to properly determine a correct value.

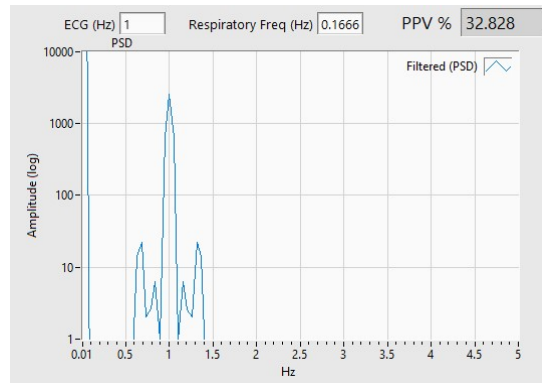


Figure 31. PSD Second harmonic, proportionally raised 2x respiratory sideband

2 nd Harmonic x2		
θ_c deg PPV simulated 20 (%)	Aboy Algorithm (%)	Error %
0	32.3	61.5
45	34.4	72
90	34.7	74
135	34.3	72
180	32.9	64.5

Table 8. Percentage error with changing respiratory signal phase θ_c 2nd harmonic x2

5.0 Data Collection Software for Philips Intellivue Monitor

The Philips Medical System MP Series of Patient Monitor (MP40/50/60/70/90) and its newer MX series models are highly sophisticated machines that use single or multi-parameter modules to provide and display clinical parameters including waveform, numeric and calculated indices. As part of hospital-wide patient networks, such patient monitors can feed into patient information management systems, and store 72-96 hours of data in local databases for trend analysis of all clinical events for later review. This ability to look back is useful since during emergency episodes clinicians are busy looking after the patient directly. Furthermore, the ability to use this information is highly desirable for researchers.

Limitations to the accessing of this data include the need to purchase expensive systems, proprietary hardware and software, but that even with this expense, outputs may only be in particular file or database format; and these may not allow the data to be used easily by other programs. HL7 is a universal output of most proprietary systems, but at the moment outputs are limited to numeric data since waveform data, for example, the ECG, plethysmography or in the case of PPV calculations based on Arterial Blood Pressure ABP are not available. For this study, a LabVIEW version of an Intellivue communication program was sought as it would allow direct programmability with any other LabVIEW routines in real-time.

However, although the Philips Intellivue, Data Export Interface Programming Guide [49] has been available since its creation in 2002, apart from marketed proprietary software, there are only two published examples of the successful creation of systems based on the information presented in the 220-page guide. Vinecore et al. [50] used the data export capability of the Intellivue monitor RS232 connection, although there is no information about what software was created and whether this was a proprietary device and used in real-time. Gjermundrod et al. [51, 52] developed open-source middleware for accessing information from Intellivue series in Intensive Care Units. As far as can be determined, this thesis is the first successful attempt to create software to communicate with LabVIEW's - *Virtual Instrument* (Vi) coding. It was only made possible through working with simpler communication protocols from other devices, these two systems being the Novamatrix, Novaterm 3 protocol and the GE Healthcare S/5 Computer Interface. Examples of these LabVIEW VI's are included in Appendix 2 as these were preliminary and necessary to creating the Intellivue Interface.

5.1 Requirements for Intellivue LabVIEW communication program

5.1.1 Design requirements

Factors that are required of the program's ability:

1. to use the software in the clinical environment at any time to record from Philips Intellivue monitor onto a laptop computer easily during surgical operations,
2. to work on both Windows and Macintosh platforms,
3. to acquire multiple numerical and wave information at the same time,
4. to store acquired data in CSV file format, and
5. be a sub-Vi for other LabVIEW programs

5.1.2 Extra software tools required

Apart from LabVIEW other programming tools were required to enable communication with the Philips MP70 monitor and return Hexadecimal code:

1. Microsoft Network Monitor V3.4 set up to parse communications between Universal Data Protocol (UDP) connected Monitor and Laptop for particular ports and IP, this allowed messages to be captured and scrutinised via notepad or excel.
2. When an attempt was made using RS232 communications the program Realterm 2.0.0.70 was used because it could send and receive messages via RS232 communications protocol.

5.1.3 Connectivity to Laptop

RS232 or LAN outputs can make a connection to the laptop; however, it was determined early in the design process that the Cyclic Redundancy Check or CRC (described further in Appendix 4) used with the MIB/RS232 interface would only be attempted after UDP communication through the LAN interface had been achieved. Since the patient monitor is standalone in the operating theatre and not connected to a LAN, it was possible to connect via a Unshielded Twisted Pair (UTP) crossover cable (Figure 32) and connect to an RJ45 LAN socket on the patient monitor (Figure 33).

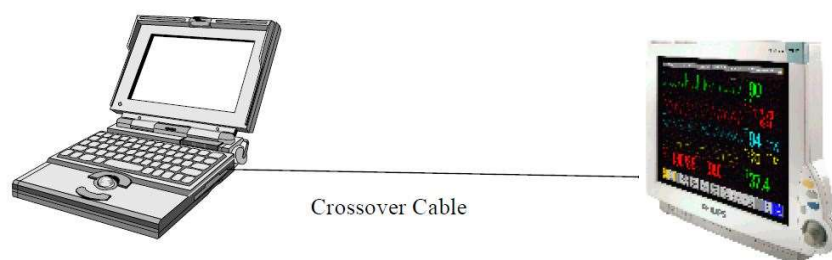


Figure 32. Crossover cable connection for Laptop to Monitor communications

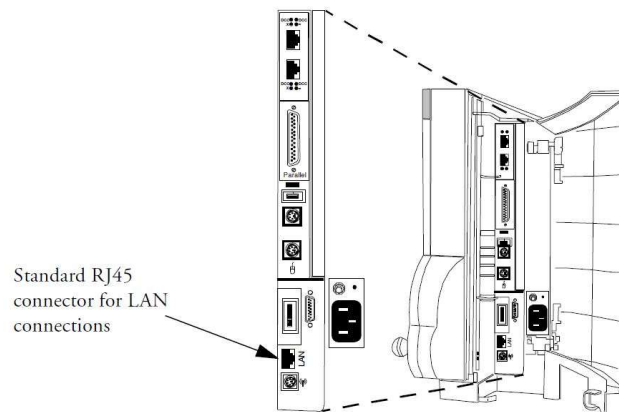


Figure 33. RJ45 LAN connection location Philips MP70

It is important to note that the crossover cable must be an UTP cable to avoid current leakage. Where there is a network switch, a straight-through UTP cable can be used between computer and switch, and from the switch to the patient monitor.

5.1.4 Configuring Network Address and Network Settings

Since the monitor is set to work on a LAN, a smaller LAN connection is set up between the Laptop and the Patient monitor. Most contemporary computers rely on wireless connectivity, which leaves the laptop's LAN network adapter free to be used solely for connectivity to the Patient Monitor.

A small static network can be created by adjusting settings in the MP70 and the laptop.

- In the Laptop under Ethernet Properties -> Internet Protocol Version 4 (TCP/IPv4) properties -> Set Use the following IP address: IP Address: 10.0.0.1 and subnet mask 255.255.255.0
- In the MP70, Central Monitoring should be set to Optional, and a static IP set in the configuration menu. For simplicity, the IP Address: 10.0.0.2 and subnet mask 255.255.255.0 can be set.

Using a Ping command from the computers Command Prompt to the IP of the MP70 will confirm that there is connectivity.

Further explanation on the setup of the patient monitor can be found in the Intellivue configuration guide (M8000-9306X).

5.2 Data Export Interface

All information in this section is from the Data Export Interface Guide[49], M8000-9305C. Descriptions have been simplified and reduced to save repetition, but some areas have a further additional explanation.

5.2.1 Supported Protocols

There are two methods for sending and receiving data from the Intellivue Monitor

1. Universal Datagram Protocol (UDP) and accessed via LAN.
2. Medical Information Bus (MIB/RS232) communication interface protocol

The Intellivue monitor cannot be accessed via LAN if connected to a patient monitoring network (connected to a central monitor), and in this case, RS232 communication can be used. However, if the monitor is not connected to a LAN, then UDP can be used to access real-time data. It is recommended in the programming guide to use and establish UDP communications first while developing software, before determining RS232 form of the communication.

The data export protocol is a connection-orientated, message-based request/response protocol on top of the transport protocol. The protocol needs some handshaking before the transfer begins, and continual communication is required to ensure that the monitor does not timeout and lose Association. It is also a server/client relationship whereby the Patient monitor acts as a server, maintaining a logical connection with the client laptop.

5.2.2 Protocol Model

The protocol is based on an objected-orientated modelling concept. All information available through the Data Export protocol is modelled as attribute values of information objects. The following table (Table 9) shows different objects that can be polled for different types of information

Object	Description	Example
Medical Device System (MDS)	The MDS object contains attributes representing: <ul style="list-style-type: none">- dynamic state information- static device-specific identification information	Current operating Model Serial Numbers
Alert Monitor	The Alert Monitor object contains attributes representing the current technical and patient alarms	Alarms as displayed on the Intellivue monitor
Numeric	Numeric objects contain attributes representing the state and value of numerical measurements	Heart Rate
Waves	Real-time sample array objects contain attributes representing the state and value of wave data	ECG

Table 9. Different Objects available with examples of their attributes [49].

Essential for this project is the ability to poll the Numeric and Waves objects, although communications must be established and maintained between the Server/Client relationship.

5.2.3 Protocol Diagram

Figure 34 shows the protocol diagram for the Intellivue monitor; each step in this communication protocol requires messages to be sent and parsed to extract necessary information. In particular, and where for example individual waveforms are to be desired, then polling messages must be created to inform the monitor/server which waveforms to send. Otherwise, the server will determine for itself which waveforms it will send, based on its own internal tables.

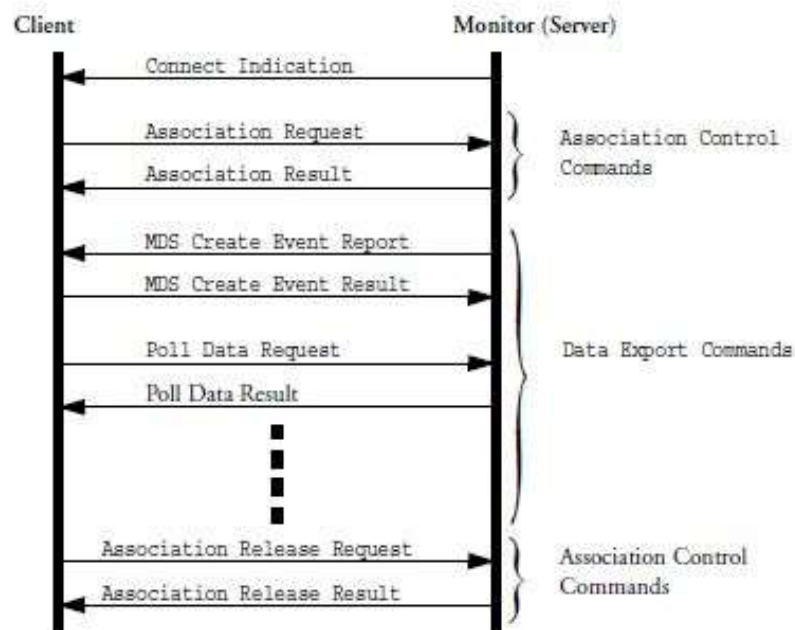


Figure 34. Protocol diagram for communication between Server (MP70) and Client (Laptop) [49].

The protocol is also controlled by a Time-out Mechanism that automatically closes the connection if a time-out condition occurs, and this relates to the negotiated minimum polling interval that is set up during the connection phase. The minimum time out period is 10 s and maximum is 130 s; however, the negotiated connection is 3x the minimum poll period time.

If the monitor times out, then a new Association Request can be sent to set up another logical connection. However, whilst programming, and to avoid loss of connection, it was deemed simpler to routinely make an MDS monitor request as this was a simple way to keep communication open. Figure 35 summarises the protocol diagram above, with additional descriptions for each of the programming steps.

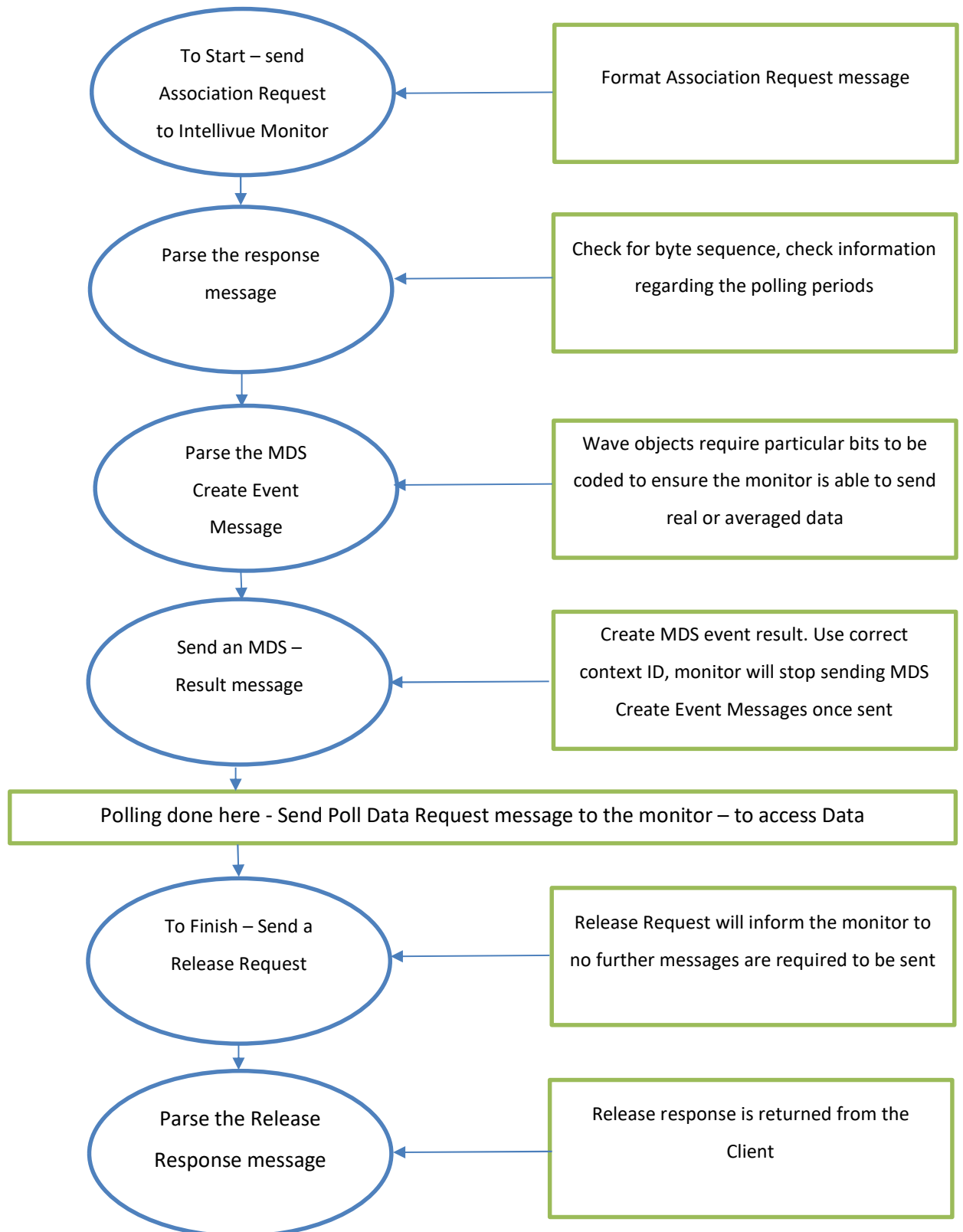


Figure 35. Steps for establishing a communications, polling data and releasing client Intellivue Monitor

5.2.4 Selection of Wave and Numerical Data.

To limit the amount of data to be parsed by the client monitor, Wave and Numeric polling requires the message to be created from the selected list of available parameters. However, to do this, there is limited bandwidth. The following table (Table 10.) shows the limits and indicates that wave data may be returned as an array of a particular size.

Wave Type	Sample Period	Sample Size	Array Size	Update Period	Bandwidth Requirement ¹
500 samples/s (ECG)	2 ms	16 bits	128 samples	256 ms	1064 bytes/s
250 samples/s (Compound ECG)	4 ms	16 bits	3*64 samples	256 ms	1640 bytes/s
125 samples/s	8 ms	16 bits	32 samples	256 ms	296 bytes/s
62.5 samples/s	16 ms	16 bits	16 samples	256 ms	168 bytes/s

Table 10. Polling frequency and sample period and size [49].

Due to bandwidth limitations, as a maximum there can be only two ECG waves and five other waves polled. The selection of waves is made by sending a request for the polling table, priority to be set differently to that decided by the monitor. Also returned numerical data can be set to reduce the number of packets that must be parsed by the client.

5.3 Program Output

Coding for this project was performed and contained within LabVIEW's *Virtual Instruments* (VIs); examples are shown in Appendix 2. The appendix describes the elements for building messages to poll the patient monitor in hexadecimal code and also the receipt, parsing and storage of the hexadecimal message. A *Graphic User Interface* GUI (otherwise known as LabVIEW 'front panel') was created to display received waveforms in real-time.

5.3.1 Parsing polled messages

As a sophisticated instrument, the Philips Intellivue monitor is capable of handling hundreds of different patient parameter signals, with many ways of displaying them on the screen in the SI Units that describe them. For waveform data, the raw data is translated into a form that can be re-scaled in the x and y dimensions on any monitor.

For this PPV calculation and as an example for the ABP waveform to be displayed correctly, a patient simulator was used to create Y scale pressure (mmHg) on the patient monitor. Output hexadecimal values were collected and converted to binary and shown as x (Table 11 below). Solving for y, a simple linear equation is used to determine that the correct scale is used. This was based on the information within the returned waveform parameter.

IBP hex	x	Simulated Y scale mmHg	y IBP mmHg ($y=x/16-50$)	
	160	-40	-40	Extrapolated -ve
320	800	0	0	
04F8	1272	30	29.5	
06D3	1747	60	59.1875	
0A8B	2699	120	118.6875	
	9120	520	520	Extrapolated +ve

Table 11. Solving for y to determine a scaling factor for Invasive Blood Pressure measurement

Only after this equation was solved could the invasive blood pressure be displayed correctly. If a different scale is used on the monitor, then the x value will also change for the same blood pressure. For example, if the type of screen configuration is changed from Adult to Paediatric, the scaling factor would also change, so that the smaller magnitude wave would display correctly on the monitor. For

this thesis patient configuration for the monitor is set to Adult. Figure 36 below shows the parsed patient data waveform using the scaling factor calculated above.

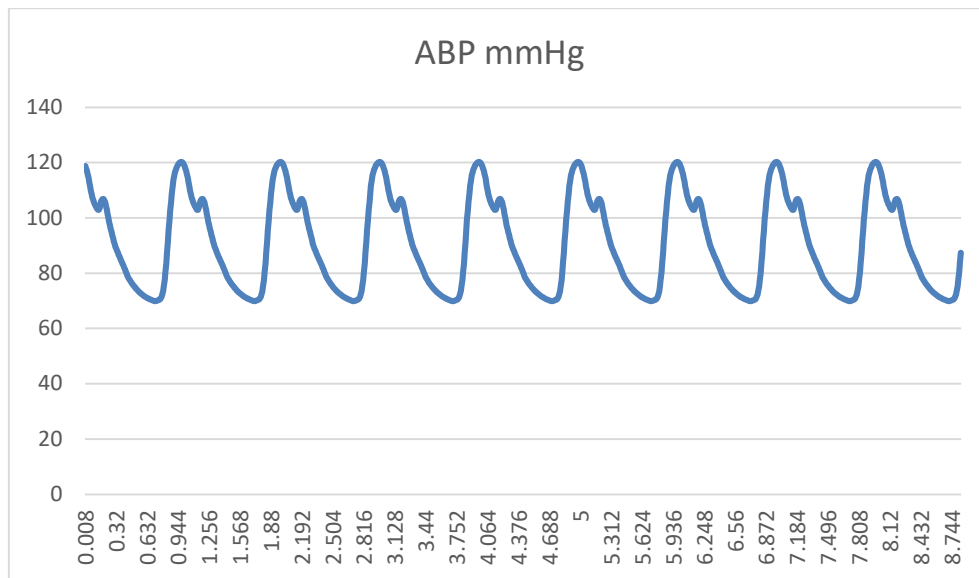


Figure 36. Arterial blood pressure waveform scaled correctly

5.3.2 Screen layout

The final screen layout is shown below in Figure 37, in this instance, the recording of three waveforms and six numerical values directly from the patient monitor. The values were also collected and stored in an Excel spreadsheet, samples of this data are also found in Appendix 1

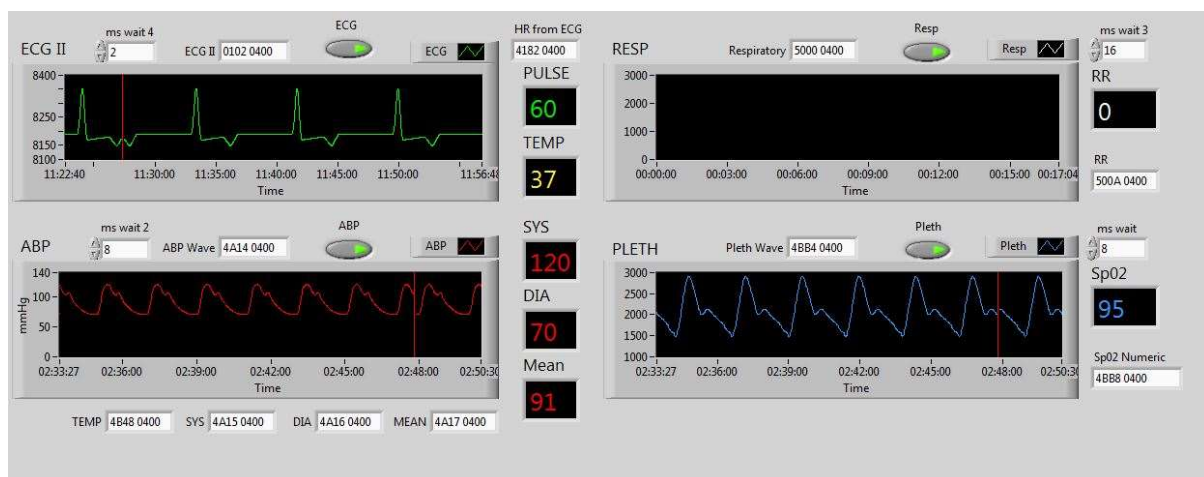


Figure 37. LabVIEW screen layout for communication with Philips MX800 with simulated data

6.0 Method

To this point, the software for communication, data collection, and the Aboy algorithm have been completed and tested with simulation data. The next stage was to obtain recorded clinical data and compare this to the Aboy algorithm and to a novel “test” algorithm.

The following section will outline the method for the clinical study and analysis techniques. Firstly, this section describes the test algorithm and secondly the clinical study to compare both algorithms' efficacy. To differentiate between the methods, either calculated or measured $\%PPV$ values, the following descriptions will be used: the Aboy algorithm developed for this project will be called $\%PPV_{Aboy}$, those recorded from the patient monitor are $\%PPV_{rec}$, and the test algorithms will be known as $\%PPV_{test}$.

6.1 Method Summary

Test algorithm: A novel algorithm for calculation of PPV using power spectral analysis (“test algorithm”)

6.1.1 Measurements

The duration of data collection in each patient varied between 5 minutes and 15 minutes, depending on the time constraints of the surgical procedure. The reference measurement $\%PPV_{rec}$ is delivered by the Philips monitor using the Aboy algorithm [1]. This is updated whenever the displayed value changed during the measurement period.

6.1.2 Statistical analysis

Agreement between PPV from the Philips monitor (based on the method of Aboy et al.[1]) and the test algorithm is provided using Bland-Altman statistics (bias and 95% limits of agreement LoAs).

6.1.3 Primary endpoint

The primary comparison was the incidence of misclassification of the predicted fluid responsiveness of patients according to the criteria of Cannesson et al. [18], i.e. where reference measurement was $>13\%$, and test measurement was $<9\%$, or vice versa. What this implies, is that if a patient was considered to be a fluid responder before with a $\%PPV_{rec} > 13\%$ but the test algorithm calculates $PPV_{test} < 9\%$ (now a non-responder) this would be considered a misclassification, conversely a $\%PPV_{rec} < 9\%$ (non-responder) but the test algorithm calculates $PPV_{test} > 13\%$ (now a responder) is also considered to be a misclassification.

6.2 Clinical Study

Due to the nature of the environment, ethics approval was sought and approval given by both Austin Health Human Research and Ethics Committee HREC and La Trobe University, University Ethics Committee, and considered as a Low-Risk application due to the observational nature of the project. This is because only *data collection* was required in patients already undergoing anaesthesia and surgery, with appropriate monitoring routinely in place for clinical management. Due to the nature of working in a hospital environment, the Principal Investigator determined which patients were selected, and under what clinical criteria.

6.2.1 Patient selection

Selection required any patient over the age of 18 years, undergoing relaxant general anaesthesia and controlled ventilation for surgery, in whom an arterial blood pressure monitoring line was inserted for routine cardiovascular monitoring by the attending anaesthetist. For this project, the study size was nominally 20 patients. Patients undergoing open-heart, or open-chest operations were excluded, as a good PPV signal relies on the patient's thorax or chest being closed.

6.2.2 Data collection

To enable data collection from selected patients, the Principal Investigator was to be present in the operating suite during surgical procedures. A notebook computer was connected to the patient monitor following patient anaesthetic induction, intubation and stabilization. PPV display was enabled on the Philips patient monitor. Data download was automated so that no additional workload was required from the attending anesthetic staff. The computer was to be disconnected at the end of the case, and data download ceased. Continuous data download of relevant variables from the monitor was performed. These could include any of the following, but the arterial blood pressure waveform is of primary concern:

- Arterial pressure waveform (ABP)
- Capnography waveform (Airway Pressure)
- ECG
- Numeric data: heart rate, rhythm, PPV, respiratory rate, SpO₂

6.3 Data Collection and Analysis

Data analysis is completed off-line, though the following aspects are required to ensure data sets are correct. The Main-VI automatically compares the techniques to produce tabular and graphical results.

6.3.1 Dataset Length

As described previously in Section 5.2.4, any waveform data from the patient monitor is collected at a specific sampling rate. For an ABP signal, this is at 125 samples per second or a sampling frequency of $f_s = 125$. Therefore 1250 samples are required for 10 seconds of data. However, Section 4.3.6 also described the calculation of the pulse pressure estimate for the Aboy method, a median filter ω_t is employed, and can be between $3 \leq \omega_t \leq 10$ respiratory cycles ($\omega_t = 3$ giving a fast response to change, and $\omega_t = 10$ a stable window, but where fast changes could be lost). Therefore for 10 respiratory cycles at an approximate maximum of 6 breaths per minute, 60 seconds of data or 7500 samples were collected for each analysis dataset.

6.3.2 Correlation Plot

For this study, correlation is used to determine how closely the calculated or test PPV is to that measured by the monitor, therefore an r value close to $r=1$ would be considered a good correlation, and $r=0$ as no correlation. The plot is also used to help categorize the responders who have been misclassified as non-responders, and vice versa; as described in 6.1.3.

6.3.3 Bland-Altman Plot

Bland-Altman or the Tukey Mean-difference plot is used to show when any two methods or measurement techniques have a good correlation between them, particularly when one is referenced as the 'gold standard' or test. For each set of measurements, the difference between them is plotted against the mean of the two values. If the difference between the two points is zero, then this shows that the two measurements are in agreement; however, *Limits of Agreement* (LoAs) are set so that outliers become apparent and where the two methods are not interchangeable.

7.0 Results

As initially laid out in Section 1.1 Project Scope, some of the work in this project is entirely software development, and of the two Sub-VIs, one is for data collection and the other an attempt at replicating the Aboy algorithm. Now with access to clinical data to obtain $\%PPV_{rec}$, both correlation and Bland-Altman statistics can be used to test the efficacy of $\%PPV_{test}$ and $\%PPV_{Aboy}$.

7.1 Clinical Results $\%PPV_{rec}$ vs $\%PPV_{test}$

When used with 20 ventilated surgical patients (211 measurements), assuming a PPV grey zone [1] of 9-13%, the algorithm for Aboy et al. gave results which showed that only 5.7% of measurements would misclassify a patient as fluid responder or non-responder (correlation plot is shown Fig 38). There is an 8.8% reduction of responders, with an increase of 11.8% non-responders and a 5.6% increase in cases within the “grey zone” samples across the dataset. The overall change in classification of any type is 36.4% comparing the two datasets.

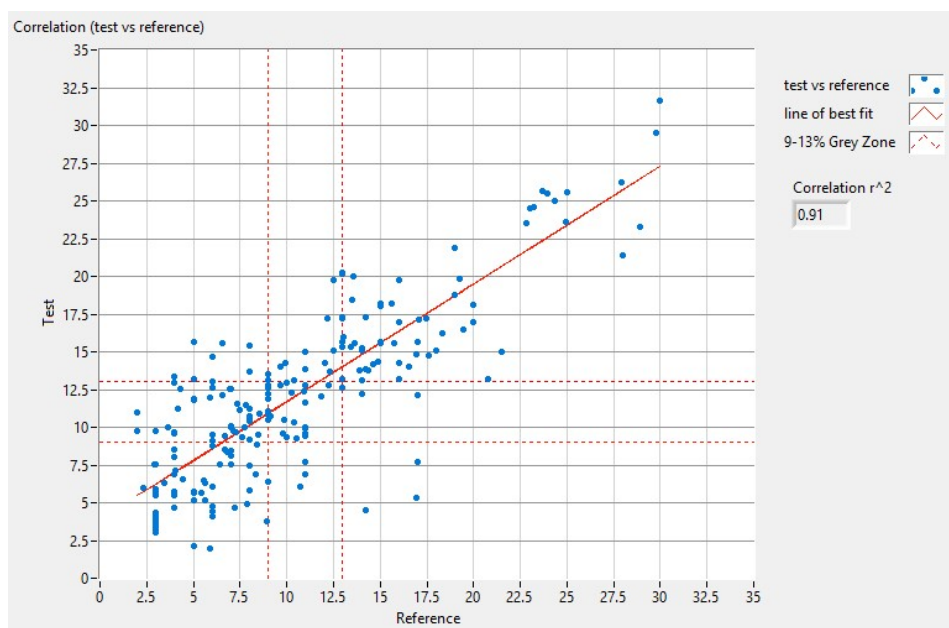


Figure 38. Correlation plot $\%PPV_{test}$ vs reference $\%PPV_{rec}$

Figure 39 below shows the Bland Altman plot for the $\%PPV_{rec}$ vs $\%PPV_{test}$, twelve paired outliers are outside the two standard deviations, or 95% percentile limit, similarly, the error is 5.7%.

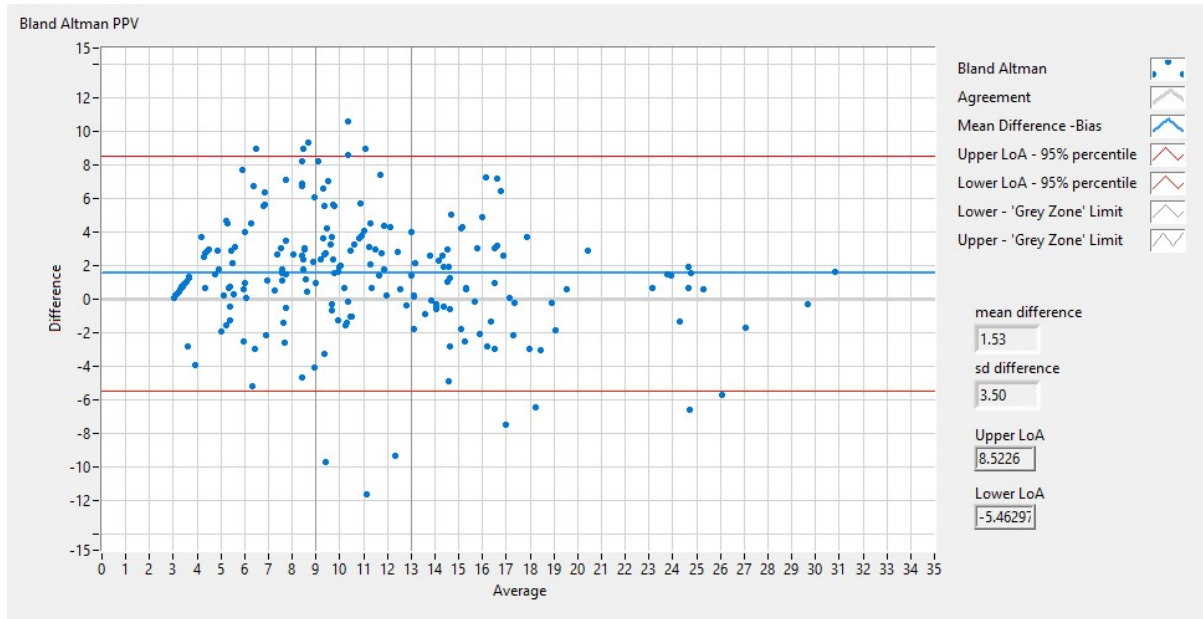


Figure 39. Bland Altman plot $\%PPV_{test}$ vs reference $\%PPV_{rec}$

7.2 Clinical Results $\%PPV_{Aboy}$ vs $\%PPV_{rec}$

The next set of graphs shows the comparison of the developed Aboy algorithm against the recorded data from the Philips Monitor. Figure 41 below shows the developed Aboy method correlated to the data recorded from the patient monitor.

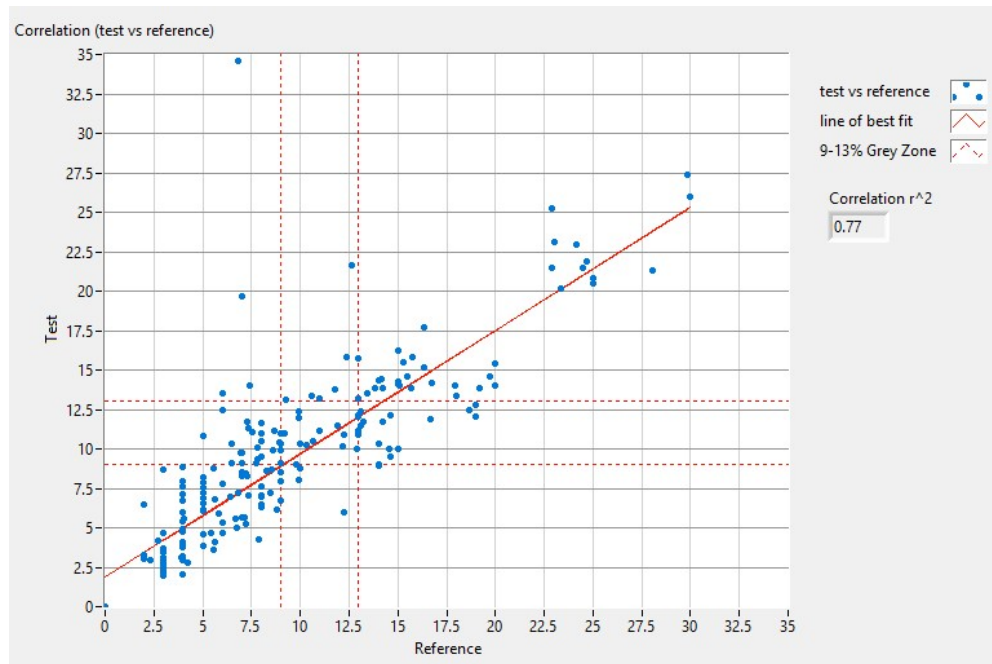


Figure 40. Correlation plot $\%PPV_{Aboy}$ vs reference $\%PPV_{rec}$

Figure 41 below shows the developed Aboy method Bland-Altman plot compared to the data recorded from the patient monitor. There was a negligible mean bias, and the standard deviation of the difference between methods was 5.03%. There is an 1.0% increase of responders, an increase of 4.1% non-responders and a 10.2% decrease in samples within the “grey zone” across the dataset. The overall change in any type of classification comparing the two datasets 19.1%

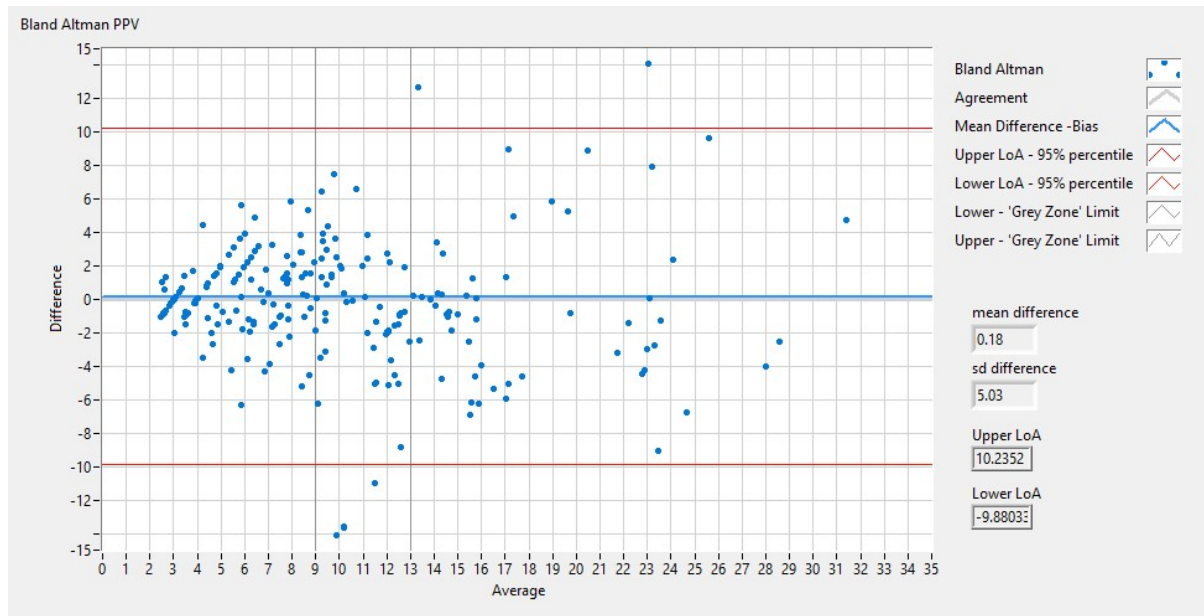


Figure 41. Bland-Altman plot $\%PPV_{Aboy}$ vs reference $\%PPV_{rec}$

8.0 Discussion

Most of the work completed in this thesis is software development, and many challenges were faced to achieve this goal. The clinical results show that the data collection software works well, and our attempt to replicate the Aboy algorithm is to a degree acceptable, based on method criteria as outlined in Section 6.1.3. An attempt using a test algorithm as a novel method of calculating PPV also provided a similar result to the developed Aboy algorithm: for the overall misclassification of fluid responsiveness. However, both methods were unable to match the performance of the algorithm used by the Philips patient monitor. This section will start with a discussion regarding the development of the communication software and Aboy algorithm, followed by clinical results observations, and finally, using observations to suggest future development.

8.1 Software Development

Previously it was mentioned that LabVIEW programs had been written to connect to and access data from two other types of patient monitors. The communications protocols of these monitors were relatively simple, and data could be parsed easily for storage. However, even with these earlier attempts providing a good programming basis, the task of communicating with the Philips Intellivue monitor was difficult. But the success of creating the program ensures that it could be used to collect the many other hundreds of parameters for future research.

For the development of the Aboy algorithm, the difficulty was to create Virtual Instruments that would replicate not only the steps of the Aboy et al. method but replicate what is happening inside the circuitry of the Intellivue monitor, with a blood pressure signal that had been pre-processed by the monitor. Assumptions have been made, regarding both the use of the Aboy et al. method in the Intellivue monitor and whether the signal output from the monitor is of high enough quality, and in some way, the results reflected the difference or errors in signal quality.

8.1.1 Data Collection Software Sub-VI

The Philips Intellivue monitor is used throughout the hospital environment. Critical care areas, including operating theatres and ICU, require only particular parameters and waveforms to be displayed or stored. Accessing these at a later time or date may be necessary for clinical reasons, and therefore monitors are networked and connected to databases for storage. The Philips Intellivue Data Export Interface Programming Guide [49] was designed to allow access to the processed signals; these could be polled and displayed on a central monitor in an ICU nurses station, or stored short term in a small database for access during the patients stay.

Since the signals are only used for display or storage, they are not raw signals; therefore, much of the filtering and smoothing to remove artefacts or environmental noise is already performed, and some data compression with loss of raw signal may have occurred. Sampling rates for the output signals are lower than would be necessary to see all of the parts of a waveform, this introduces additional loss of information that, depending on the research, may be required. Finally, the waveforms are then displayed or stored digitally, and to do so can introduce quantization noise; if the waveforms are re-sampled for research purposes, a small amount of fidelity will again be lost. It was not apparent in the Data Export Guide how many bits of information were used to construct the signal, and therefore, however small this error, it was not taken into account in the comparisons we made of our method PPV outputs against PPV from the Intellivue.

The Intellivue monitor has two output ports, RS232 and UDP, according to the Data Export Guide. For the scope of this Thesis, only UDP communications were accessible as, and after many attempts, it was clear that *Cyclic Redundancy Check* (CRC) used with the MIB/RS232 protocol could not be determined. Possibly failure to understand RS232 CRC description in the data export protocol is the reason why so few researchers have been able to access information in this way, and that only Philips authorised proprietary vendors have been able to fully utilise the RS232 output. It is fortunate for this study that the monitor was in an operating theatre, where the monitor situated on an anaesthetic machine did not have a network connection, and therefore the network port could be accessed by the laptop for data collection.

Finally, programming was made difficult because all messages and polled results were hexadecimal. The programming guide did give most descriptions; however, the programming guide is not complete, and some of the examples required considerable effort to reverse engineer. However, regardless of the difficulties, a program was written to access data using the LabVIEW programming language; so that any future attempts to collect blood pressure or any other patient parameters are now a possibility and this is a successful outcome of the current study.

8.1.2 Aboy Algorithm Sub-VI

Replicating the Aboy Algorithm required interpreting the step-by-step guide of Aboy et al. 2004, plus previous works as recommended were also consulted. Creating each step required the use of LabVIEW program basic signal connections and Sub-VIs, however, after completion, it was soon determined that however well the Aboy et al. steps were followed, for some patients the agreement was limited. The main focus became the use of filtering, and the effect this might have on the amplitudes of signals. However, although the Aboy method initially uses filters to determine the parameters for beat detection, the final detection is used on the raw signal. So, to help understand why the agreement

was limited, power spectral density was used to visualise the different ABP signals. When this was done, the components of the signal were not the clean amplitude-modulated simulated signal, but with physiological variation either beat-to-beat or breath-to-breath. Table 1 showed the different types of ABP signal.

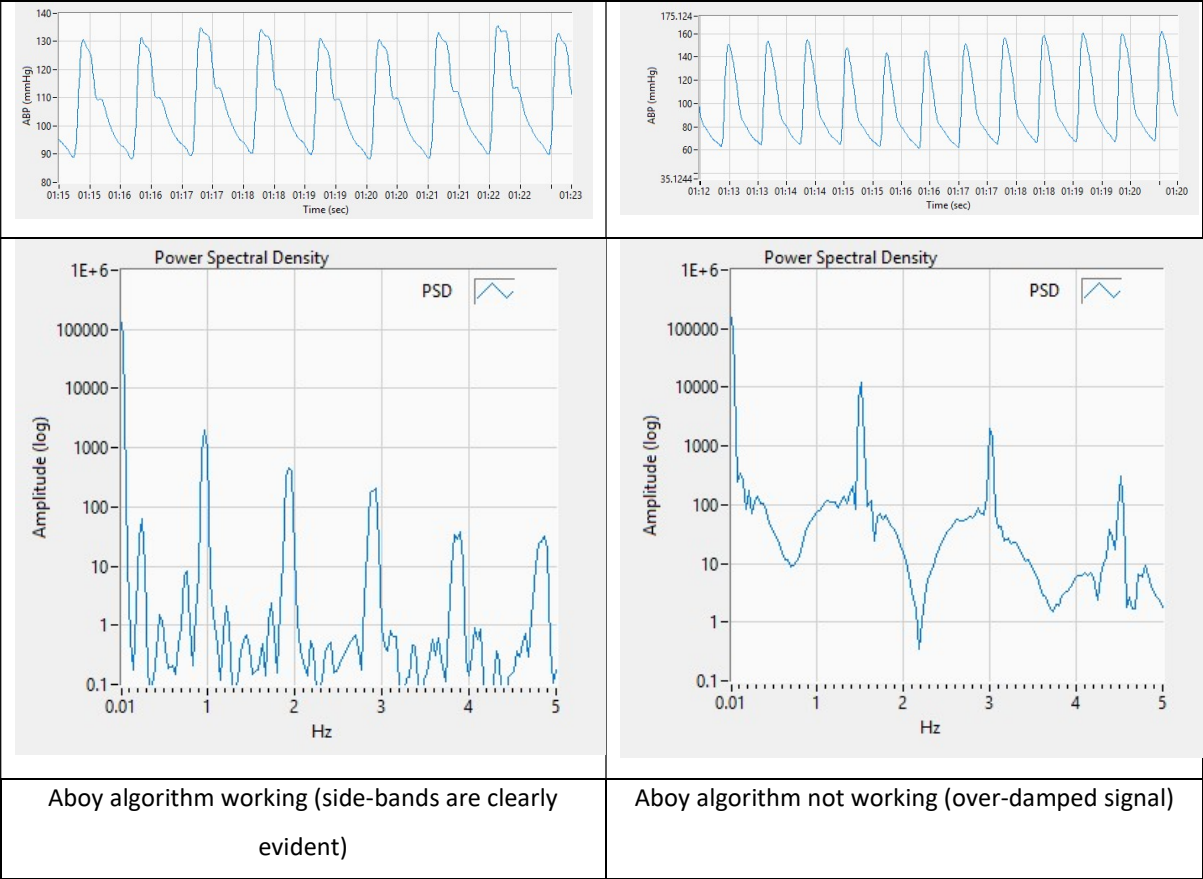


Table 12. Different PSDs for different wave-types

In many cases signals contained many harmonics, some with considerable power or artifact. On the left of Table 12 the Aboy algorithm is working because the respiratory sidebands are clear, on the right respiratory bands are unclear and the algorithm does not work. It was shown previously in Figure 29, that when spectral components for the second harmonic exceeded the first harmonic, large amounts of error could occur, and this is the case when there are no visible respiratory side-bands or other spectral components. Also, signal quality will compromise the ability for the Aboy to work well, examples shown in table 13.

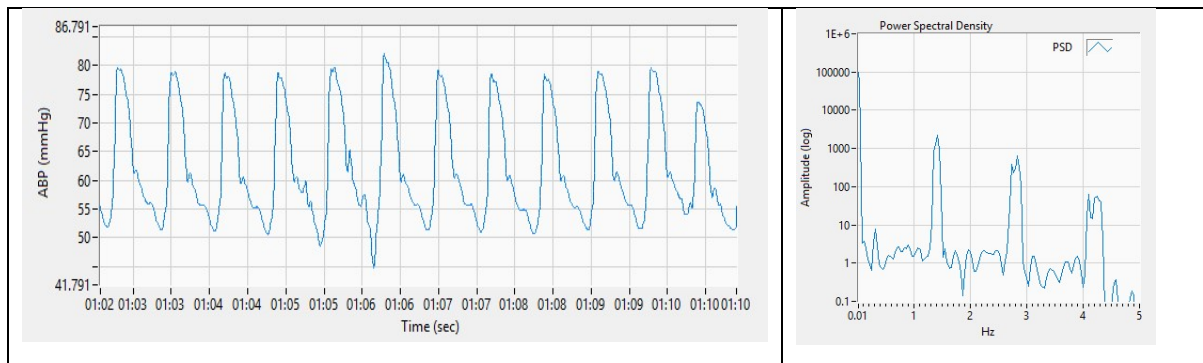


Table 13. Signal quality affected the ability of PPV Algorithm

The presumption of the Aboy et al. algorithm is that the ABP signal is amplitude modulated only at the respiratory frequency. What became apparent is that the additive effect of the respiration plus other harmonics made it difficult to determine the modulation amount and therefore, the amount of PPV using the Aboy method. Attempts were made to use band-pass filtering to remove the effects of respiration and harmonics; however, this also did not give the results required when compared to the Philips Intellivue PPV output.

This then brings into question whether the PPV from the Intellivue monitor is not processed in some other way before making the PPV calculation, as stated the Philips PPV is only *based* on the Aboy method and incorporates, in fact, something further to enable it to remove artefact and harmonic frequencies.

Finally, the lack of heart rate did affect the operation of the algorithm because heart rate is calculated from power spectral density for use in the algorithm filters, and the interbeat interval required for beat-to-beat nearest neighbour calculations. The lack of heart rhythm due to any type of reason meant the algorithm no longer had some inputs for it to work; the effect was that it would abruptly stop giving PPV values. Therefore, the Lead Investigators' observations that the Aboy drops out with even very brief and transient irregularities in heart rhythm were replicated after the creation of the algorithm.

8.1.3 Novel 'Test' Algorithm

The test algorithm is based on observations of the relative amplitudes of the HR and RR frequencies from a power spectrum. It was established in Section 4.2 that due to the relationship of Spectral Heart Rate and Respiratory Rate peaks, Equation (4) could become a surrogate for %PVV.

Most researchers, including Aboy et al. use the frequency domain to determine HR and RR frequencies but only to determine filter cut-off frequencies for their subsequent time-domain filtering. However, with the new test algorithm, the time-domain is not considered. Specific frequency-domain work has been performed by Thiele et al. [41]. Using a Spectral Peak Ratio (*SPeR*), Equation (13), for

consideration of the correlation of PPV from two separate sites (radial and femoral arteries) with SPeR, they concluded that it may offer a useful alternative to time-domain-based metrics.

$$SPeR = \frac{SP_{RR}}{SP_{HR}} \quad (13)$$

As previously mentioned, their reasoning was that the time-domain based estimates of respiratory variation such as PPV and SSV are dependent on the site at which they are measured, whereas frequency-domain estimates were not.

Thiele's work did not give a specific PPV value in calculations, but the novel test algorithm presented in this thesis estimates the PPV via equation (4), and Spectral Peaks provide relative information of the amount strength of a particular frequency.

Time-domain PPV equation (1) is calculated from the maxima and minima of the effect of the respiration on the blood pressure. In the time-domain calculations the blood pressure becomes modulated with an index-related strength of the respiratory frequency. Frequency-domain calculation does not rely on modulation but takes the ratio of the relative power of the HR and RR frequencies as they are measured within the blood pressure signal.

However, as previously mentioned, AM radio transmission uses amplitude modulation with a carrier at a fixed higher frequency since radio signals cannot be transmitted effectively at audio frequencies. In the case of PPV, the higher frequency "carrier" is constituted by the heart rate, and the lower frequency (modulation) is the respiratory rate. Heart rate and respiratory rate are much closer in frequency than typical AM radio frequency signals. The heart rate is not as constant as an AM carrier and has variability beat-to-beat, and this would appear as slight shifts of the heart rate frequencies. With the carrier now changing due to heart rate variability this would also be similar to a form of frequency modulation.

With variability of the heart rate frequency the spectral ratio required for the test method equation (4) will be affected. Moreover, the test algorithm is also affected by issues similar to the Aboy method as HR and RR frequency peaks are susceptible to signal dropouts, complex physiological inputs, under/overdamping of BP, poor signal quality, noise and other artefacts. However, this simple test algorithm was able at times to estimate PPV and further work in the frequency domain is encouraged.

8.2 Clinical Results Observations

The mean bias in PPV of 1.5% shown in Figure 40 between the spectral power test Algorithm method and the Philips Intellivue may reflect one of the limitations of the test method theory, that is, that the formula used equation (4) recovers a given simulated level of PPV specifically where the variation in systolic and diastolic pressure is identical, as illustrated in Figure 37. Other possible types of pulse pressure variation, for example, purely systolic pressure variation, will produce different results.

Another factor found in the simulation was the presence of harmonics in the pulse pressure signal. With 36.4% pairs of data changing classification between responders, non-responders or grey zone, the simplistic model was unable to work in the presence of harmonics and other noise in the recorded signal. In exploring our test method, using measured spectral power, we took advantage of the simultaneous presence of the downloaded capnograph waveform to identify the primary respiratory frequency to minimise the risk of serious error in the calculation of PPV from the presence of strong harmonics. Similarly, the heart rate was identified from the pulse pressure waveform. However, the presence of a second harmonic did cause some overestimation of PPV relative to Philips Intellivue.

Given that the agreement between the Philips Intellivue PPV and our Aboy PPV was imperfect, for the reasons discussed above, the agreement of the Spectral power test method with the Philips Intellivue PPV appears to be as good as can be expected using real physiological signals in the clinical environment. From the point of view of clinical management implications, the 5.7% misclassification rate in predicted fluid responsiveness we found is likely to be seen as clinically acceptable given the imperfect nature of patient monitoring and fluid and volume status assessment using currently available tools.

The potential for the Spectral power test method to deliver reliable estimates of PPV and fluid responsiveness in the presence of irregularity in heart rate and respiratory rate is worthy of further exploration. Certainly, the Aboy method implemented in the Philips Intellivue monitor fails to deliver a PPV value with only brief changes in heart rate and will produce no PPV value at all in the presence of atrial fibrillation. The conditions required for the Spectral power test method to produce reliable PPV estimates are still to be determined. In particular, the required sampling time window to generate a reliable measurement in the presence of e.g. atrial fibrillation is likely to be quite wide, much wider than the 60-second window we used in our sample of patients who were all in regular sinus rhythm during the sampling period.

8.3 Other observations and improvements

Both the developed Aboy algorithm and the Test Method were able to work when the conditions of the signal supported the algorithm's construction. For the Aboy algorithm, there is a requirement for the signal to have a respiratory sideband (modulation) at the heart rate frequency. On the other hand, the Test Method model did not require any signal modulation at all: but only required good heart and respiratory rate peaks. During observations of the recorded waveforms, it can be seen harmonics affect the top and bottom envelopes differently, and mask the modulation and skew the amplitudes of the signal, the phase relationship of each of the component harmonics works differently on the top envelope when compared to the bottom. Figure 42. below illustrate normal patient data envelopes

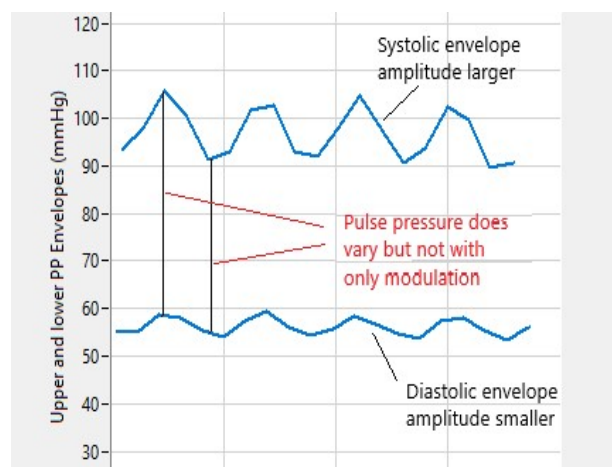


Figure 42. Patient data, normal pulse pressure with PPV \approx 30%

prior to subsequent de-meaning (inappropriate for the Aboy method). The test method envelope in Figure 43 below is comparable to Figure 42, except that when using the Aboy algorithm this will give a result of PPV \approx 0%; however, the shape and the type of envelopes can be said to be more representative of true physiological scenarios in comparison to the purely modulated waveform shown below in Figure 44.

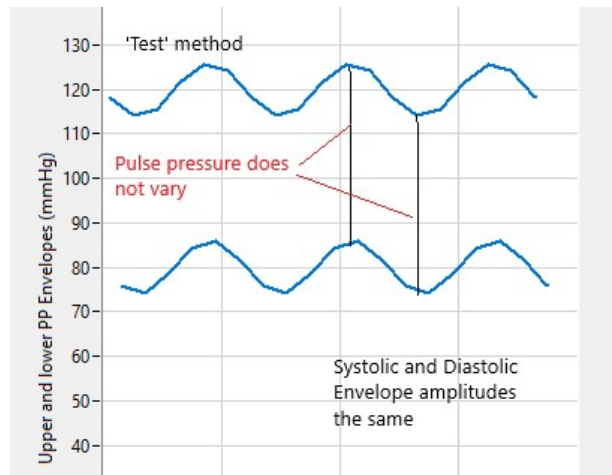


Figure 43. PP Envelope for Test method 30% envelope change

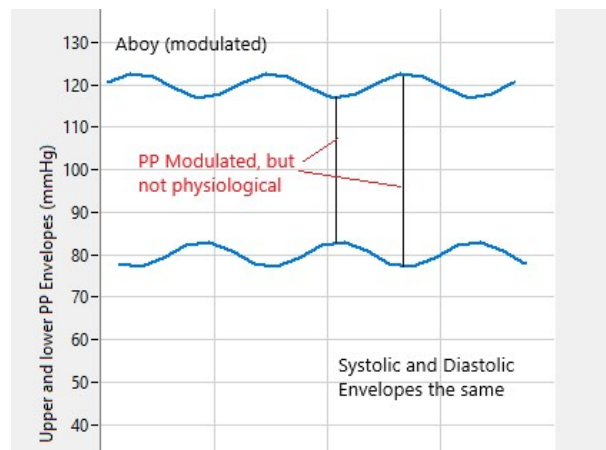


Figure 44. PP Envelope that satisfies Aboy algorithm PPV= 30%

After filtering harmonics, the patient waveform takes a shape similar to that of Figure 44. However, the wave is also modulated: the Aboy algorithm requires such modulation for its operation. Therefore, through the separation of waveform components, it may be possible for a hybridised model to be created to give a better PPV value by using the strengths of both methods to give a more stable PPV.

9.0 Conclusion

A system was successfully constructed using LabVIEW to interface and download waveform data, in real-time from the Philips Intellivue patient monitor, in an operating room environment. The system was implemented in ventilated patients undergoing surgery with invasive arterial blood pressure monitoring to conduct proof of concept testing of a method for estimation of PPV using analysis of Spectral power ratio at the cardiac and respiratory frequencies. This was found to have a clinically acceptable agreement with PPV delivered by the Philips Intellivue monitor with overall miss classification of 5.7%. Performance of both the developed Aboy algorithm and the test method did have difficulty replicating the algorithms used from the Philips monitor. However, from the results of the test algorithm, frequency-based methods are worthy of further investigation, as a clinical tool for estimation of fluid and volume status: during anaesthesia and critical care.

Appendix 1. Philips monitoring LabVIEW Documentation

This section comprises the various stages of LabVIEW circuits broken into different sections, some of which have been simplified. It also shows examples of each part of the code used to ensure to initiate and keep communication active whilst receiving and processing messages. Due to the nature and complexity of the protocol, some components of each LabVIEW virtual instrument (.vi) needed considerable research and trial before perfecting them. In addition, making a LabVIEW specific translation of a protocol designed for the C++ language also requires consideration for messaging and message creation in hexadecimal rather than the higher-level language.

UDP Communications

Required for opening UDP ports on the Philips monitor and Client PC, the Protocol requires that port 24105 could be used, and in this case, the monitor IP 10.0.0.2 is the address.

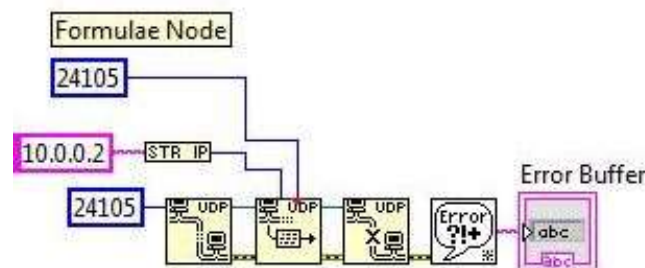


Figure 45. Initiate and Close UDP

However, since UDP communications are in real-time and filling the computer's read buffer, it is required that the data is received and processed by the LabVIEW VI in time to receive the next message; otherwise, the computer buffer will overflow, and packets will be lost.

To help overcome this, the computer's UDP buffer must be set to higher than that specified by a Windows system. This was only applicable to the Windows computer and was required to be removed from the Macintosh version of the software as buffering is done differently. See Figure 46 below.

Message format examples

All messages, whether sent or received, are in hexadecimal format contain information to parse as required. In some circumstances, it was not necessary to do so because standard requests matched examples within the protocol. However, when receiving messages, it was necessary to understand which part of the message had the information to extract.

Following are two examples of messages sent to the server from the laptop client. The first (Figure 49) is an association request that is quite standard except it was necessary to inform the server that real-time data instead of trend data was required and this required specific bits to be set towards the end of the message after the request is made the server responds and informs the client that this has been done.

Association Request

```
0DEC 0508 1301 0016 0102 8000 1402 0002
C1DC 3180 A080 8001 0100 00A2 80A0 0300
0001 A480 3080 0201 0106 0452 0100 0130 8006
0251 0100 0000 0030 8002 0102 060C 2A86 48CE
1402 0100 0000 0101 3080 060C 2A86 48CE 1402
0100 0000 0201 0000 0000 0000 6180 3080 0201
01A0 8060 80A1 8006 0C2A 8648 CE14 0201
0000 0003 0100 00BE 8028 8006 0C2A 8648 CE14
0201 0000 0001 0102 0102 8148 8000 0000 4000
0000 0000 0000 8000 0000 2000 0000 0000 0000
0001 002C 0001 0028 8000 0000 000F DE80 0000
3000 0000 3000 0000 0000 6000 0000 0001 000C
F001 0008 8800 0000 0000 0000 0000 0000 0000
0000 0000 0000 0000 0000
```

Figure 49. Request to start communication

Another example Figure 50 shows a single poll data request that tells the server to send all Numeric data available when available or the next poll period.

Single Poll Data

```
E100 0002 0001 001C 0001 0007 0016 0021
0000 0000 0000 0000 0C16 0008 0001 0001
0006 0000
```

Figure 50. Single Poll Data (numeric)

Deconstructing wave signal

The following is a breakdown of a sample waveform data for blood pressure, and the client is to parse this information quickly, parameters are in red and described in italics. Not all parameters have a meaning, and the programming guide recommended to be careful to parse signals correctly.

E100 0002 0002 01F0 0001 0007 01EA 0021 0000 0000 F13B 01E0 0001 0040 000B 6000 FFFF FFFF FFFF FFFF 0001 0009
0000 0002 01C6 0000 0000 0000 0001 0003 01BA 0423 0001 004A – *Header information*

0356 000F 0134 – *Unknown*

Following is information describing how to display the Arterial Blood pressure:

0921 0002 0356 – *Object Handle*

092F 0004 0001 0009 – *Object Type*

093F 000C 0000 0800 0001 4280 0000 0000 – *Metric Specification*

096D 0006 0020 100D A000 – *Array specification – 16 bit Smooth Curve static scale with 14 significant bits*

098D 0004 0000 0040 – *Samples 64 per second*

0924 0004 0002 4A14 – *Label ID – this is Arterial Blood Pressure*

0927 0010 000E 0041 0042 0050 0020 0020 0000 – *Label - ASCII A.B.P.*

0996 0002 0F20 – *dimension - mmHg*

0911 0002 0001 *color - red*

0964 0010 0000 0000 0000 0078 0320 0AA0 0280 0001 – *sample array calibration specification from 0 to 7,*

0940 0002 0000 *Metric State - ok*

096F 000C 00FF FFD8 0000 0208 00A0 23A0 – *lower -40 to upper 520, 160 to 9120*

096A 0004 0260 0C60 – *Physiological range of scaled values 608 – 3186 (of 12 bit sample)*

091A 005C 000B 0058 0000 0000 0320 0000 0000 000C 03E0 0002 0000 0018 04A0 0002 0000 0024 0560 0002 0000 0030
0620 0002 0000 003C 06E0 0001 0000 0048 07A0 0002 0000 0054 0860 0002 0000 0060 – *boundaries of grid to display on
the monitor*

0920 0002 0000 006C – *unknown*

09E0 0002 0000 0078 – *unknown*

0AA0 0000 096E 0046 4A14 8000 0040 0A9D 0A9D 0A9D 0A9E 0A9D 0A9D 0A9D 0A9D 0A9D 0A9D 0A9C 0A9C 0A9C
0A9C 0A9C 0A9C 0A9D 0A9D 0A9D 0A9D 0A9E 0A9E 0A9D 0A9D 0A9D 0A9D 0A9C 0A9D 0A9D 0A9D 0A9D – *waveform data
32 Samples returned*

Numeric Data - Float Conversion

All numeric data is in a 32-bit float, and a VI was required to be designed to handle the range of numbers available using a 32-bit wide place holder structure with an 8bits signed exponent MSB, 24-bit mantissa bits upper part, signed plus lower 24 bit, signed LSB.


```
typedef u_32  FLOATType;
```

The FLOAT-Type must be interpreted as follows:

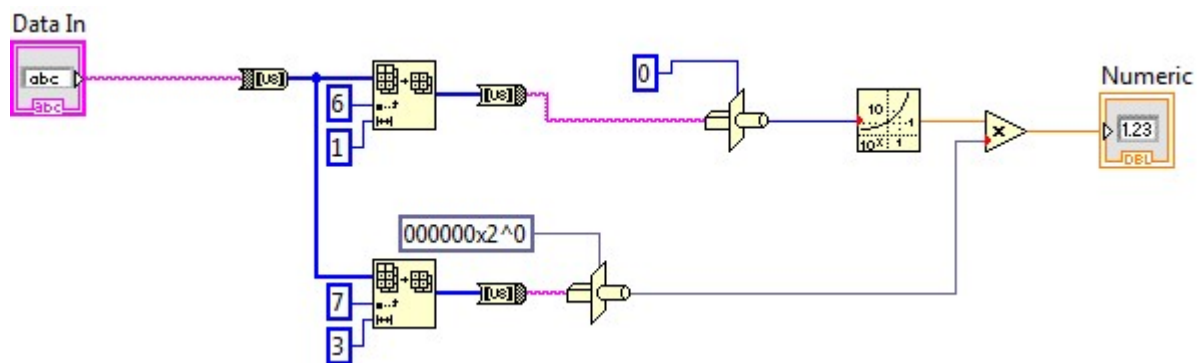
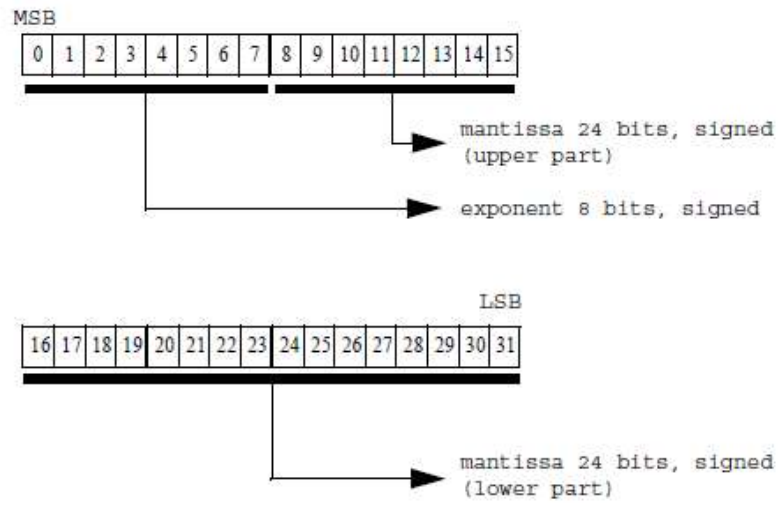


Figure 51. Vi for conversion from 32-bit hex to float type numeric display

Timing

The Intellivue monitor uses Absolute and Relative time to give information to the Client; however, the Absolute time is only given during Association request and is based on milliseconds since the 1st of January 1970. Relative time in milliseconds is provided after this time to when the monitor is cold booted; however, the minimum time capable of receipt is 2ms division. Conversion of a relative timestamp to the current time is still a challenge that has not been completed; however, the relative time is calculated as follows.

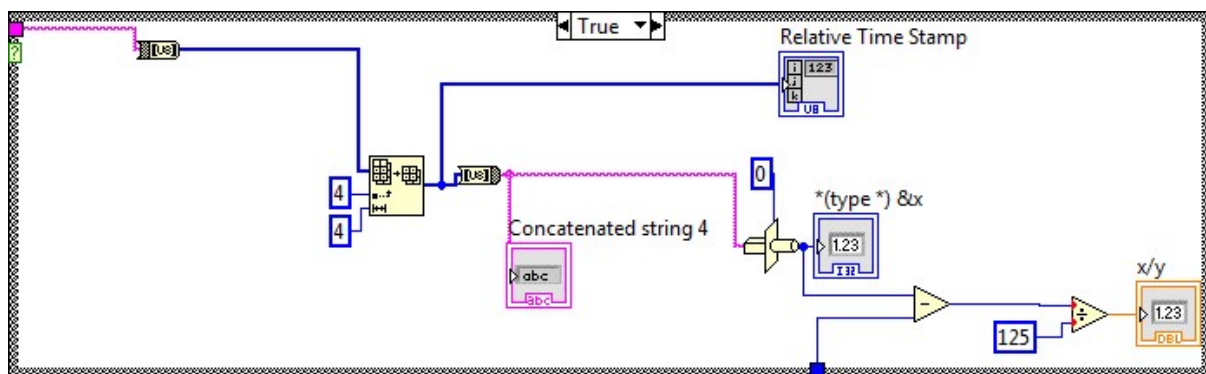


Figure 52. Conversion of relative time Hex to Integer data in milliseconds

Selection of Wave and Numerical Data.

To limit the amount of data to be parsed by the client monitor, Wave and Numeric polling requires the message to be created from the selected list of available parameters. However, to do this, there is an available bandwidth limit. The following table shows the limits and indicates that some wave data may be returned as a part of an array.

Wave Type	Sample Period	Sample Size	Array Size	Update Period	Bandwidth Requirement ¹
500 samples/s (ECG)	2 ms	16 bits	128 samples	256 ms	1064 bytes/s
250 samples/s (Compound ECG)	4 ms	16 bits	3*64 samples	256 ms	1640 bytes/s
125 samples/s	8 ms	16 bits	32 samples	256 ms	296 bytes/s
62.5 samples/s	16 ms	16 bits	16 samples	256 ms	168 bytes/s

Table 14. Polling frequency and sample period and size

However, it is common that there can be two ECG waves, and five other waves are polled as a maximum. The selection of waves is made by sending a request for the polling table priority to be set

differently to that decided by the monitor. Also returned numerical data can be set to reduce the number of packets that must be parsed by the client.

A means of creating a polling message is required, and this needs to have the ability to incorporate all the message length information so that the polling message meets the programming rules.

The following VI, Figure 53, takes the requested parameters and creates the polling message for real-time waveforms.

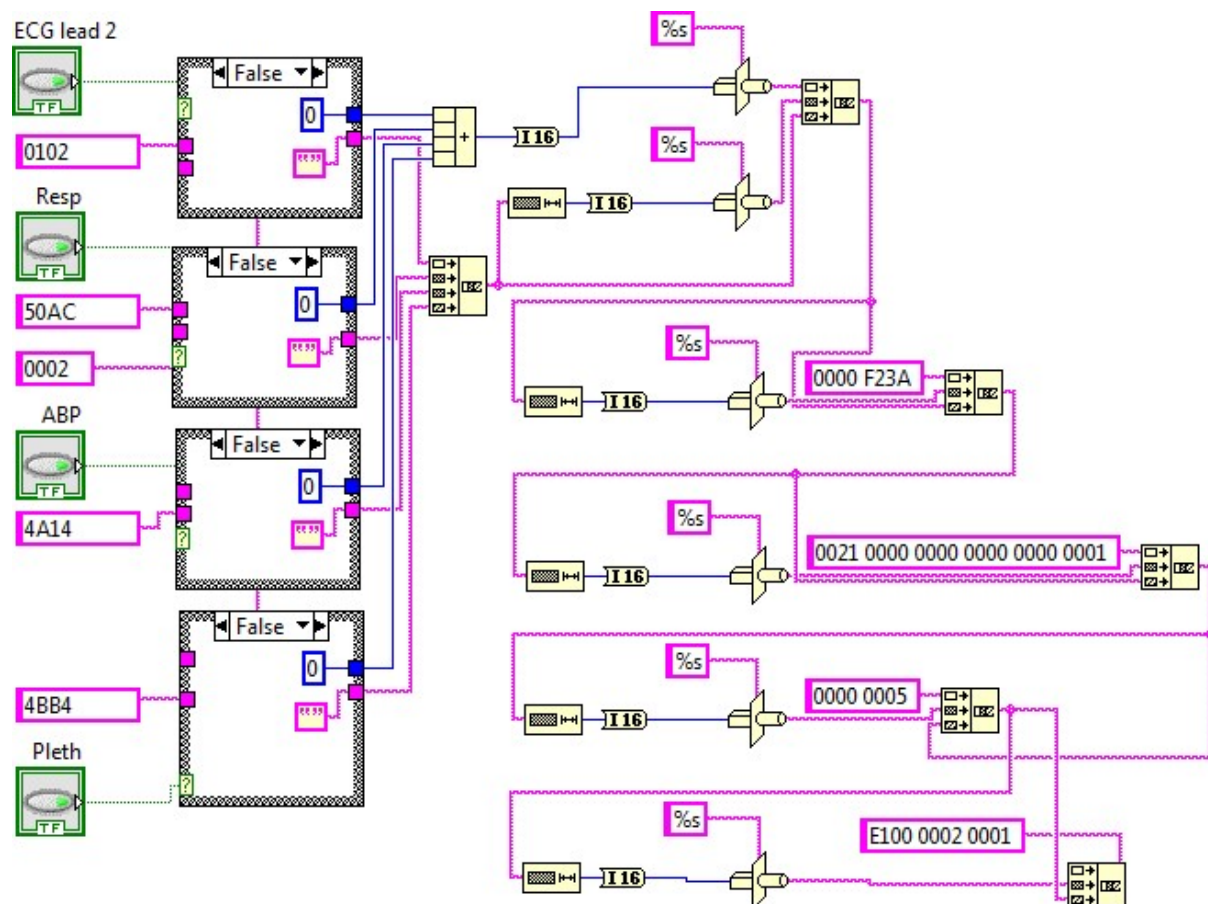


Figure 53 Selection of polled waveforms and numerics

Data recording

The final part of the project is recording waveform to excel file for later use this is currently achieved by a simple method of writing directly to an opened file. Figures 54 and 55 show the code and the resultant output.



Figure 54. Writing to *.CSV file

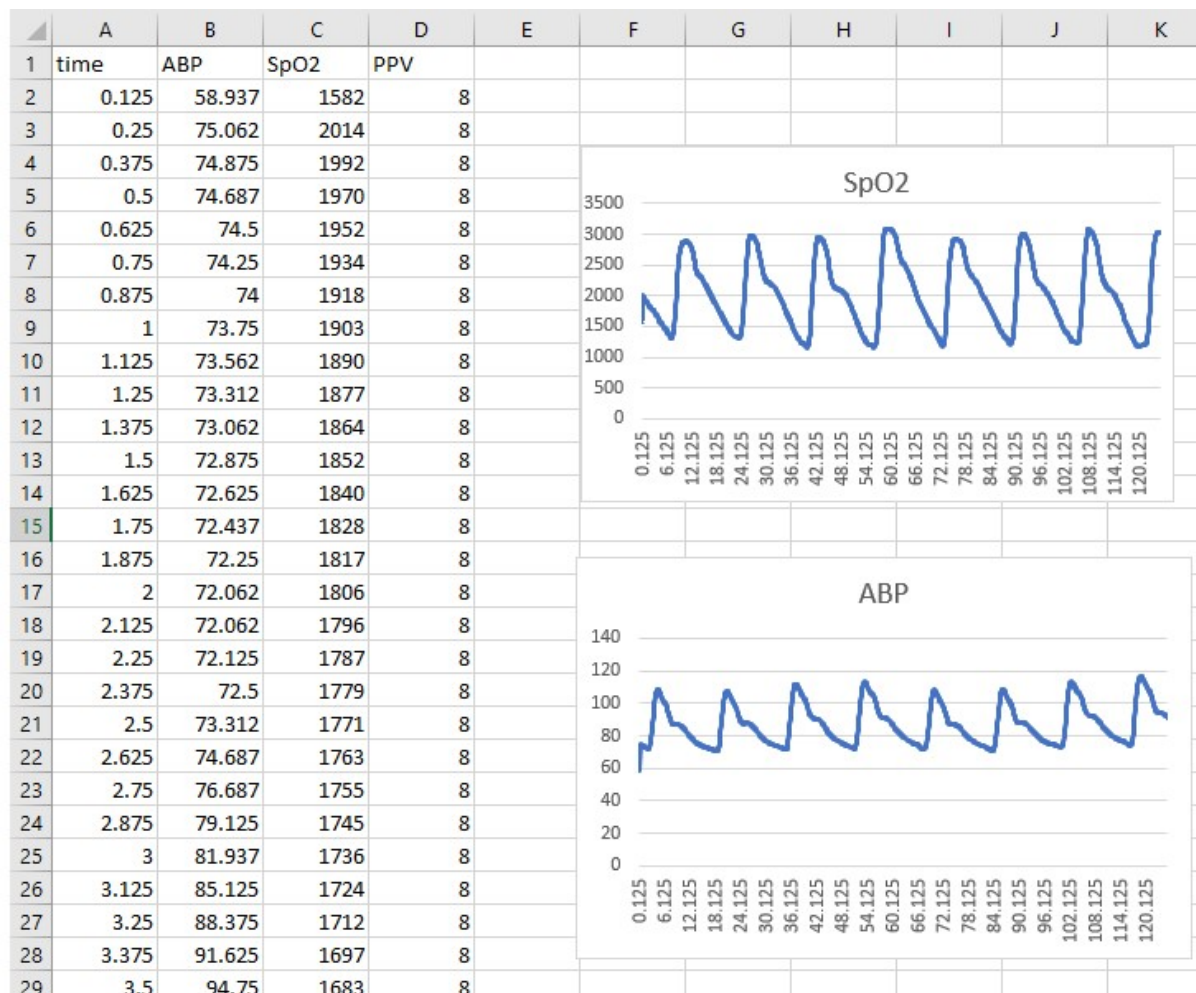


Figure 55. Sample Excel data recorded from the monitor

Appendix 2 – Aboy Algorithm coding

Below are Figures 56 and 57 are examples of coding and Sub-VI front panel, respectively.

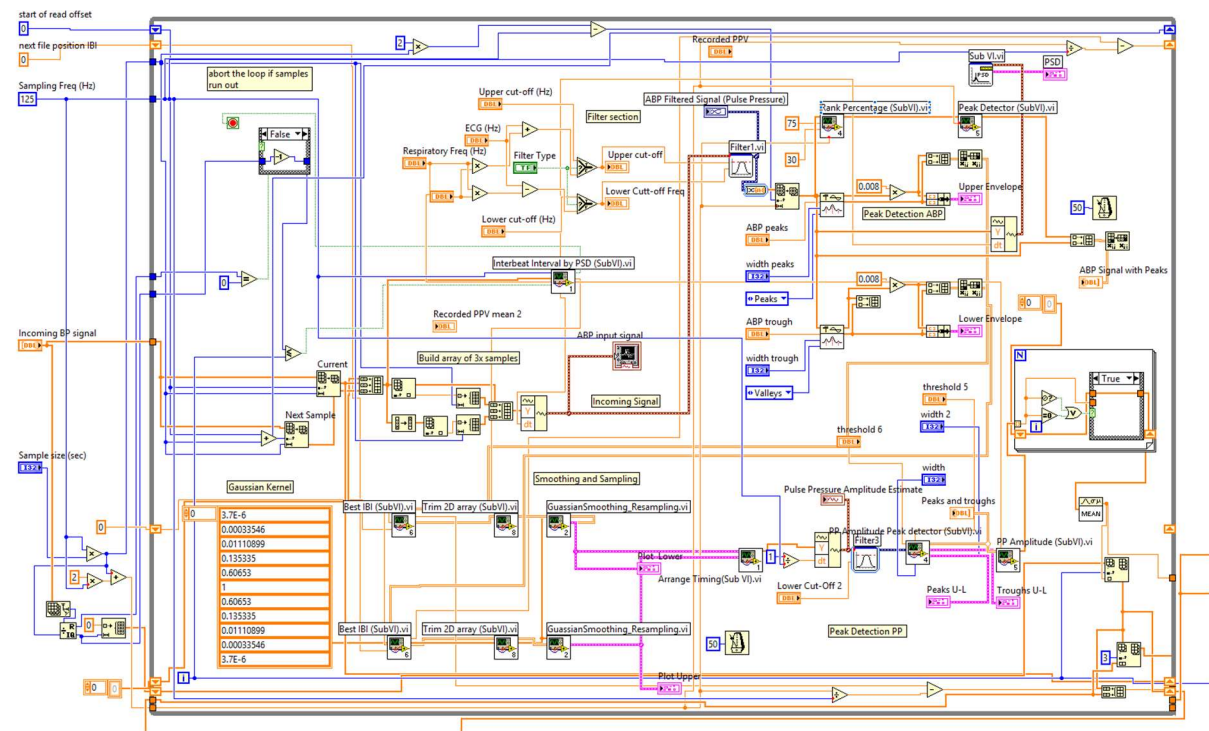


Figure 56. Aboy Algorithm Sub-VI coding snippet

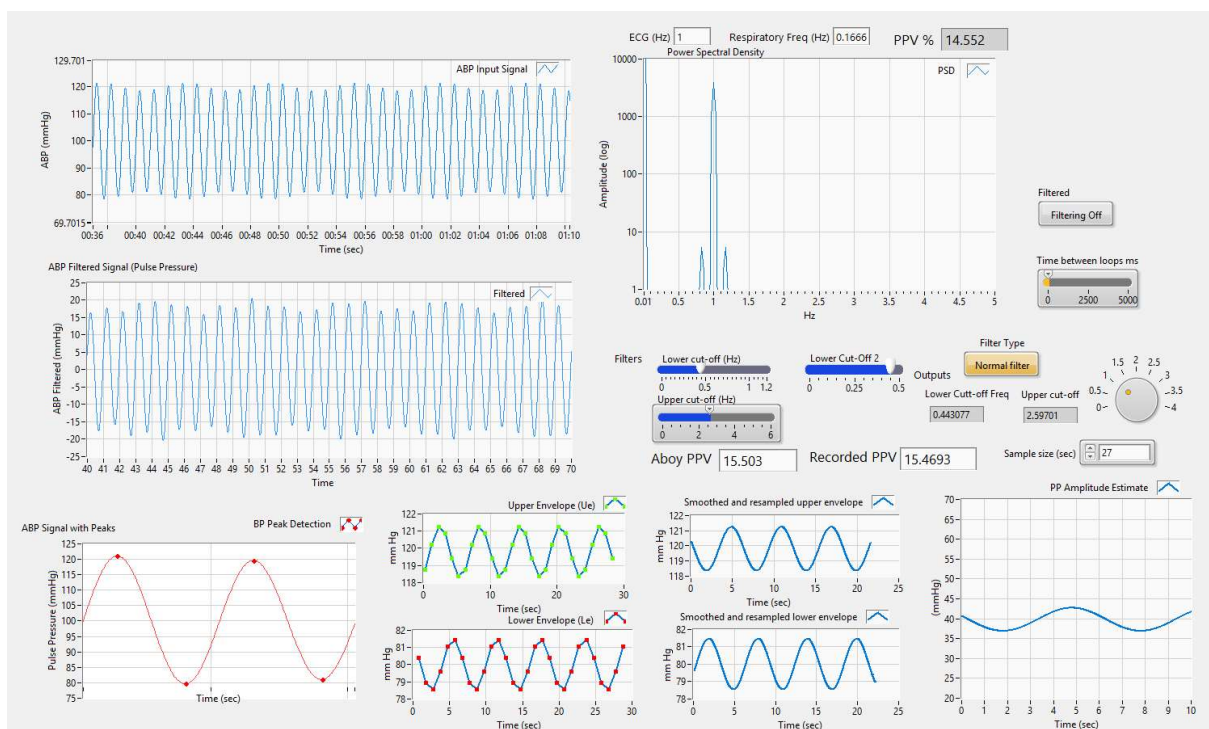


Figure 57. Front panel created for Aboy Algorithm thesis

Appendix 3 – Communication with Other Monitors

Waveform and Patient Data Acquisition with CO2SMO+ with Results

There is a requirement therefore in the first instance to access CO2 waveform, plus the VCO2 and SpO2 waveforms. The following is part of the method to achieve this, please see Figure 1 for a copy of the VI made in LabVIEW.

Streaming data is sent via RS232 when a control signal is sent to the CO2SMO+ to start the process.

Start Waveform/Data Mode (Command B0h)

Command:

B0h - NBF - WMB - [DP1 - ... - DPn] - CKS

Command Type:

Continuous Response Command

Response:

B0h - NBF - WMB - WMV - DPV - DP1 - ... - DPn - CKS

In the “Response” allows for multiple waveforms WMB (Waveform) and DP1 to DPn (Patient Numerics)

Waveforms are continuous; however, there is a control signal (every 100 samples/ for timing) and Patient Parameters (numeric) are interleaved with the waveform at the start of inspiration (end of expiration).

The patient parameters are transmitted interleaved with waveform data starting at the start of inspiration of each breath. In cases of high respiration rate and/or a large number of patient parameter selections, transmitting all the parameters on a breath by breath basis may not be possible. In these cases, the selected list of patient parameters will continue to be transmitted through the next breath(s). When the full list of all patient parameters is transmitted, the next set of patient parameters will be sent beginning at the start of inspiration of the next breath.

After successfully interpreting this command, the Flow/CO₂ module will start the Waveform/Data Mode. A continuous stream of *Multi-Waveform/Data Mode* packets, Command B1h, will be transmitted to the host. The continuous data transmission will continue until the *Stop Continuous Mode* command, Command C9h, is received from the host.

Waveform Gaps with RS232

So there will be gaps in the waveform, and when the Parameter packets are sent these need to be dealt with but are to be expected, the waveform can be averaged or smoothed out. The important part is to make sure the waveform timing is complete.

One final issue is that the device will require a zero every 1-10 minutes depending on how its stability, this is to eliminate drift. This requires solenoids to open and will take 1-2 secs; during this time, the waveform will not be sent out.

VCO2

If we want VCO2 then we need to send the request for it to be sent in the Data Packet, DP1 = 82 and DP1 = 83

DPI = 82

Volume CO₂ Expired, per breath measurement (VCO_{2b})

Description: The volume of CO₂ in a breath is calculated by summing the product of CO₂ (in percent) and volume over the entire breath. The expired CO₂ volume is computed by calculating the total volume CO₂ and subtracting the inspired CO₂ volume to compensate for rebreathing. The Volume CO₂ Expired is reported in STPD units.

Resolution: 0.1 mL (0.0 - 800.0 mL)

Updated: each breath

Length = 2 bytes

Conversion = (128 * DP1) + DP2

DPI = 83

Volume CO₂ Expired, per minute average (VCO₂)

Description: The Volume CO₂ Expired is a moving average of the VCO₂ calculated per breath. The Volume CO₂ Expired is averaged over several different periods: 8 breath, 1 minute, 3 minute, 5 minute, or 10 minute, based on the settings in the Flow/CO₂ module.

Resolution: 1 mL/min (0 - 800 mL/min)

Updated: each breath

Length = 2 bytes

Conversion = (128 * DP1) + DP2

SpO2

If we want SpO2 is also a parameter and not a waveform, but if that is to be sent, then we need to request it as well.

DPI Parameter Table - Pulse Oximetry Specific Parameters

DPI = 10	<p><i>Pulse Rate</i></p> <p>Description: This parameter returns the pulse rate as read from the pulse oximeter. Pulse Oximetry hardware support is required for this parameter.</p> <p>Resolution: 1 beat/minute (30 - 250 b/min), 0 = invalid</p> <p>Updated: each breath</p> <p>Length = 2 bytes</p> <p>Conversion = $(128 * DP1) + DP2$</p>
DPI = 11	<p><i>O₂ Saturation</i></p> <p>Description: This parameter returns the oxygen saturation as read from the pulse oximeter. Pulse Oximetry hardware support is required for this parameter.</p> <p>Resolution: 1 % (0 - 100 %)</p> <p>Updated: each breath</p> <p>Length = 1 byte</p> <p>Conversion = DP1</p>

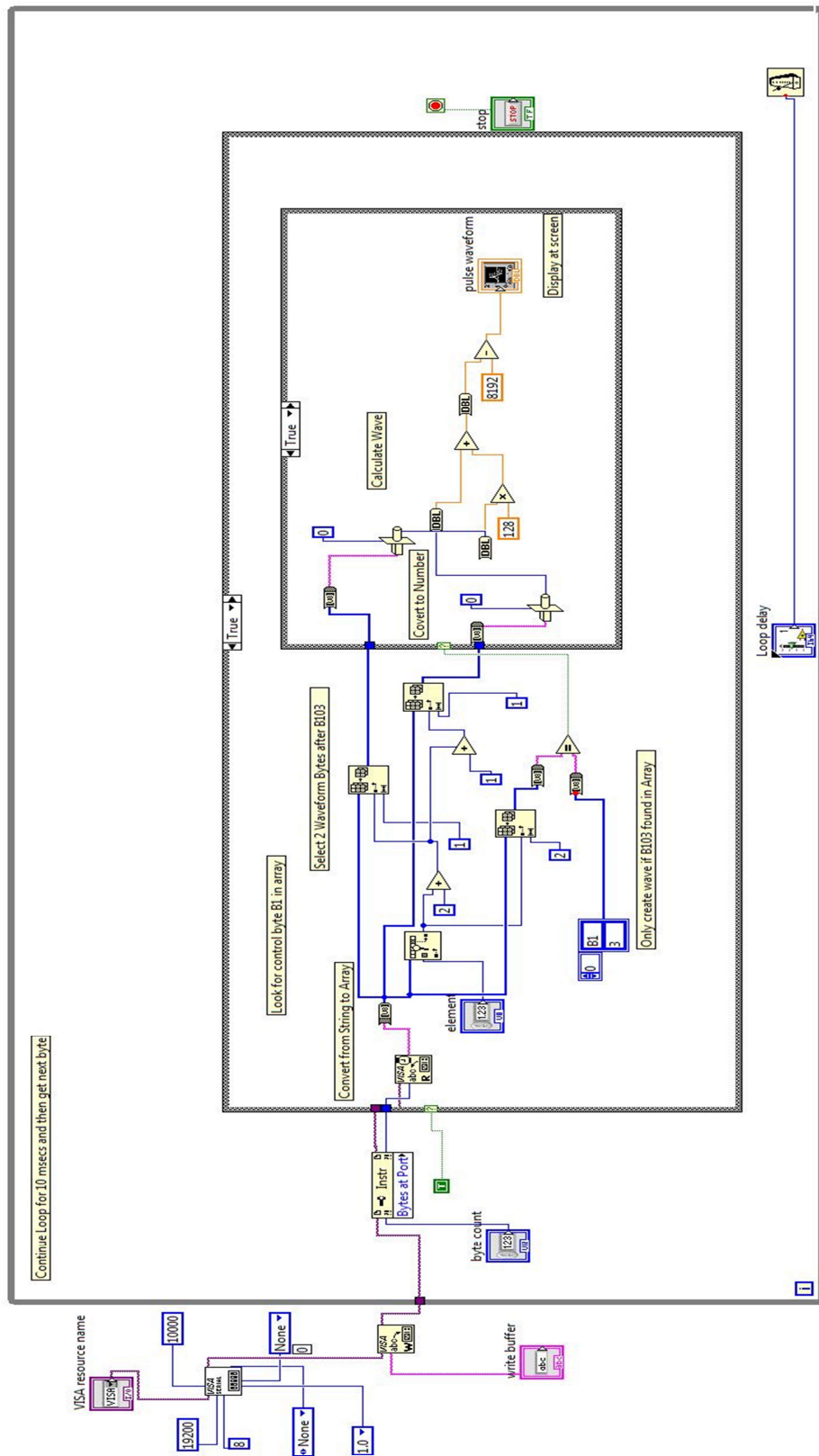


Figure 58 Sub-VI for CO2 wave capture

The resultant waveform in real-time is, as shown in Figure 60.

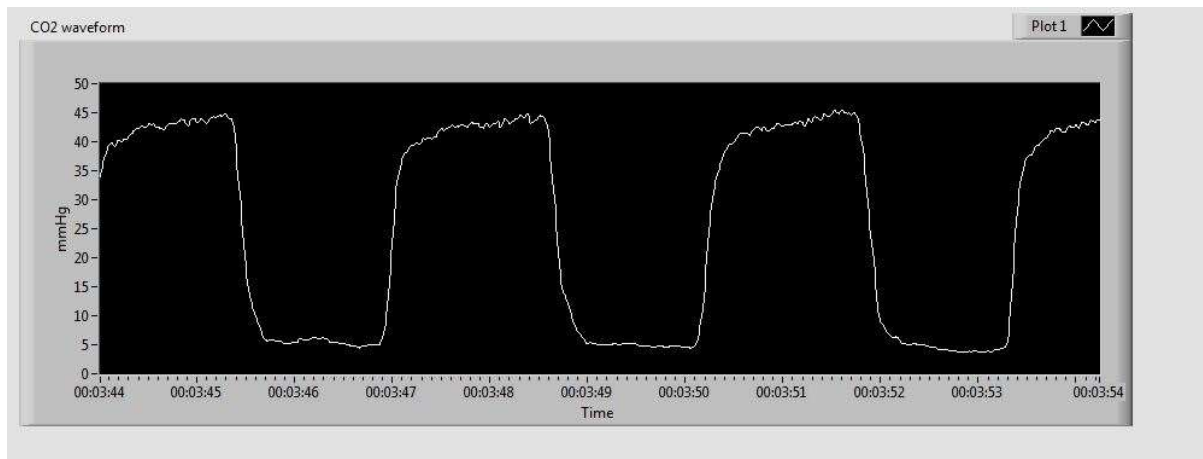


Figure 59. Resultant CO2 waveform

It was decided by Lead Investigator that this waveform was acceptable the VI was subsequently placed into the existing program used for the "Capnotracking" method. However, there is some issue with the VISA usage with the Apple computer compared to the PC and therefore, more work is required.

The NOVAMETRIX unit will be used as a portable version for research until the Philips Monitoring is ready for use during surgery for Cardiac output determination.

Waveform and Patient Data Acquisition with GE Patient Monitor

After initially spending a great deal of time trying to work through the protocol of the Philips Monitor it was decided to pursue the GE monitor that had been supplied by GE Medical. The interest from GE is that if the software could be developed and shown to work using their monitor, then the future possibility of this being included in an anaesthetic machine may result.

Work to date has been the ability to easily connect to the monitor via RS232 because the protocol has in-built handshaking and therefore it worked on the first go using proper cabling.

Where the project is at the moment for waveform and data extraction from the GE monitor for future work is that programming is in HEX code very similar to that used by the CO2SMO+. The code structure

is like standard C+ programming, but the actual coding for LabVIEW requires that in some cases, individual bits be recognisable and decoded to make sure the wave or numeric data is easy to extract.

Example code: this starts allows data to be extracted

How to request displayed values (DRI_PH_DISPL)

Example code for generating the request:

```
struct datex_record requestPkt;
struct dri_phdb_req *pRequest;
// Clear the packet
memset(&requestPkt, 0x00, sizeof(datex_record));
// Fill the header
requestPkt.hdr.r_len = sizeof(datex_hdr) +
sizeof(struct dri_phdb_req);
requestPkt.hdr.r_maintype = DRI_MT_PHDB;
// The packet contains only one subrecord
// 0 = Physiological data transmission request
requestPkt.hdr.sr_desc[0].sr_type = 0;
requestPkt.hdr.sr_desc[0].sr_offset = (byte)0;
requestPkt.hdr.sr_desc[1].sr_type =
(short) DRI_EOL_SUBR_LIST;
// Fill the request
pRequest =
(struct dri_phdb_req *)&(requestPkt.rcrd.ph_rcrd);
pRequest->phdb_rcrd_type = DRI_PH_DISPL;
pRequest->tx_ival = 10; // 10 = 10s interval
pRequest->phdb_class_bf =
DRI_PHDBCL_REQ_BASIC_MASK | DRI_PHDBCL_REQ_EXT1_MASK |
DRI_PHDBCL_REQ_EXT2_MASK | DRI_PHDBCL_REQ_EXT3_MASK;
```

Hexadecimal representation of the request:

```
7e 31 00 00 00 00 00 00 00 00 00 00 00 00 00 00
00 00 00 00 00 00 00 ff 00 00 00 00 00 00 00 00
00 00 00 00 00 00 00 00 00 00 01 0a 00 0e 00 00
00 00 49 7e
```

Figure 60. GE Code Example Code sample

After some investigation, the GE monitor it became apparent the coding was more complex than the CO2 monitor. However, it was intuitive, and after interpretation of the code methods it be could be determined that with the correct request messages, subsequent physiological output was sent.

Numeric data would be sent if it were displayed on the screen, whereas a call for Wave data was required however this was returned

```

START PRESSURE WAVEFORM
7E48 0000 0000 0000 0000 0000 0000 0001 0000
0000 0000 FF00 0000 0000 0000 0000 0000 0000
0000 0000 0000 0000 0004 FF00 0000 0000 0000
0000 0000 0000 0000 0000 0000 0000 0000 0000
004B 7E

STOP WAVEFORM
7E48 0000 0000 0000 0000 0000 0000 0001
0000 0000 0000 FF00 0000 0000 0000 0000
0000 0000 0000 0000 0001 0000 00FF 0000
0000 0000 0000 0000 0000 0000 0000 0000
0000 0000 0000 0000 0048 7E

STOP DATA
7E31 0000 0000 0000 0000 0000 0000
0000 0000 0000 0000 FF00 0000 0000
0000 0000 0000 0000 0000 0000 0001
0000 0000 0000 0000 317E

DATA
7E31 0000 0000 0000 0000 0000 0000 0000 0000
0000 FF00 0000 0000 0000 0000 0000 0000 0000
0001 0A00 0E00 0000 0000 497E

START ECG AND IBP
7E48 0000 0000 0000 0000 0000 0000 0001 0000
0000 0000 FF00 0000 0000 0000 0000 0000 0000
0000 0000 0000 0000 0004 0001 FF00 0000 0000
0000 0000 0000 0000 0000 0000 0000 0000 0000
004C 7E

```

Figure 61. Hex commands for GE Carescape monitor for the initiation of Wave and Numerical data

After success with GE monitor, it is likely that this work may be useful to work by the Austin Hospital in the future but with the change to a second project, this work was not completed in entirety.

Appendix 4. Cyclic Redundancy Checks used in Philips Intellivue Monitor

Frame Check Sequence

The Frame Check Sequence FCS used by the Philips Intellivue Monitor is a slightly modified version of the Infrared Data Association Serial Infrared Physical Layer Link Specification Version 1.1, October 1995. Section 5.3.2.5 of this specification defines the binary polynomial that is used to determine the FCC.

Bits that are sent via RS232 or Ethernet are subject to distortion due to resistance, capacitance and inductance of the cable and fittings or electrical interference from other sources such as electromagnetic fields.

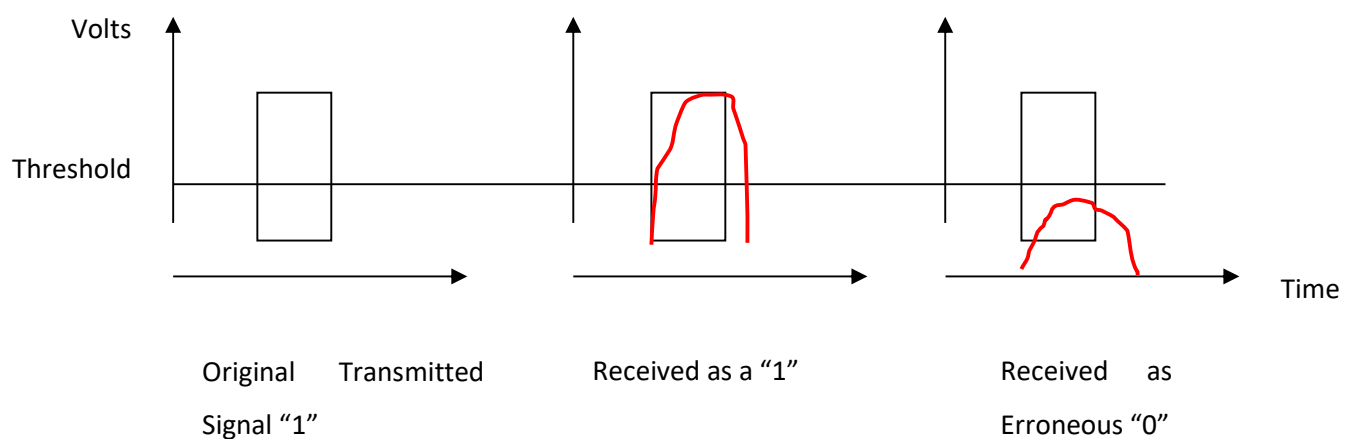


Figure 62. Electrical interference on the bit

Parity Bit

Originally schemes for packet checking included a parity bit, the simplest form of error detection. If a pattern of 7 bits is sent, then an 8th parity bit is included to ensure the byte is either odd or even in number of bits, depending on the parity scheme used.

For 7 bits and an Even Parity bit (>):

0 0 0 1 0 1 1 (1) parity bit, makes it 4 bits sent and therefore even

0 1 0 1 0 1 1 (0) parity bit, also makes it 4 bits sent and therefore even

On receipt, this simple method can be verified by checking if the byte is even in number of “one” bits.

However, this scheme is prone to error since during transmission if two or four or six bits where to change state, the received byte would still give a “correct” byte.

Therefore, more robust methods are employed that are more mathematically safer, and where the probability of an error due to the method is extremely small.

Simple Checksum

Better methods may be to sum to the bytes in a message and append the “checksum” to the byte, this is transmitted, and message checked on receipt. For one byte (8-bit) or modulo 256 checksums:

Message 6 23 4, and the checksum is 33 (6+23+4)

Sent packet: 6 23 4 33

Received packet: 6 27 4 33 (calculated Checksum is 37, therefore Error)

In this case, it is a safe error detection where the packet is determined to be faulty and a packet requested to be resent.

However, if the checksum (or the data) is incorrect such that the packet is a valid packet:

Sent packet: 6 23 4 33

Received packet: 6 27 4 37 (calculated Checksum is 37, in this case no Error)

Or Received packet: 3 27 3 33

Data corruption will occur if the method is still not robust enough; errors are unavoidable.

Cyclic Redundancy Check (CRC) Checksum

One byte or an 8-bit register will give a 1/256 chance of error not being detected, to improve these two bytes or 1/65536 chance for an error to go undetected in the checksum.

This is still better, but there is a good likelihood that random unsafe corruptions will occur, logically by making the register wider, the probability for error reduces, but computer processors only have a finite size processor, plus there is still a chance the error will go undetected. A better method is to utilize a mathematically strong method that allows for each individual bit to have an effect on the CRC for the FCS.

The method that employed is to take a “binary polynomial” (polynomial) and perform long division on the data, in the case of the Philips system it is performed on the header and user data and use the remainder of this binary - long division is the CRC for the FCS.

The width (W) of the CRC is obtained by appending the message (header + user data) with (W) zeros calling this M, then dividing the M by the polynomial G. The remainder is going to be of width W.

Binary long division uses an XOR function to subtract:

$$0-0=0$$

$$0-1=1$$

$$1-0=1$$

$$1-1=0$$

Also which number goes into another number during the long division is based around the order of magnitude of the highest bit being equal to or greater than the highest bit into the second number.

For example, W = 4 bits:

Original message : 11011

Polynomial (G) : 1011

Message after appending W (zeros) M= 110110000

111011 = Quotient (not used)

1011) 110110000

1011

1111

1011

1000

1011

0110

0000

1100

1011

1110

1011

0101 Remainder = CRC Checksum

Transmitted message would be Original Message + CRC = 11011+0101 or 110110101 without BOF and EOF.

The Philips Intellivue monitor utilizes a CRC-CCITT polynomial is chosen for and provides a 2 byte or 16-bit Width CRC:

$CRC(x) = x^{16} + x^{12} + x^5 + 1$: this is 11021 in hex, but as a 16-bit polynomial is required this reduces to:

This is 1021 in HEX or 0001 0000 0010 0001 in BINARY

The binary polynomials are chosen for their strength in detecting single and multiple error detection and the method of implementation in code where much of the work requires the use of XOR and shifting the register through the data until the CRC is calculated.

References

- [1] M. Aboy, J. McNames, T. Thong, C. R. Phillips, M. S. Ellenby, and B. Goldstein, "A novel algorithm to estimate the pulse pressure variation index ΔPP ," *IEEE Trans Biomed Eng*, vol. 51, no. 12, pp. 2198-203, Dec 2004.
- [2] M. Cannesson *et al.*, "The ability of a novel algorithm for automatic estimation of the respiratory variations in arterial pulse pressure to monitor fluid responsiveness in the operating room," (in eng), *Anesth Analg*, vol. 106, no. 4, pp. 1195-200, table of contents, Apr 2008.
- [3] M. Aboy, C. Crespo, and D. Austin, "An enhanced automatic algorithm for estimation of respiratory variations in arterial pulse pressure during regions of abrupt hemodynamic changes," *IEEE Trans Biomed Eng*, vol. 56, no. 10, pp. 2537-45, Oct 2009.
- [4] F. Michard *et al.*, "Clinical use of respiratory changes in arterial pulse pressure to monitor the hemodynamic effects of PEEP," *Am J Respir Crit Care Med*, vol. 159, no. 3, pp. 935-9, Mar 1999.
- [5] R. A. Massumi, D. T. Mason, Z. Vera, R. Zelis, J. Otero, and E. A. Amsterdam, "Reversed pulsus paradoxus," *N Engl J Med*, vol. 289, no. 24, pp. 1272-5, Dec 13 1973.
- [6] Gccwang, "Diagram of the circulatory system," *Diagram_of_human_circulatory_system.gif*, Ed., ed. Wikimedia Commons, 2014.
- [7] B. Medical, "Sectional Anatomy of the Heart," 600px-Blausen_0457_Heart_SectionalAnatomy.png, Ed., 0457 ed: Blausen Medical Communications, 2013, p. Heart Sectional Anatomy.
- [8] H. J. Guyton AH, *Text Book of MEDICAL PHYSIOLOGY*, 10th ed. (Heart Muscle; The Heart as a Pump). Elsevier, 2003.
- [9] D. Chemla *et al.*, "Total arterial compliance estimated by stroke volume-to-aortic pulse pressure ratio in humans," *Am J Physiol*, vol. 274, no. 2 Pt 2, pp. H500-5, Feb 1998.
- [10] F. Michard, "Changes in arterial pressure during mechanical ventilation," *Anesthesiology*, vol. 103, no. 2, pp. 419-28; quiz 449-5, Aug 2005.
- [11] M. Cannesson, M. Aboy, C. K. Hofer, and M. Rehman, "Pulse pressure variation: where are we today?," *J Clin Monit Comput*, vol. 25, no. 1, pp. 45-56, Feb 2011.
- [12] B. C. Morgan, E. W. Crawford, and W. G. Guntheroth, "The hemodynamic effects of changes in blood volume during intermittent positive-pressure ventilation," *Anesthesiology*, vol. 30, no. 3, pp. 297-305, Mar 1969.
- [13] J. Wiesen, M. Ornstein, A. R. Tonelli, V. Menon, and R. W. Ashton, "State of the evidence: mechanical ventilation with PEEP in patients with cardiogenic shock," *Heart*, vol. 99, no. 24, pp. 1812-7, Dec 2013.
- [14] RnCeus. ""Arterial Blood Pressure Monitoring". " <http://www.rnceus.com/hemo/artline.htm>
- [15] U. H. Solutions. ""Features of the Pulse Waveform". " <http://www.uhsmed.com/bp-management/features-of-the-pulse-waveform.php>
- [16] Gomersal C. ""Arterial Line Damping". " <https://www.aic.cuhk.edu.hk/web8/art%20line.htm>
- [17] P. E. Marik, M. Baram, and B. Vahid, "Does central venous pressure predict fluid responsiveness? A systematic review of the literature and the tale of seven mares," *Chest*, vol. 134, no. 1, pp. 172-8, Jul 2008.
- [18] X. Yang and B. Du, "Does pulse pressure variation predict fluid responsiveness in critically ill patients? A systematic review and meta-analysis," *Crit Care*, vol. 18, no. 6, p. 650, 2014.
- [19] A. Kramer, D. Zygun, H. Hawes, P. Easton, and A. Ferland, "Pulse pressure variation predicts fluid responsiveness following coronary artery bypass surgery," *Chest*, vol. 126, no. 5, pp. 1563-8, Nov 2004.
- [20] F. Michard *et al.*, "Relation between respiratory changes in arterial pulse pressure and fluid responsiveness in septic patients with acute circulatory failure," *Am J Respir Crit Care Med*, vol. 162, no. 1, pp. 134-8, Jul 2000.

- [21] F. Michard and J.-L. Teboul, "Predicting Fluid Responsiveness in ICU Patients: A Critical Analysis of the Evidence," *Chest*, vol. 121, no. 6, pp. 2000-2008, 2002/06/01/ 2002.
- [22] C. K. Hofer, S. M. Muller, L. Furrer, R. Klaghofer, M. Genoni, and A. Zollinger, "Stroke volume and pulse pressure variation for prediction of fluid responsiveness in patients undergoing off-pump coronary artery bypass grafting," *Chest*, vol. 128, no. 2, pp. 848-54, Aug 2005.
- [23] M. Cannesson *et al.*, "Assessing the diagnostic accuracy of pulse pressure variations for the prediction of fluid responsiveness: a "gray zone" approach," *Anesthesiology*, vol. 115, no. 2, pp. 231-41, Aug 2011.
- [24] P. Grassi, L. Lo Nigro, K. Battaglia, M. Barone, F. Testa, and G. Berlot, "Pulse pressure variation as a predictor of fluid responsiveness in mechanically ventilated patients with spontaneous breathing activity: a pragmatic observational study," *HSR Proceedings in Intensive Care & Cardiovascular Anesthesia*, vol. 5, no. 2, pp. 98-109, 2013.
- [25] T. J. Gan *et al.*, "Goal-directed intraoperative fluid administration reduces length of hospital stay after major surgery," *Anesthesiology*, vol. 97, no. 4, pp. 820-6, Oct 2002.
- [26] P. E. Marik, R. Cavallazzi, T. Vasu, and A. Hirani, "Dynamic changes in arterial waveform derived variables and fluid responsiveness in mechanically ventilated patients: a systematic review of the literature," (in eng), *Crit Care Med*, vol. 37, no. 9, pp. 2642-7, Sep 2009.
- [27] F. Michard, "Volume management using dynamic parameters: the good, the bad, and the ugly," *Chest*, vol. 128, no. 4, pp. 1902-3, Oct 2005.
- [28] K. Lakhal *et al.*, "Respiratory pulse pressure variation fails to predict fluid responsiveness in acute respiratory distress syndrome," *Crit Care*, vol. 15, no. 2, p. R85, 2011.
- [29] C. D. Oliveira-Costa, G. Friedman, S. R. Vieira, and L. Fialkow, "Pulse pressure variation and prediction of fluid responsiveness in patients ventilated with low tidal volumes," *Clinics (Sao Paulo)*, vol. 67, no. 7, pp. 773-8, Jul 2012.
- [30] P. A. Wyffels, P. Sergeant, and P. F. Wouters, "The value of pulse pressure and stroke volume variation as predictors of fluid responsiveness during open chest surgery," *Anaesthesia*, vol. 65, no. 7, pp. 704-9, Jul 2010.
- [31] J.-L. Teboul, X. Monnet, D. Chemla, and F. Michard, "Arterial Pulse Pressure Variation with Mechanical Ventilation," *American Journal of Respiratory and Critical Care Medicine*, vol. 199, no. 1, p. 22, 2019.
- [32] C. Morelot-Panzini, Y. Lefort, J. P. Derenne, and T. Similowski, "Simplified method to measure respiratory-related changes in arterial pulse pressure in patients receiving mechanical ventilation," *Chest*, vol. 124, no. 2, pp. 665-70, Aug 2003.
- [33] D. Jacques, K. Bendjelid, S. Duperret, J. Colling, V. Piriou, and J. P. Viale, "Pulse pressure variation and stroke volume variation during increased intra-abdominal pressure: an experimental study," *Crit Care*, vol. 15, no. 1, p. R33, 2011.
- [34] D. De Backer, F. S. Taccone, R. Holsten, F. Ibrahimi, and J. L. Vincent, "Influence of respiratory rate on stroke volume variation in mechanically ventilated patients," (in eng), *Anesthesiology*, vol. 110, no. 5, pp. 1092-7, May 2009.
- [35] M. Aboy, J. McNames, T. Thong, D. Tsunami, M. S. Ellenby, and B. Goldstein, "An automatic beat detection algorithm for pressure signals," *IEEE Trans Biomed Eng*, vol. 52, no. 10, pp. 1662-70, Oct 2005.
- [36] M. Cannesson, B. Vallet, and F. Michard, "Pulse pressure variation and stroke volume variation: from flying blind to flying right?," *Br J Anaesth*, vol. 103, no. 6, pp. 896-7; author reply 897-9, Dec 2009.
- [37] D. Austin, C. Staats, and M. Aboy, "A novel approach to pulse pressure variation estimation," *Conf Proc IEEE Eng Med Biol Soc*, vol. 2006, pp. 1391-3, 2006.
- [38] J. McNames and M. Aboy, "Statistical modeling of cardiovascular signals and parameter estimation based on the extended Kalman filter," *IEEE Trans Biomed Eng*, vol. 55, no. 1, pp. 119-29, Jan 2008.

- [39] S. Kim, M. Aboy, and J. McNames, "Pulse pressure variation tracking using sequential Monte Carlo methods," *Biomedical signal processing and control*, vol. 8, no. 4, pp. 333-340, 2013.
- [40] M. Cannesson, N. P. Tran, M. Cho, F. Hatib, and F. Michard, "Predicting fluid responsiveness with stroke volume variation despite multiple extrasystoles," *Crit Care Med*, vol. 40, no. 1, pp. 193-8, Jan 2012.
- [41] R. H. Thiele, D. A. Colquhoun, J. M. Tucker-Schwartz, G. T. Gillies, and M. E. Durieux, "Radial-femoral concordance in time and frequency domain-based estimates of systemic arterial respiratory variation," *J Clin Monit Comput*, vol. 26, no. 5, pp. 393-400, Oct 2012.
- [42] K. Soltesz, "Robust computation of pulse pressure variations," *Biomedical Signal Processing and Control*, vol. 39, no. C, pp. 197-203, 2018.
- [43] M. Schmid, H. Prettenhaler, C. Weger, and K. H. Smolle, "Evaluation of a novel automated non-invasive pulse pressure variation algorithm," *Comput Biol Med*, vol. 43, no. 10, pp. 1583-9, Oct 2013.
- [44] R. B. P. Wilde *et al.*, "Non-invasive continuous arterial pressure and pulse pressure variation measured with Nexfin® in patients following major upper abdominal surgery: a comparative study," *Anaesthesia*, vol. 71, no. 7, pp. 788-797, 2016.
- [45] O. Desebbe *et al.*, "A Novel Mobile Phone Application for Pulse Pressure Variation Monitoring Based on Feature Extraction Technology: A Method Comparison Study in a Simulated Environment," *Anesth Analg*, vol. 123, no. 1, pp. 105-13, Jul 2016.
- [46] O. Desebbe, J. L. Vincent, B. Saugel, J. Rinehart, and A. Joosten, "Pulse pressure variation using a novel smartphone application (Capstesia) versus invasive pulse contour analysis in patients undergoing cardiac surgery: a secondary analysis focusing on clinical decision making," *J Clin Monit Comput*, vol. 34, no. 2, pp. 379-380, Apr 2020.
- [47] P. Hoppe, F. Gleibs, L. Briesenick, A. Joosten, and B. Saugel, "Estimation of pulse pressure variation and cardiac output in patients having major abdominal surgery: a comparison between a mobile application for snapshot pulse wave analysis and invasive pulse wave analysis," *Journal of clinical monitoring and computing*, 2020.
- [48] National Instruments. "RF Academic Bundle: Amplitude Modulation." <http://www.ni.com/tutorial/5421/en/>
- [49] P. M. Systems, P. M. Systems, Ed. *Data Export Interface Programming Guide, Intellivue Patient Monitor MP40/50/60/70/90*. 2002.
- [50] K. Vinecore *et al.*, "Design and implementation of a portable physiologic data acquisition system," *Pediatr Crit Care Med*, vol. 8, no. 6, pp. 563-9, Nov 2007.
- [51] H. Gjermundrod, M. Papa, D. Zeinalipour-Yazti, M. D. Dikaiakos, G. Panayi, and T. Kyprianou, "Intensive Care Window: A Multi-Modal Monitoring Tool for Intensive Care Research and Practice," in *Twentieth IEEE International Symposium on Computer-Based Medical Systems (CBMS'07)*, 20-22 June 2007 2007, pp. 471-476, doi: 10.1109/CBMS.2007.64.
- [52] N. Stylianides, M. D. Dikaiakos, H. Gjermundrod, G. Panayi, and T. Kyprianou, "Intensive care window: real-time monitoring and analysis in the intensive care environment," *IEEE Trans Inf Technol Biomed*, vol. 15, no. 1, pp. 26-32, Jan 2011.